7-1-2013

Elastomeric Capture Microparticles (ECμPs) and Their Use with Acoustophoresis to Perform Affinity Capture Assays

Kevin Cushing

Kevin W. Cushing
Candidate

Biomedical Sciences Graduate Program
Department

This dissertation is approved, and it is acceptable in quality and form for publication:

Approved by the Dissertation Committee:

Bruce Edwards Ph.D., Chairperson

Gabriel P. Lopez Ph.D.

Steve Graves, Ph.D.

Dimiter Petsev, Ph.D.

James P. Freyer, Ph.D.

Elastomeric Capture Microparticles (ECμPs) and Their use with Acoustophoresis to Perform Affinity Capture Assays

by

Kevin Wallace Cushing

B.S., Biology, University of Arizona
Tucson, Arizona 2001

M.S., Chemistry, Northern Arizona University
Flagstaff, Arizona 2004

DISSERTATION

Submitted in Partial Fulfillment of the
Requirements for the Degree of

Doctor of Philosophy

Biomedical Science

The University of New Mexico
Albuquerque, New Mexico

July 2013

ACKNOWLEDGMENTS

I would like to sincerely thank my research advisor Gabriel P. Lopez for all his support over the course of my dissertation research. I am also very grateful for Professors Bruce Edwards and Steven Graves, who without their continual guidance and support I would have never been able to complete my dissertation research. I am also very indebted to all my other committee members, Dimiter Petsev and James Freyer, who have helped fine tune my understanding of emulsion science and flow cytometry over the years. I am also extremely thankful to Menake Piyasena who was instrumental in my understanding of acoustophoresis and the fabrication of acoustofluidic devices. I would also like to thank and show appreciation for my undergraduate students, Gian Maestas and Beth Ann Lopez, who were very helpful in the fabrication of the acoustofluidic devices and elastomeric particles.

Elastomeric Capture Microparticles (ECμPs) and Their Use with Acoustophoresis to Perform Affinity Capture Assays

by

Kevin Wallace Cushing

B.S., Biology, University of Arizona
Tucson, Arizona 2001

M.S., Chemistry, Northern Arizona University
Flagstaff, Arizona 2004

Ph D., Biomedical Sciences, University of New Mexico
Albuquerque, New Mexico 2013

Abstract

This dissertation describes the development of elastomeric capture microparticles (ECμPs) and their use with acoustophoresis to perform affinity capture assays. ECμPs that function as negative acoustic contrast particles were developed by crosslinking emulsion-based droplets composed of commercially available silicone precursors followed by functionalization with avidin/biotin reagents. The size distribution of the ECμPs was very broad or narrow depending on the emulsion system that was used during the synthesis process. Elastomeric particles exhibited a very broad size distribution when a bulk-emulsion process was used; however, when microfluidic systems were utilized, their size distribution became comparatively narrow. The functionalization of elastomeric particles was accomplished by the non-specific adsorption of avidin protein followed by bovine serum albumin (BSA) blocking and bio-specific adsorption of a biotinylated-capture antibody. Polydisperse ECμPs were functionalized to bind prostate specific

antigen (PSA) or IgG-phycoerythrin (PE) in aqueous media (buffer, plasma, blood); whereas monodisperse ECμPs were functionalized to bind a high density lipoprotein in the aqueous media. Polydisperse ECμPs functionalized to bind PSA in a physiological buffer (PBS pH 7.4) demonstrated nanomolar detection using flow cytometry analysis; whereas ECμPs functionalized to bind IgG-PE demonstrated picomolar detection in 10% porcine plasma. ECμPs have a specific density of ~1.03 and are more compressible than their surrounding aqueous media; which allowed the ECμPs to exhibit negative acoustic contrast properties under an ultrasonic acoustic standing wave field. The negative acoustic contrast property of ECμPs was advantageously utilized in an IgG-PE assay conducted in 0.1% whole porcine blood. The ligand-bound ECμPs suspended in the diluted blood sample were flowed through an acoustofluidic device where the application of an ultrasonic acoustic standing wave field focused the ligand-bound ECμPs to pressure antinodes and the positive acoustic contrast blood cells to the central pressure node of the microchannel. As a result of laminar flow, focused ligand-bound ECμPs and blood cells were flowed into properly aligned outlet channels at the downstream trifurcation, where they where collected separately off-chip. The cell-free fraction containing ligand-bound ECμPs was analyzed using flow cytometry; where the detection of IgG-PE was in the picomolar range. This approach has potential applications in the development of rapid assays that detect the presence of low concentrations of biomarkers in a number of biological sample types.

Table of Contents

List of Figures

Chapter 1 Introduction

Chapter 3 Synthesis of Elastomeric Particles

Chapter 4 Elastomeric Particles Biofunctionalized and Used in Flow Cytometry-Based Assays

Chapter 5 Elastomeric Particles Function as Negative Acoustic Contrast Particles

Chapter 6 Elastomeric Negative Acoustic Contrast Particles for Affinity Capture Assays

Chapter 1 Introduction

Acoustofluidics

Microfluidics deals with the flow and manipulation of small amounts of liquids and suspensions (e.g., microparticles) in channels with dimensions in the tens to hundreds of micrometers.[1] The small dimensions of the microchannels allow for the absence of turbulent flow patterns and the appearance of laminar flow-based streamlines. Under such a flow regime, laminar flow streamlines allow for predictable spatial and temporal control over the flow of solutes and suspensions under the influence of an external field.[2] The application of using microfluidics in conjunction with applied external fields allow for the precise manipulation of particle suspensions and cells (e.g., concentrations, separations, trapping) in microfluidic devices that can be advantageously used for biomedical applications (e.g., cell sorting, and enrichment). Some of the commonly used microfluidic-based manipulation methods are: magnetic,[3] dielectrophoresis,[4] optical tweezers,[5] inertia,[6] and acoustophoresis.[7] Some advantages for using microfluidic devices in conjunction with external fields are: high-throughput capabilities, inexpensive to fabricate, require low consumption of reagents and power, give rapid particle manipulation times, and are generally portable for field usage.

Acoustofluidics is a subset of microfluidics that deals with the application of mechanical sound waves in microfluidic environments;[2] it is also generally used to perform acoustophoresis.[7] According to Thomas Laurell, acoustophoresis can simply be defined as "migration with sound." Acoustophoresis performed using an acoustofluidic device is a gentle, non-contact method to manipulate micro objects (e.g., cells, microparticles) based on size, shape, density, and compressibility.[7] Acoustophoresis has

many biomedical and biotechnical applications such as: elimination of lipid emboli from shed blood in thoracic surgery,[8] blood component fractionation and particle sizing,[9] contaminated blood plasma replacement and buffer media exchange,[10] plasmapheresis[11] and positioning and trapping of cells,[12] and stream-line focusing of particles and cells for flow cytometry analysis.[13] Furthermore, acoustophoresis can easily be integrated with magnetic separators,[14] dielectrophoresis,[4] and other automated systems.[15]

Acoustophoresis Theory

Acoustophoresis is generally based on an acoustic standing wave field that is produced within the fluid-filled cavity of an acoustofluidic chip. Particles (or cells) suspended in this fluid-filled cavity can experience a primary acoustic radiation force that can be expressed with the following primary acoustic force equation (1)[16] that was partly derived from the work of Gor'gov et al.[17]

$$F_p = -\left(\frac{\pi p^2 V_p \beta_o}{2\lambda}\right) \varphi(\beta,\rho) \sin(2kx) \qquad \textbf{(1)}$$

$$\varphi(\beta,\rho) = \frac{5\rho_p - 2\rho_o}{2\rho_p + \rho_o} - \frac{\beta_p}{\beta_o} \qquad \textbf{(2)}$$

The magnitude of the primary acoustic force (Fp) is directly proportional to the volume of the particle (V_p), the pressure amplitude of the field (p^2), the applied frequency ($1/\lambda$), and the acoustic contrast factor $\varphi(\beta,\rho)$. The value of the acoustic contrast factor depends on the density of the particle (ρ_p) and the surrounding media (ρ_o) and the

compressibility of the particle (β_p) and the surrounding media (β_o). If $\varphi(\beta, \rho)$ has a positive value then the acoustic field will exert a time-averaged force moving the particle to the acoustic pressure node of a standing wave (positive acoustic contrast particles). However, if $\varphi(\beta, \rho)$ has a negative value then the acoustic field will exert a time-averaged force moving the particle to acoustic pressure antinodes in a standing wave (negative acoustic contrast particles). The acoustic forces exerted on particles (or cells) are to a large extent independent of the ionic strength and pH of the surrounding medium, or the surface charge of the particles.[18] A more detailed description of the acoustic forces exerted on particles under an acoustic standing wave field can be found in Bruus et al.[19]

In regards to this dissertation report, the most pertinent application of the acoustophoretic theory is the binary separation of particles with different acoustic contrast properties (negative and positive acoustic contrast). The concept of separating particles with different acoustic contrast properties was originally patented by Kaduchak et al. where they were able to demonstrate that hollow, compressible glass spheres function as negative acoustic contrast particles and can be separated from positive acoustic contrast particles.[20] In their patent application they discussed methods (which were never implemented or published) to use negative acoustic contrast capture particles to capture protein biomarkers in biological solutions containing cells (positive acoustic contrast particles) followed by acoustophoresis and on-chip spectroscopic analysis (e.g., on-chip flow cytometry).

Acoustofluidic devices have been fabricated using glass, steel, quartz, and silicon-based microfluidic devices. These microfluidic devices are easily converted into acoustofluidic devices by coupling an actuating lead zirconate titanate piezoelectric

transducer (PZT) ceramic to their surfaces. Coupling of an actuating (drive) PZT to the surfaces of microfluidic devices can be performed by using cyanoacrylate glue or some other type of super glue. PZTs are generally operated using a high power RF (radio frequency) amplifier where the frequency is modulated using a waveform generator. The operating frequencies of the actuating PZT is determined based on the thickness of the actuating PZT crystal. Acoustofluidic devices are generally referred to as acoustic "resonators." An acoustic resonator is an acoustofluidic device that naturally vibrates (or oscillates) at specific frequencies called resonance frequencies. Vibration at these resonance frequencies leads to the formation of an acoustic standing pressure wave within the fluid-filled cavity of the microchannel. An acoustic resonator has natural resonance frequencies that are dependent upon the width of its microchannel. The fundamental resonance frequency (1st harmonic) of an acoustic resonator is the frequency that allows half the wavelength (1/2λ) of the acoustic standing wave to fit within the fluid-filled cavity of the microchannel; thus the fundamental resonance frequency is 1/2λ, which gives 2 pressure antinodes at the side walls and a pressure node at the center of the microchannel. Utilizing fractional harmonics (1/2λ, λ, 3/2λ, 4/2λ....) the number of pressure nodes (pressure minima) and pressure antinodes (pressure maxima) can be modulated with a PZT with the appropriate thickness.

The acoustic resonator that is most pertinent to this dissertation is fabricated from silicon. Silicon has exceptional sound reflecting properties that minimize acoustic losses. The minimization of acoustic losses during the reflection of the sound wave in a silicon-based acoustic resonator is due to the high characteristic acoustic impedances of the silicon (~19.79 x 10^6 kg m^{-2}s) compared to the fluid-filled cavity (water~1.49 x 10^6 kg m^{-}

^{2}s).[18] Further, the high acoustic impendence of the actuated PZT (30.8 x 10^{6} kg m^{-2}s) along with the acoustic impendences of the silicon material and the fluid-filled cavity allow easy acoustic energy transfer from the PZT to the silicon material and then finally into the fluid-filled cavity.[18,22] These physical characteristics of silicon make it one of the most common materials used for the fabrication of acoustofluidic devices.

Silicon acoustofluidic devices can be easily microfabricated using silicon wafers, pre-established photolithography and deep reactive ion etching (DRIE); these methods are explicitly discussed by Austin-Suthanthiraraj et al.[22] These microfabricated processes are versatile and allow silicon microchannels to be designed with a diversity of microchannel patterns (e.g., straight channels, bifurcations, trifurcations) with precise spatial control of microchannel dimensions (e.g., depth, width, and length). Further, the use of DRIE as a method to etch silicon microchannels allows rectangular microchannels to be microfabricated with straight vertical side walls that contribute to the longitudinal sound wave reflecting properties of silicon-based acoustofluidic devices. Once the microchannels have been etched into the silicon, a transparent Pyrex® glass slide is anodically bonded onto the silicon etched microchannels.[22] Sealing the silicon microchannels with a transparent glass slide allows visual observation of acoustophoresis using microscopy and imaging technologies; this observation can aide in the optimization and fine tuning of the acoustic standing wave within the microchannel. The versatility in how silicon acoustofluidic microchannels are designed and microfabricated can allow silicon acoustofluidic devices to be developed for a diversity of biomedical and biotechnology applications that utilize acoustophoresis, such as: 1-dimensional focusing for low-cost flow cytometry,[22] acoustic trapping,[12] continuous washing of cells and assay

particles,[10] and a binary separation system for particles with different acoustic contrast properties.[8]

The microfabricated silicon acoustofluidic device utilizes a rectangular microchannel along with an actuating PZT to perform acoustophoresis. To prevent visual interference of acoustophoresis using microscopy, the PZT can be attached to the bottom of the device (Figure 1.1); although the PZT can be effectively used for acoustophoresis when attached to the bottom, side, or on top of the glass slide.[10] The actuation of the PZT at the appropriate resonance frequency (1/2λ) generates a 1-dimensional, longitudinal acoustic standing wave within the silicon microchannel. The generation of this acoustic standing wave at 1/2λ exerts a time-averaged acoustic radiation force that positions positive acoustic contrast particles (e.g., cells) at the central pressure node, and negative acoustic contrast particles (e.g., lipids) at the pressure antinodes at the side walls of the microchannel (Figure 1.1).

Acoustofluidic Assays

Many bioassay systems (e.g., Enzyme-Linked Immunosorbent Assay: ELISA, and mass spectrometry-based assays) performed in biological samples, e.g., plasma or sera, necessitate removal of blood cells and dilution of plasma (e.g., 1000 fold) prior to performing the assay. In the case of biomarker (e.g., PSA) detection and quantification in human plasma using ELISA or mass spectrometry, removal of blood cells is necessary as they are typically present at very high concentrations ($5x10^9$ cells per mL) so that they represent a large source of background "noise" relative to the biomarker "signal" of interest.[23] Removal of background generating blood cells therefore increases signal-to-

noise (S/N ratio) to improve accuracy, sensitivity, limit-of-detection (LOD), and reproducibility of the assay system.

Centrifugation is the most common method for blood cell removal, but can be problematic. Centrifugation can often be time consuming (10-20 minutes); damaging to cells -leaving behind large amounts of cellular debris in plasma; often requires large volumes of blood (2.5-10 mL); and is generally not very portable for field usage.
The use of a silicon-based acoustofluidic device for obtaining cell-free plasma has several advantages over centrifugation, such as it 1) allows the usage of small volumes (microliters) of whole or diluted blood; 2) is a rapid (seconds), non-contact method for separation that does not damage (i.e., lysis) blood cells; and 3) can be performed in a portable, silicon-based acoustofluidic device.

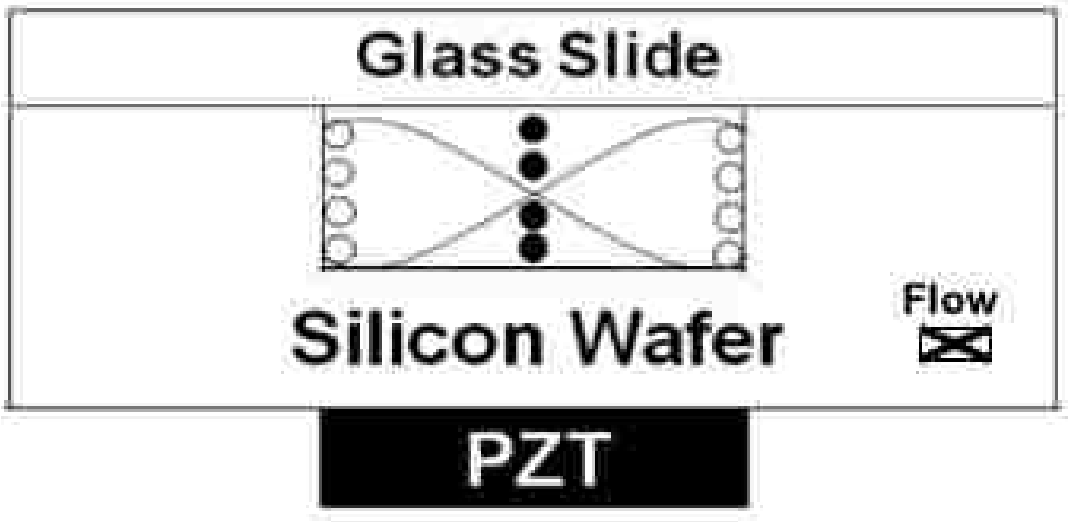

Figure 1.1 Cross-section of a silicon-based acoustofluidic device with the positive acoustic contrast particles (black) focused at the pressure node and the negative acoustic contrast particles (white) focused at the pressure antinodes under an acoustic standing wave field.

Although the use of a silicon-based acoustofluidic device for obtaining cell-free plasma has advantages over centrifugation, the use of common analysis techniques such as ELISA or mass spectrometry still requires multiple additional processing steps to enable accurate and sensitive analysis. Cell-free plasma protein assays performed using ELISA requires an initial dilution (e.g., 1000-fold) followed by multiple washing steps to obtain accurate and sensitive analysis; whereas mass spectrometry often requires dilution followed multiple protein purification steps (e.g., 2-D gel electrophoresis, chromatography, filtration methods, trypsin digestion) prior to analysis. To obviate these excessive processing steps, capture particles can be designed that will be able to 1) capture a plasma protein biomarker present in an undiluted or minimally diluted blood sample; 2) have negative acoustic contrast properties that allow separation from background generating blood cells (positive acoustic contrast particles) in an applied acoustic standing wave field and 3) can produce a fluorescence signal quantitatively proportional to the amount of captured protein which is immediately measurable in a flow cytometer without prior washing steps (Figure 1.2).

The ability to perform the biospecific capturing of a biomarker-analyte (e.g., PSA) in a whole blood sample without dilution (or with minimal dilution) has potential to enhance detection and quantification of biomarkers (PSA) that are present at low concentration levels (e.g., picomolar, femtomolar). Once negative acoustic contrast capture particles have bound the desired biomarkers, the removal of high quantities of blood cells using acoustophoresis becomes crucial for accurate flow cytometry analysis of ligand-bound capture particles; as large quantities of blood cells can overwhelm the electronic systems of most flow cytometers (e.g., Accuri C6).

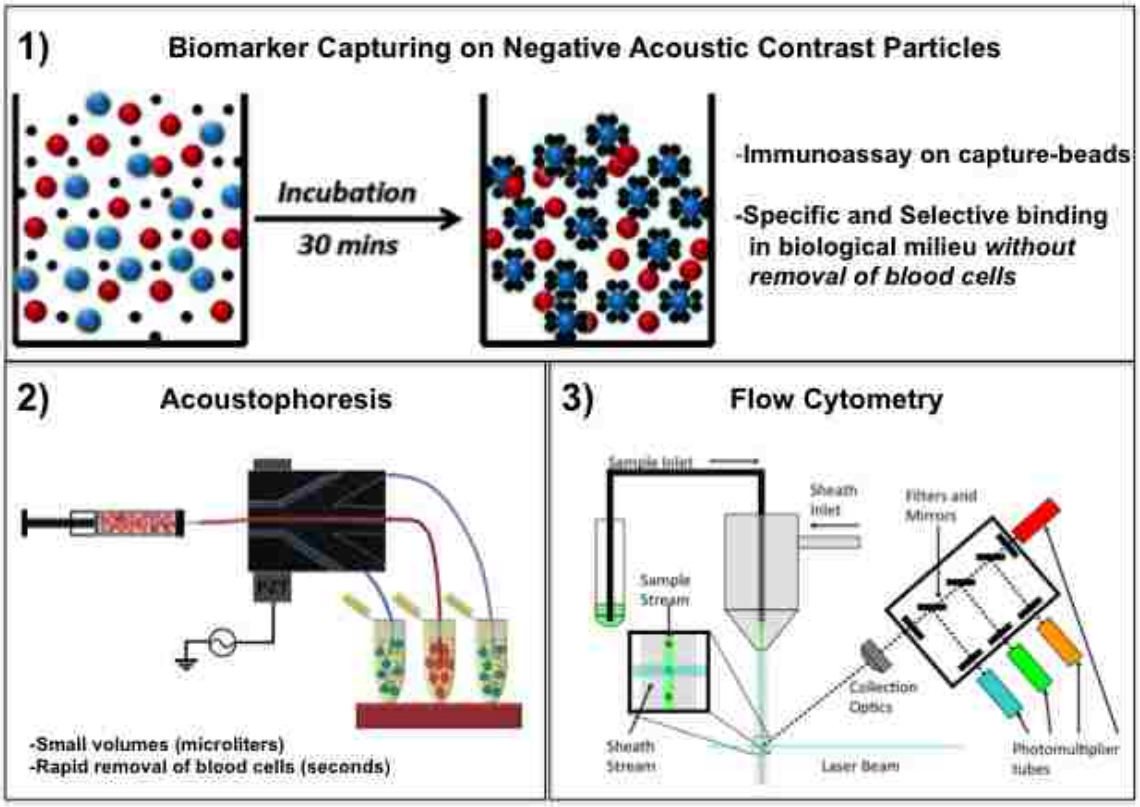

Figure 1.2 Schematic diagram outlining the proposed bioassay strategy for using acoustophoresis as a method to separate biomarker (black)-bound elastomeric capture microparticles (blue) from blood cells (red) prior to performing flow cytometry analysis without prior washing steps.

Particle Design

One of the core objectives of this project is to synthesize negative acoustic contrast particles that can be separated from positive acoustic contrast particles (e.g., cells) using acoustophoresis. To achieve this objective, a material that possesses a negative acoustic contrast value for the acoustic contrast factor (equation 2) must be used to synthesize negative acoustic contrast particles. To function as a negative contrast particle, the material must have a compressibility and density that allow $\frac{5\rho_p - 2\rho_o}{2\rho_p + \rho_o} < \frac{\beta_p}{\beta_o}$; when this is the case the acoustic contrast factor exhibits a negative value and the synthesized particles function as negative contrast particles. However, if the opposite occurs, if $\frac{5\rho_p - 2\rho_o}{2\rho_p + \rho_o} > \frac{\beta_p}{\beta_o}$, then the acoustic contrast factor value is positive and the synthesized particles function as positive contrast particles.

To simplify the design of negative contrast particles, if the densities of the material and their surrounding medium display negligible differences, then the acoustic contrast factor formula can be simplified into $1 - \frac{\beta_p}{\beta_o}$; thus the value of the acoustic contrast factor becomes exclusively dependent upon the compressibility ratio of the suspended particles and their surrounding medium. Under such a circumstance, if $\beta_p > \beta_o$, then the acoustic contrast factor value is negative and the synthesized particles function as negative contrast particles; however, if $\beta_p < \beta_o$, then the acoustic contrast factor value is positive and the particles function as positive contrast particles.

This simplification of the acoustic contrast formula gives insight into the type of material needed to produce a negative contrast particle. Sylgard 184 is a type of polydimethylsiloxane (PDMS) that can be crosslinked into a compressible rubber-like

material. The compressibility of the Sylgard 184 can be modulated based on the amount of crosslinking agent added to the prepolymer prior to the curing process (also referred to as crosslinking process); which forms a crosslinked Sylgard 184 elastomer. The less crosslinking agent added to the prepolymer, the more compressible will be the resulting particle and the more likely that it will have negative acoustic contrast properties. The conventional 10:1 ratio of Sylgard 184 prepolymer to crosslinking agent results in a particle that is more compressible than water. Sylgard 184 particles also have a specific gravity of 1.03 and are therefore approximately the same density as water ($specific\ gravity = \frac{density\ of\ Sylgard\ 184}{density\ of\ water}$). This indicates that compressibility will be the major factor determining acoustic contrast and that conventionally crosslinked Sylgard 184 particles will have negative acoustic contrast properties in aqueous media. The specific gravity of Sylgard 184 particles has an additional advantage in that the particles will tend to remain in suspension in aqueous media such as PBS. This will facilitate flow cytometry analysis in which particle suspension is required.

The significant portion of research presented in this dissertation relates to the synthesis of negative contrast particles using Sylgard 184; however, other compressible, water-insoluble elastomeric materials may possess negative acoustic contrast properties that can be modulated based on addition of crosslinking reagents, such as: other silicones, natural rubbers, polyurethanes, butyl rubbers, polybutadienes, styrene butadienes, fluoroelastomers, polyether block amides, ethylene-vinyl acetates, polyacrylic rubbers, and many others...etc.

References

1. Whitesides, G. M., The origins and the future of microfluidics. *Nature* **2006,** *442* (7101), 368-373.

2. Bruus, H., Acoustofluidics 1: Governing equations in microfluidics. *Lab on a Chip* **2011,** *11* (22), 3742-3751.

3. Degre, G.; Brunet, E.; Tabeling, P., Improving agglutination tests by working in microfluidic channels. *Lab on a Chip* **2005,** *5* (6), 691-694.

4. Wiklund, M.; Günther, C.; Lemor, R.; Jäger, M.; Fuhr, G.; Hertz, H. M., Ultrasonic standing wave manipulation technology integrated into a dielectrophoretic chip. *Lab Chip* **2006,** *6* (12), 1537-1544.

5. Enger, J.; Goksör, M.; Ramser, K.; Hagberg, P.; Hanstorp, D., Optical tweezers applied to a microfluidic system. *Lab Chip* **2004,** *4* (3), 196-200.

6. Kuntaegowdanahalli, S. S.; Bhagat, A. A. S.; Kumar, G.; Papautsky, I., Inertial microfluidics for continuous particle separation in spiral microchannels. *Lab Chip* **2009,** *9* (20), 2973-2980.

7. Lenshof, A.; Magnusson, C.; Laurell, T., Acoustofluidics 8: Applications of acoustophoresis in continuous flow microsystems. *Lab on a Chip* **2012,** *12* (7), 1210-1223.

8. Petersson, F.; Nilsson, A.; Holm, C.; Jönsson, H.; Laurell, T., Continuous separation of lipid particles from erythrocytes by means of laminar flow and acoustic standing wave forces. *Lab on a Chip* **2005,** *5* (1), 20-22.

9. Petersson, F.; Åberg, L.; Swärd-Nilsson, A.-M.; Laurell, T., Free flow acoustophoresis: microfluidic-based mode of particle and cell separation. *Analytical chemistry* **2007,** *79* (14), 5117-5123.

10. Evander, M.; Lenshof, A.; Laurell, T.; Nilsson, J., Acoustophoresis in wet-etched glass chips. *Analytical chemistry* **2008,** *80* (13), 5178-5185.

11. Lenshof, A.; Ahmad-Tajudin, A.; Järås, K.; Swärd-Nilsson, A.-M.; Åberg, L.; Marko-Varga, G. r.; Malm, J.; Lilja, H.; Laurell, T., Acoustic whole blood plasmapheresis chip for prostate specific antigen microarray diagnostics. *Analytical chemistry* **2009,** *81* (15), 6030-6037.

12. Evander, M.; Johansson, L.; Lilliehorn, T.; Piskur, J.; Lindvall, M.; Johansson, S.; Almqvist, M.; Laurell, T.; Nilsson, J., Noninvasive acoustic cell trapping in a microfluidic perfusion system for online bioassays. *Analytical chemistry* **2007,** *79* (7), 2984-2991.

13. Goddard, G.; Martin, J. C.; Graves, S. W.; Kaduchak, G., Ultrasonic particle-concentration for sheathless focusing of particles for analysis in a flow cytometer. *Cytometry Part A* **2006,** *69* (2), 66-74.

14. Adams, J. D.; Thévoz, P.; Bruus, H.; Soh, H. T., Integrated acoustic and magnetic separation in microfluidic channels. *Applied physics letters* **2009,** *95* (25), 254103-254103-3.

15. Augustsson, P.; Barnkob, R.; Wereley, S. T.; Bruus, H.; Laurell, T., Automated and temperature-controlled micro-PIV measurements enabling long-term-stable microchannel acoustophoresis characterization. *Lab on a Chip* **2011,** *11* (24), 4152-4164.

16. Laurell, T.; Petersson, F.; Nilsson, A., Chip integrated strategies for acoustic separation and manipulation of cells and particles. *Chemical Society Reviews* **2007,** *36* (3), 492-506.

17. Gor'Kov, L. In *On the forces acting on a small particle in an acoustical field in an ideal fluid*, Soviet Physics Doklady, **1962**; p 773.

18. Lenshof, A.; Evander, M.; Laurell, T.; Nilsson, J., Acoustofluidics 5: Building microfluidic acoustic resonators. *Lab on a Chip* **2012,** *12* (4), 684-695.

19. Bruus, H., Acoustofluidics 7: The acoustic radiation force on small particles. *Lab on a Chip* **2012,** *12* (6), 1014-1021.

20. Kaduchak, G.; Ward, M. D., Apparatus for separating particles utilizing engineered acoustic contrast capture particles. **2011**, Patent No., US 8,083,068 B2.

21. Cushing, K. W.; Piyasena, M. E.; Carroll, N. J.; Maestas, G. C.; Lopez, B. A.; Edwards, B. S.; Graves, S. W.; Lopez, G. P., Elastomeric Negative Acoustic Contrast Particles for Affinity Capture Assays. *Analytical chemistry* **2013**, 85 (4), 2208-2215.

22. Austin Suthanthiraraj, P. P.; Piyasena, M. E.; Woods, T. A.; Naivar, M. A.; Lopez, G. P.; Graves, S. W., One-dimensional acoustic standing waves in rectangular channels for flow cytometry. *Methods* **2012**, 57 (3), 259-271.

Chapter 2 Goals and Specific Aims

A core objective of this dissertation is to synthesize a particle that functions as a negative acoustic contrast capture particle under an acoustic standing wave. Negative acoustic contrast particles can be used in blood-based assays (or other types of biological assays) where biomarker-bound negative acoustic contrast particles are continuously separated from blood cells using a silicon-based acoustofluidic device with a downstream trifurcation. Once biomarker-bound negative acoustic contrast particles are collected, without high concentration levels of blood cells, they can be accurately analyzed using flow cytometry. We hypothesize that 1) elastomeric capture microparticles (ECμPs) will function as negative acoustic contrast particles; and 2) can be used in bioassays in which they can be rapidly separated and collected from blood cells prior to flow cytometry analysis using a silicon-based acoustofluidic device. Four specific aims must be accomplished to complete development of this system.

1) Develop a protocol for the synthesis of elastomeric particles.

2) Develop a method to functionalize elastomeric particles to serve as platforms for affinity capture bioassays.

3) Demonstrate that functionalized elastomeric particles function as negative acoustic contrast particles and can be acoustically separated from blood cells using a silicon-based acoustofluidic device.

4) Demonstrate the use of ECμPs in the capturing of a biomarker in a blood sample, followed by acoustophoresis and subsequent flow cytometry analysis.

Chapter 3 Synthesis of Elastomeric Particles

Polydimethylsiloxane (PDMS)

Polydimethylsiloxane (PDMS) is a rubber-like material that belongs to an organosilicon group referred to as silicones.[1] Synthesized silicone is composed of an alternating sequence of silicon and oxygen atoms that constitute the basic structure and backbone of the silicone polymer (Figure 3.1).[2] The silicon atoms in PDMS are bonded to organic groups (Me: $-CH_3$). The presence of organic groups (methyl groups) and an inorganic backbone (-Si-O-Si-) give PDMS unique physical and chemical properties (e.g., optically transparent, inert, non-toxic, and non-flammable) that allow them to function as fluids, emulsions, compounds (e.g., silicone surfactants), resins, contact lenses, medical devices and elastomers, food, caulking, and lubricating oils.[2]

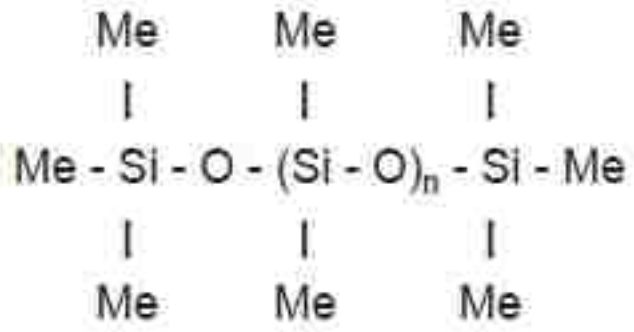

Figure 3.1 Chemical structure of the PDMS prepolymer composed of organic groups ($-CH_3$) and an inorganic backbone (-Si-O-Si-).[1]

Silicone precursors can be polymerized into PDMS prepolymers with different chain lengths.[2] Increased polymerization results in an increased number of PDMS monomers being incorporated into the PDMS prepolymers;[2] thus the molecular weight of the PDMS prepolymers is controlled based on the degree of polymerization. As the molecular weight of the PDMS prepolymers increases, the viscosity of the PDMS prepolymer also becomes greater.[2] According to Dow Corning, their PDMS fluids range in kinematic viscosity from 0.65 cSt to 20,000,000 cSt -which is thicker than chewing gum. In regards to this dissertation report, the type of PDMS that is predominantly used is Sylgard 184; which has a molecular weight of 20,000 g/mole[3] and on average 270 dimethylsiloxane repeat units;[4] corresponding to a kinematic viscosity of 5000 cSt.[5] The synthesized PDMS prepolymers come in the form of loosely entangled prepolymers that can be crosslinked to form a compressible, water-insoluble elastomer. The crosslinking of PDMS prepolymers into a 3-dimensional polymeric network, consists of forming chemical bonds (or links) between individual PDMS prepolymers.[6]

Sylgard 184 is a heat curable type of PDMS that comes commercially from Dow Corning® as a kit composed of two separated parts (parts A and B) in which part (A), with a viscosity of 5000 cSt, is composed of siloxane prepolymers with reactive terminal vinyl groups (base), along with a platinum catalyst, and the second part (B), with a viscosity of 100 cSt, is composed of siloxane prepolymers with silicon-hydride groups (curing agent: or referred to as crosslinking agent). When siloxane (A) and (B) are mixed together, in the presence of the platinum-based catalyst, an addition of the Si-H (silicon hydride) across the double bonds (vinyl groups) forms -(Si-CH_2-CH_2-Si)- linkages (or crosslinks);[7] this method is commonly referred to as hydrosilylation of the double bonds

(Figure 3.2), or more generically referred to as cross-linking.[4] These cross-links will thus convert the liquid-like properties of the PDMS prepolymers into a more dense crosslinked polymeric network that now contains rubber-like elastic (or compressible) properties.

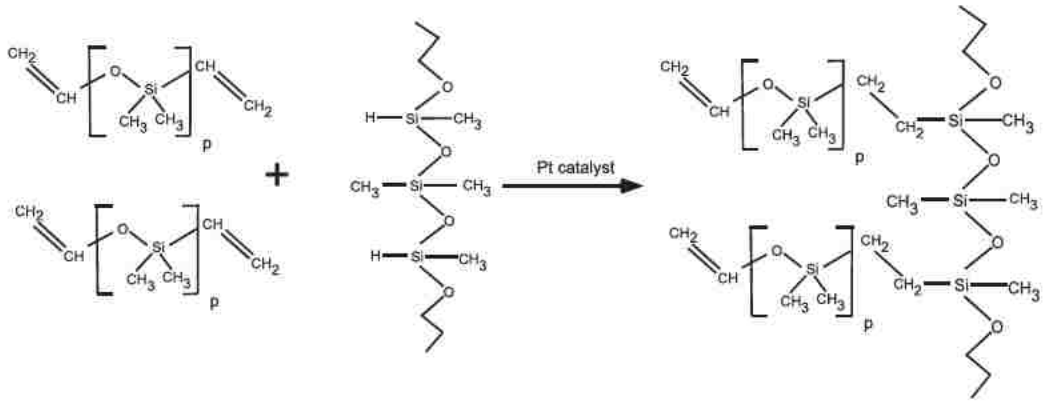

Figure 3.2 The crosslinking in the formation of the PDMS elastomer involving the reaction of vinyl end-capped siloxane oligomers and the dimethylmethylhydrogen siloxane cross-linker by hydrosilylation with a platinum catalyst.[4]

When PDMS is not crosslinked, the siloxane polymers exist is a loosely entangled configuration, giving PDMS a high viscoelasticity, i.e., exhibiting both viscous and elastic characteristics when undergoing deformation. Upon crosslinking, using the above-mentioned mechanism (Figure 2.2), PDMS becomes stiffer, with less compressibility, depending on the concentration of curing agent (crosslinking agent) incorporated in the crosslinking procedure; thus the degree of stiffness and compressibility can be manually controlled by altering the base to crosslinking agent ratio. The shear modulus *G* (~measurement of a material's stiffness) of PDMS may vary from 100 kPa to 3 MPa

depending of the preparation conditions (e.g., monomer ratios during synthesis, amount of crosslinking agent).[8]

PDMS, along with all silicones, are relatively stable as a result of the strong polar covalent bonds that exist between the silicon and oxygen atoms of the siloxane backbone; the bond energies of these polar covalent bonds are on the order of 452 kJ/mol.[1] PDMS is also characterized with a surface tension that is within the biocompatible range for elastomers (20-30 mN/m).[1] PDMS also adopts a structural configuration that exposes the methyl groups (organic groups) to the surrounding environment. The surface tension of PDMS along with its hydrophobic surface (organic surface), make PDMS a stable biocompatible polymer. It must also be noted that these physical properties of PDMS are virtually unaffected by the crosslinking process; and thus PDMS remains a stable biocompatible polymer rather it is crosslinked or not.

PDMS is a water-insoluble elastomer with unique physical properties that make it ideal for conversion into negative acoustic contrast particles. PDMS is relatively low-cost, chemically inert, compatible with biological cells, permeable to gases and selective agents, optically transparent, and has a broad shear modulus or compressibility that can be modulated based on preparation conditions.[9,10] As a result of this, we pursued emulsion-based methods to synthesize polydisperse and monodisperse elastomeric particles; with the intention of using them as negative acoustic contrast particles for affinity capture assays with flow cytometry. Emulsion systems are well established and have predetermined protocols and systems, e.g., bulk[11] and microfluidic systems,[4,5] that have worked well in previously published reports. Herein we synthesized elastomeric negative acoustic contrast particles out of PDMS-based materials using emulsion systems.

In the preceding section we describe emulsion science and give in-depth background information on the bulk and microfluidic methods that are used to synthesize elastomeric negative acoustic contrast particles.

Emulsion Science

An emulsion is a mixture of two or more immiscible liquids where one phase, the dispersed phase, is dispersed in another phase referred to as the continuous phase.[12,13] The dispersed phase (e.g., oil), in order to adopt the most stable energetic configuration,[12] usually forms spherical liquid droplets, i.e., also referred to as suspended liquid colloids, that are randomly distributed within the continuous phase (e.g., water). Some common examples of emulsions are, vinaigrettes, milk, and mayonnaise.

At constant volume and temperature, the formation of an emulsion is governed by the Gibb's free energy of the isolated system.[14] The Gibb's free energy can be described by the following equation:

$$\Delta \boldsymbol{G_{form}} = \boldsymbol{\gamma \Delta A} - \boldsymbol{T \Delta S^m} \qquad (\mathbf{1})$$

The value of Gibb's free energy is determined based on the interfacial tension (γ); the change in interfacial area (ΔA); the temperature (T); and the change in entropy (ΔS^m) upon emulsification (mixing). Generally in most cases, immiscible liquids in contact with each other generate a high interfacial tension that becomes significantly larger than the entropic contribution ($\gamma \Delta A >> T \Delta S^m$). As a result of this high interfacial tension, the formation of most emulsions are not thermodynamically spontaneous ($\Delta G_{form} >> 0$), and therefore require the input of large amounts of energy, usually in the form of shear

forces generated by homogenization, to form an emulsion. This input of energy therefore increases the entropic contribution ($\gamma \Delta A \leq T \Delta S^m$) and allows an emulsion to form ($\Delta G_{form} \leq 0$). To decrease the amount of input energy that is needed to form an emulsion, surfactants can be used to lower the interfacial tension.[14]

Surfactants can be defined as surface active agents (e.g., detergents, polymeric surfactants, proteins) that have amphiphilic properties, i.e., hydrophilic and hydrophobic components,[15] which reduce the interfacial tension between the suspended liquid colloids and the continuous phase (Figure 3.3).[16]

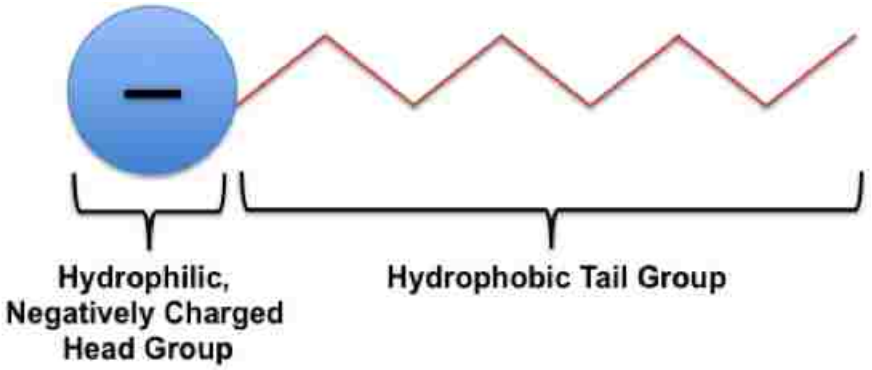

Figure 3.3 Image of a generic amphiphilic surfactant that is composed of a negatively charged hydrophilic head group and a hydrophobic tail group.

The addition of surfactant not only reduces the interfacial tension between the two phases, but increases the kinetic stability of the dispersed liquid phase; thus minimizing aggregation (also referred to as flocculation) and coalescence.[16] This kinetic stability is a consequence of the electrostatic charge or steric barrier that is provided by the adsorbed surfactants to the interface of the dispersed droplets.

Generally, surfactants that are used in the stabilization of emulsions come in the form of detergents. Detergents have an exceptional ability to solubilize biomolecules and are often used in the washing of planar and micro-bead surfaces that are used as platforms for assays (e.g., enzyme linked immunosorbent assays: ELISA). It is important to note that all detergents are considered surfactants, but not all surfactants are considered detergents. Though most emulsion stabilizing surfactants come in the form of detergents, there are also examples of proteins (e.g., casein)[15] which have been used to stabilize oil-in-water emulsions. Emulsions produced in the presence of surfactants have many applications, such as in the preparation of foods, agrochemicals, pharmaceuticals, paints, cosmetics, oil industries, and sunblock, and many others.

Many types of emulsions exist, but the two most common types of emulsions are water-in-oil and oil-in-water. Whether an emulsion of oil and water turns into a water-in-oil emulsion or an oil-in-water emulsion depends on the volume fraction[12] of both phases and the type of surfactant present.[17] Generally surfactants tend to promote the dispersion of the phase in which they do not dissolve very well. A simple example of a water-in-oil emulsion would be water droplets dispersed in a continuous mineral oil phase containing a silicone-based polymeric surfactant named Cetyl PEG/PPG-10/1 Dimethicone (ABIL EM 90). A water-in-oil emulsion results because the ABIL EM 90 surfactant is more soluble in the oil phase than the water phase, and because the volume fraction of the oil phase is significantly larger than the volume fraction of the water phase. However, if you intended to form an oil-in-water emulsion you could adjust the volume fraction of both phases and use a surfactant that was more soluble in the water phase (e.g., Pluronic® F-108) than the oil phase. This observation has been coined as the *Bancroft rule - "The*

phase in which an emulsifier (surfactant) is more soluble constitutes the continuous phase."[17]

Some surfactants that are commonly used to form water-in-oil emulsions are: sorbitan stearate, polyglyceryl oleate, lecithin, sorbitan monooleate, glyceryl monooleate, lanolin, and lanolin alcohols. Surfactants commonly used for oil-in-water emulsions are: cetyltrimethylammonium bromide (CTAB), sodium dodecyl sulfate (SDS), poly(ethylene glycol)-block-poly(propylene glycol)-block-poly(ethylene glycol) (Pluronic® F-108), and other water-soluble surfactants .

More important in regards to this dissertation report are bulk oil-in-water emulsions. Bulk oil-in-water emulsion systems are generally used to produce large quantities of polydisperse oil droplets in a relatively short period of time. Bulk oil-in-water emulsions are generally produced by depositing an oil in an aqueous phase containing a water-soluble surfactant (e.g., Pluronic F108) followed by emulsification using a hand-held homogenizer (Figure 3.4).[18] The resulting emulsion forms polydisperse (many-sizes) oil droplets that are kinetically-stabilized by the adsorbed surfactants at the surface of the droplets.[16] This bulk emulsification process using the hand-held homogenizer always leads to polydisperse droplet formation. This polydispersity results because the stresses and shear forces that are used to form droplets are not evenly distributed throughout the entire system.[19]

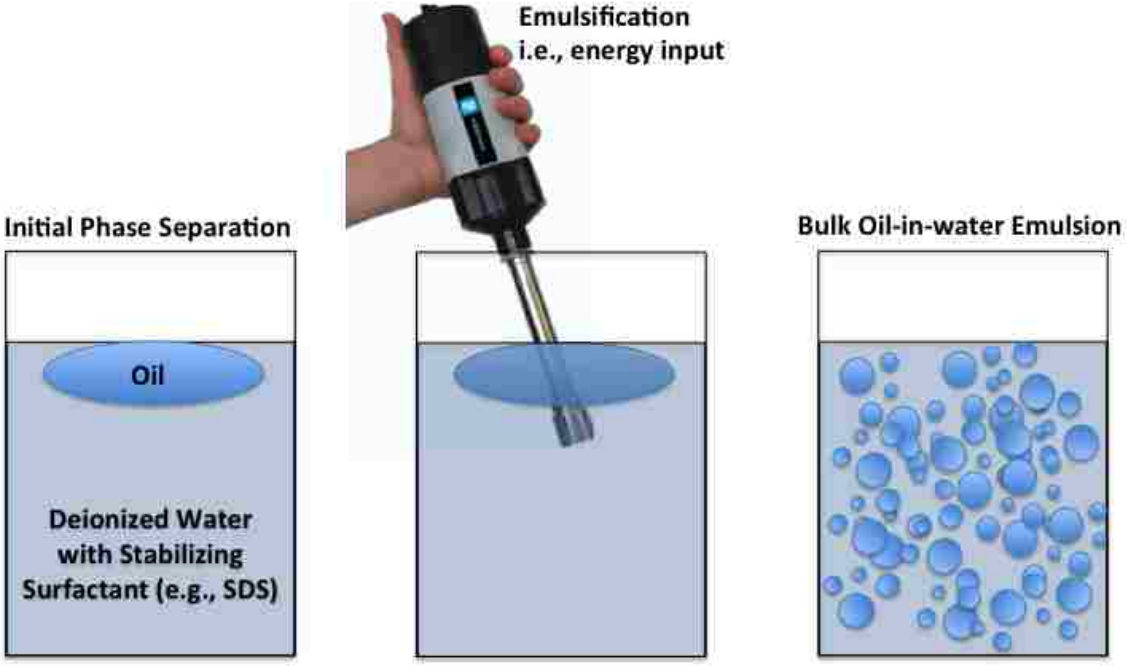

Figure 3.4 Schematic depiction of a bulk oil-in-water emulsion being formed, in the presence of a water-soluble surfactant, by the use of high energy emulsification using a hand-held, commercially-available homogenizer.

Monodisperse (same-size) droplets and particles have potential to be used for exchange resins, spacers, calibration standards, and carriers or drugs, nutrition, pharmaceutical, and cosmetics agents.[20] In order for droplets (or particles) to function properly and provide accurate and reproducible results, they must be prepared in a monodisperse fashion. To make monodisperse emulsions, droplet-based microfluidic systems can be utilized.[19] Droplet-based microfluidic systems are generally characterized by a low Reynold's number ($Re << 1$)[21] and extreme laminar flow regimes;[22] these extreme laminar flow regimes allow frictional or viscous forces to dominate inertial forces.[23] Microfluidic systems with extreme laminar flow regimes allow precise control over the emulsification and thus control of the volumes and sizes of the generated droplets.[19]

Some of the parameters that help determine the size of the produced droplets using microfluidic systems are the flow rates of the continuous and dispersed phases, the viscosities of the continuous and dispersed phases, the use of surfactants, the hydrophobicity and hydrophilicity of the microchannel walls, and the size of the junction (or orifice) where the two phases initially form an interface.[21,22] According to David Weitz at Harvard University, "...the use of microfluidic systems to form droplets, allows each droplet to be formed individually, i.e., one droplet at a time - it is this property that allows droplets to be formed in a very monodisperse fashion".

The dimensionless capillary number (Ca) plays an important role in predicting droplet breakoff within a microfluidic device.[22] The capillary number (Ca) can be defined as:

$$\boldsymbol{Ca = \frac{\eta v}{\gamma}} \qquad (\mathbf{2})$$

The value of the capillary number is determined based on the viscosity of the continuous phase (η); the velocity of the continuous phase (v); and the interfacial tension between the oil and water phases (γ). Generally, droplet breakoff occurs above a critical value, (Ca);[22] however , it has been reported in literature that (Ca) can vary depending on the geometry of the microfluidic microchannels.[24] Spherical droplets usually form at Ca < 1, where interfacial tension dominates viscous forces; and deformed and asymmetric droplets generally form at Ca >> 1.[21]

The most common type of microfluidic devices for monodisperse droplet generation are the polydimethysiloxane (PDMS) based microfluidic devices. The fabrication of PDMS based microfluidic devices using soft-photolithographic methods was pioneered by George Whitesides et al., at Harvard University.[25] The benefits of using PDMS based microfluidic devices are that they are relatively inexpensive, moldable,[25] easy to fabricate compared to other microfluidic devices (e.g., silicon, glass), allow reproducible results, and can be produced in microfluidic systems that generate 10,000 monodisperse droplets per second.[19]

The most common configurations used for monodisperse droplet generation in PDMS microfluidic devices are the T-junction[27] and flow focusing configurations.[22,26,27]

In a T-Junction microfluidic device, the dispersed phase flows perpendicular to the continuous phase in the main channel. (Figure 3.5) As a result of the pressure gradient, the two phases are forced to flow into the orifice (or junction) where they form an interface. As the dispersed phase flows through the orifice and down the main channel the asymmetrical shear forces of the continuous phase, and the pressure gradient, cause the tip of the dispersed phase to elongate and the neck of the dispersed phase to focus until pinching off to form a dispersed droplet. In a flow focusing configuration, the process of droplet formation is different in that the continuous phase is infused from the side channels and thus the dispersed phase is exposed to symmetrical (not asymmetrical as in the T-junction) shear forces. (Figure 3.6) These symmetrical shear forces cause the tip of the dispersed phase to elongate and the neck of the dispersed phase to focus until pinching off to form a droplet. The application of symmetrical shearing of the dispersed phase by the continuous phase gives extreme control over droplet size and is therefore capable of producing extremely uniform populations of droplets.

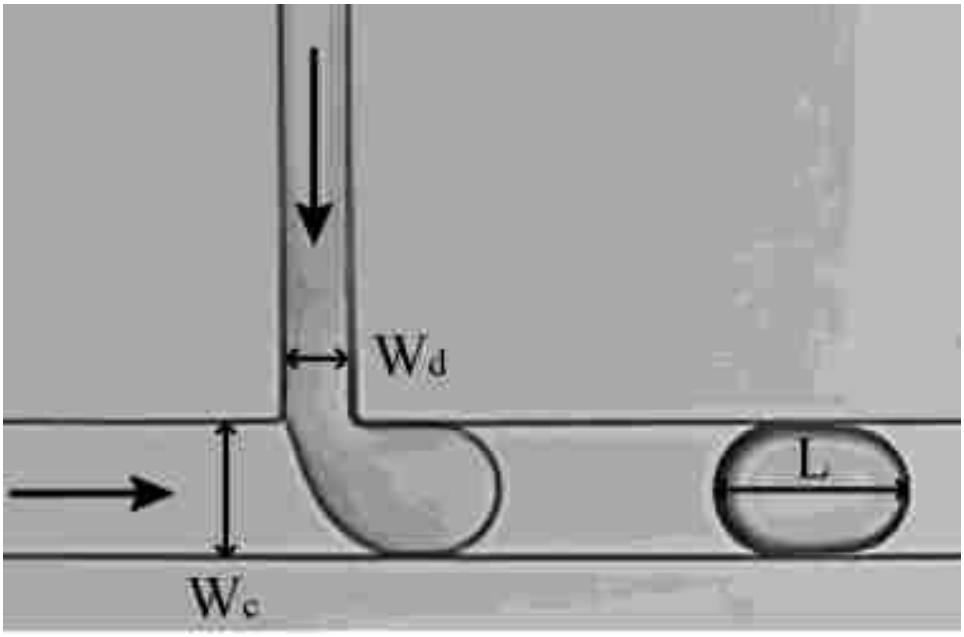

Figure 3.5 Droplet formation in a T-junction. The dispersed phase and continuous phase meet in a T-shaped junction perpendicularly. (*Wd*: 50 μm; *Wc*: 100 μm).[21]

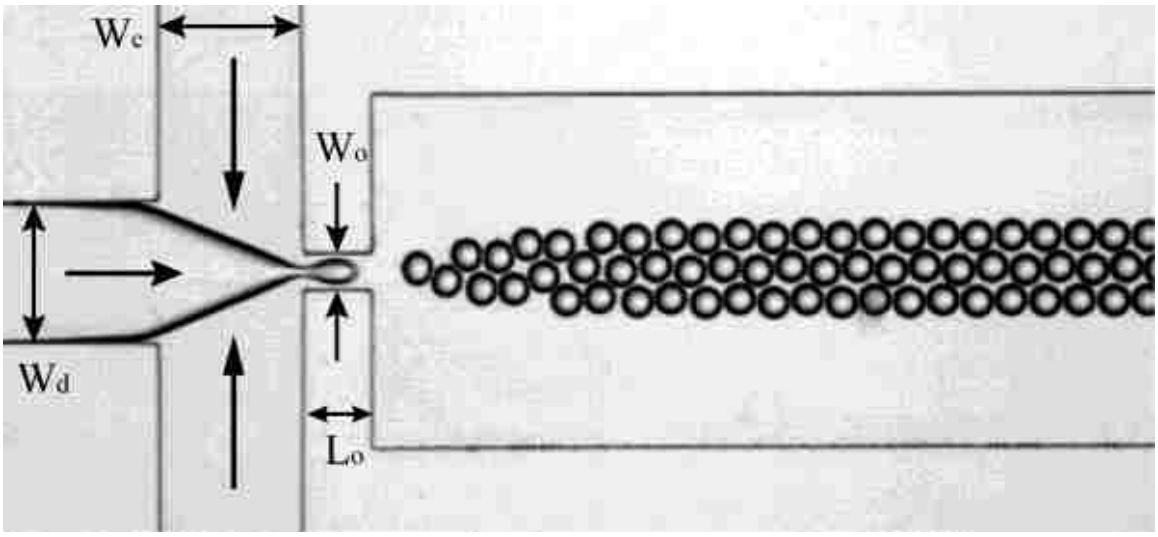

Figure 3.6 Droplet formation in flow focusing device (FFD). The widths of the inlets of dispersed phase and continuous phase, as well as the orifice are indicated as *Wd*, *Wc* and *Wo, respectively* (*Wd* = *Wc* =200 μm: *Wo* = 50 μm).[21]

In this dissertation chapter we describe the synthesis of PDMS-based elastomeric particles from two varieties of PDMS, Sylgard 184 (specific gravity ~ 1.03) and a low molecular weight PDMS (specific gravity ~ 0.97) elastomer, using emulsion-based synthesis strategies. We demonstrate that PDMS-based elastomeric particles can be synthesized in a polydisperse or monodisperse fashion using modified bulk-emulsion processes or PDMS-based microfluidic systems (flow focusing and T-junction configurations) in the presence or absence of surfactant. We also demonstrate that polydisperse elastomeric particles made in the absence of stabilizing surfactant (detergent) can be stabilized towards aggregation using protein as a stabilizing surfactant (avidin and bovine serum albumin: BSA) at the surface of elastomeric particles.

Materials and Methods

Synthesis of polydisperse elastomeric particles

Sylgard 184 (specific gravity ~ 1.03) (1 g, at 10:2 ratio of PDMS prepolymer to crosslinking agent) or low viscosity PDMS (specific gravity ~ 0.97) (1 g, at 9:1, 7:3, 5:5, 2.5:7.5, and 1.5:8.5 ratios of PDMS prepolymer to crosslinking agent) (Dow Corning Corp., Midland, MI) were emulsified in 10 mL of ultrapure water (18.2 MΩ•cm @ 25 °C; Synergy®, EMD Millipore) in the presence or absence of specific detergents (CTAB, Tween 20), using a homogenizer (Power Gen 125, Fisher Scientific) set at 6K RPM for ~ 60 seconds. The elastomeric droplets, with crosslinking agent, were cured at 100 °C for ~ 1 hour to form crosslinked elastomeric particles. Elastomeric particles were imaged using bright field microscopy (BH-2, Olympus) and a 4300 cool pix camera (Nikon). The scale bar was calibrated based on standardized monodisperse particles (mean = 30.1 μm; standard deviation = ± 2.1 μm; and a coefficient of variation = 6.6%) (Thermo Scientific).

Synthesis of monodisperse elastomeric particles

Sylgard 184

Sylgard 184 was used to form elastomeric microparticles using a T-junction microfluidic chip (polydimethylsiloxane-based). The continuous phase contained ultrapure water without the presence of stabilizing surfactant or with 1 μM of avidin protein (Molecular Probes, Eugene, Oregon). To prevent Sylgard 184 (with crosslinking agent) from wetting the micro-channel walls, the continuous phase was first injected using a syringe pump (Nexus 3000, Chemyx Inc. Stafford, TX) at a flow rate of 5-13 μL/min. The dispersed phase, Sylgard 184 at 10:2 (kinematic viscosity~ 2209 cSt) or 6:4 (viscosity~ 827 cSt) ratio of PDMS prepolymer to crosslinking agent, was then injected

into the microfluidic chip at a flow rate of 0.08-0.67 μL/min. Droplets were collected and cured at 70 °C overnight to form crosslinked monodisperse elastomeric microparticles. A Coulter counter (Z2 Coulter Particle Count and Size Analyzer, Becton Dickinson, Franklin Lakes, NJ) was used to determine the size distribution of the near-monodisperse elastomeric particles.

Low molecular weight PDMS

Low viscosity PDMS was used to form microparticles using a T-junction or flow focusing microfluidic device (polydimethylsiloxane-based). The continuous phase contained ultrapure water with the presence of stabilizing surfactants, CTAB (Millipore, Billerica, MA), SDS (Bio-Rad, Hercules, CA), and Pluronic F108 (Sigma-Aldrich). To prevent PDMS (with crosslinking agent) from wetting the micro-channel walls, the continuous phase was first injected using a syringe pump (Nexus 3000, Chemyx Inc. Stafford, TX) at a flow rate of 5 μL/min. The dispersed phase, low viscosity PDMS at 1:1 ratio (viscosity~ 450 cSt) of PDMS prepolymer to crosslinking agent, was then injected into the microfluidic chip at a flow rate of 0.08 μL/min. Droplets were collected and cured at 70 °C overnight to form crosslinked monodisperse elastomeric microparticles.

Stability Studies on Elastomeric Particles (Sylgard 184)

Time-dependent Studies

The synthesized polydisperse elastomeric particles (10:2 ratio of Sylgard 184 prepolymer to crosslinking agent) were incubated in glass scintillation vials with 10 mL of ultrapure water with 0.1% bovine serum albumin (BSA). To determine the extent of aggregation over time, elastomeric particles were imaged over a 1-week interval (days 1,2,3, and 7). The negative control was treated the same except incubation was performed

in ultra water without BSA protein.

Polydisperse elastomeric particles were functionalized by being incubated in 1μM avidin in 1X PBS. Avidinylated-elastomeric particles (~1 x 10^6 particles/mL) were subsequently incubated in a polypropylene microcentrifuge tube (Sorenson Bioscience, Inc, Salt Lake City, Utah) with 1 mL of 1X PBS with 0.1% of BSA. To ensure continuous suspension of elastomeric particles, the microcentrifuge tube was continuously rotated at room temperature using a RotoFlex rotator (Argos Technologies, Elgin, IL). The concentration of elastomeric particles was measured over time (days 0,2,4,6,9) using a flow cytometer (Accuri® C6).

Centrifugation and resuspension studies

Avidinylated-elastomeric particles (7.0 x 10^6 particle/mL) in washing buffer (1X PBS with 0.1% BSA) were centrifuged for 2 minutes at 2900 x gravity. Upon careful removal of supernatant, pelleted elastomeric particles were resuspended in 1 mL of the washing buffer. After elastomeric particles were resuspended, flow cytometry (Accuri® C6) measurements were performed to determine particle concentrations and forward scatter. A total of 7-8 sequential centrifugal washes were performed where microparticles were resuspended with the washing buffer prior to flow cytometry analysis.

Results

Synthesis of Polydisperse Elastomeric Particles (Sylgard 184)

Polydisperse elastomeric microparticles were successfully synthesized using Sylgard 184 (10:2 ratio of prepolymer to crosslinking agent) and a bulk oil-in-water emulsion process in the absence of surfactant (Figure 3.7A). To verify the conversion of elastomeric droplets into microparticles, elastomeric microparticles were dried on a glass microslide (Figure 3.7B). The elastomeric microparticles demonstrated no observable coalescence upon drying on the glass microslide; thus demonstrating successful conversion of droplets into crosslinked microparticles.

Stability Studies on Elastomeric Particles (Sylgard 184)

Time-dependent Studies

Polydisperse elastomeric microparticles (Sylgard 184 at 10:2 ratio of prepolymer to crosslinking agent) incubated in a protein-rich solution (ultra-pure water with 0.1% BSA) over a week (days 1,2,3, and 7), demonstrated stability in regards to forming particle aggregates (Figure 3.8). At the end of the week (day 7), elastomeric microparticles incubated in the protein-rich solution, demonstrated a high degree of turbidity, indicative of a solution containing few particle aggregates and a high concentration of suspended microparticles. To determine the effects of the protein-rich solution on the elastomeric particle stability, a control was performed in which elastomeric microparticles were incubated in an ultra-pure water solution without protein (Figure 3.8). Elastomeric microparticles incubated in ultra-pure water in the absence of protein, formed particle aggregates within the first few hours after being synthesized; on

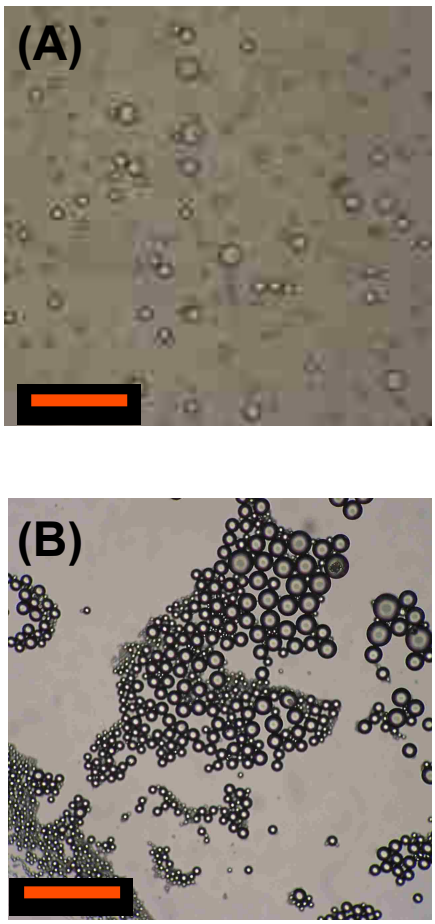

Figure 3.7 Polydisperse elastomeric particles (Sylgard 184: specific gravity~1.03) synthesized using a bulk-emulsion process without surfactant. (A) Bright field image of polydisperse elastomeric particles being suspended in an aqueous solution. (B) Polydisperse elastomeric particles dried on a glass slide. Note: Red bar equals ~ 100 μm.

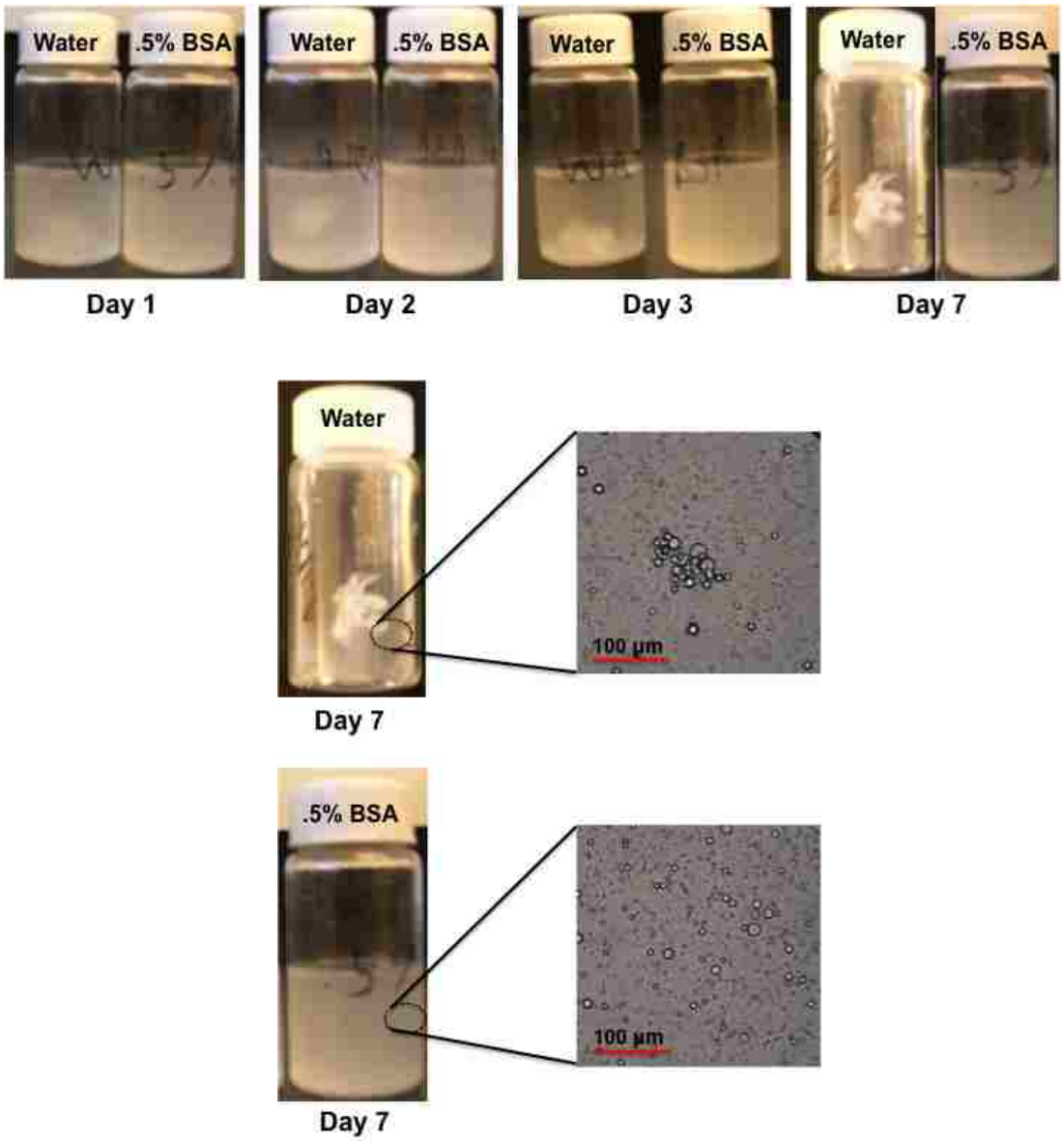

Figure 3.8 Protein (Bovine Serum Albumin: BSA) functions as a stabilizing surfactant for elastomeric particles (Sylgard 184) synthesized in the absence of surfactant.

day 7, the solution demonstrated a high degree of transparency in which a significant amount of microparticles were aggregated and less remained suspended in solution. These results demonstrate that protein can be successfully used as a stabilizing surfactant for elastomeric microparticles.

Suspended avidinylated-elastomeric particles (1 x 10^6 particles/mL) demonstrated stability in regards to particle aggregation in a protein-rich solution (1X PBS with 0.1 BSA) over a 9 day period where particle concentrations were measured using flow cytometry. During the 9 day incubation period, the avidinylated-elastomeric particle concentration hovered around 1 x 10^6 particles/mL; thus indicating that particle aggregation was being minimized (Figure 3.9). These results demonstrate that suspended avidinylated-elastomeric particles are stable enough to be used as capture particles in protein-rich solutions (e.g., solutions containing high concentrations of albumins-plasma) without significant aggregation occurring over extensive time periods.

Centrifugation and Resuspension Studies

Centrifugal washes (2900 x gravity @ 2 minutes) performed in a protein-rich solution (1X PBS with 0.1% BSA) resulted in a decrease in the concentration of avidinylated-elastomeric particles (Figure 3.10). The initial concentration of avidinylated-elastomeric particles in 1 mL of the protein-rich solution was ~ 7 x 10^6 particles/mL; following 1 wash the concentration decreased to ~ 5.7 x 10^6 particles/mL; following the 2^{nd} wash the concentration fell to ~ 4.3 x 10^6 particles/mL; and by the 8^{th} wash the particle concentration was ~ 1.3 x 10^6 particles/mL. Visual observation of the supernatants under the microscope indicated that there were significant amounts of particles remaining in the supernatants after centrifugal washes.

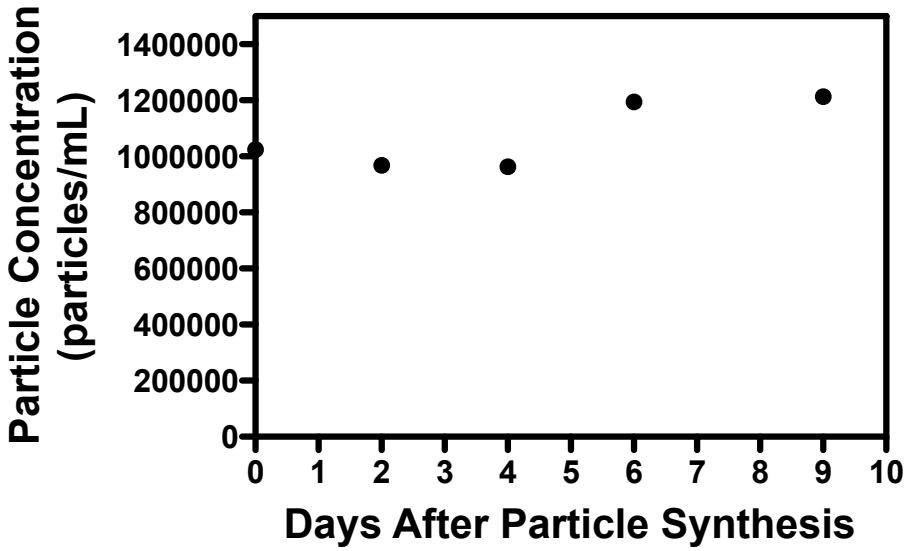

Figure 3.9 Polydisperse avidinylated-elastomeric particles (Sylgard 184) demonstrate stability overtime when suspended a protein-rich buffer (1X PBS with 0.1% BSA).

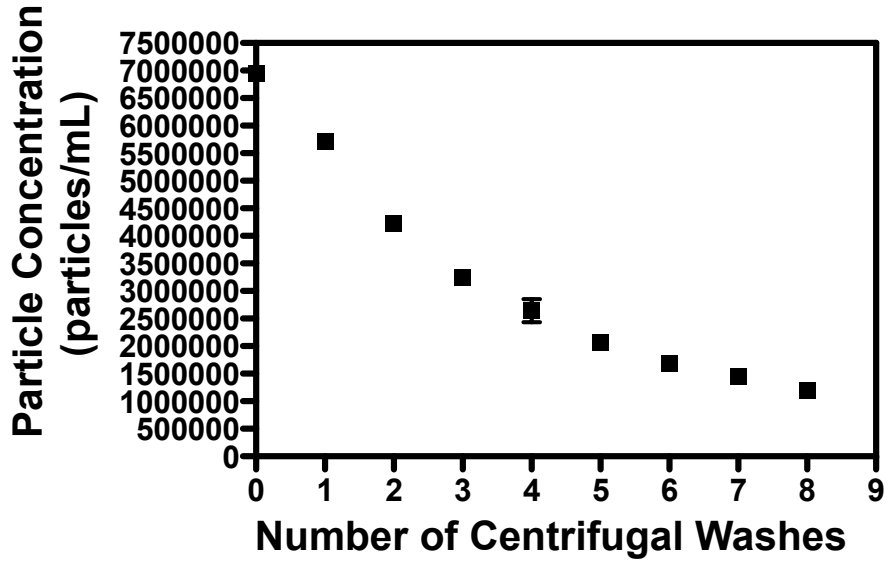

Figure 3.10 Polydisperse avidinylated-elastomeric particles (Sylgard 184) in 1X PBS (with 0.1% BSA) are lost during centrifugal washes (2900 x gravity @ 2 minutes) in polypropylene centrifuge tubes.

The significant particle losses during centrifugal washes could be explained by the density of Sylgard 184 (specific gravity ~ $\frac{density\ of\ Sylgard\ 184}{density\ of\ water}$ ~ 1.03); the similarities in densities between Sylgard 184 and the density of water make efficient recovery of elastomeric particles challenging; alternative methods to increase particle recovery during washing steps are necessitated.

To establish if significant particle aggregation was occurring during centrifugal washes (2900 x gravity at 2 minutes) forward scatter measurements were performed on resuspended avidinylated-elastomeric particles in a protein-rich solution (1X PBS with 0.1% BSA) using flow cytometry (Figure 3.11). The forward light scatter intensity of particles in suspension is a relative measure of particle size in which an increase in average scatter intensity typically (but not always) reflects an increase in average particle size. Prior to centrifugation the relative mean forward scatter intensity was ~ 683,658 intensity units; following the 1st centrifugal wash the mean forward scatter was ~ 707,294 units; and by the 7th wash the mean forward scatter was ~ 674,416 units. The lack of significant alteration in the mean forward scatter intensity measurements suggest that significant aggregation was not occurring during centrifugal washes of avidinylated-elastomeric particles suspended in a protein-rich solution; and thus the particle losses in Figure 3.8 were unlikely to be explained by particle aggregation..

To determine if prolonged time exposure to centrifugal forces might improve particle recovery, avidinylated-elastomeric particles in a protein-rich solution were centrifuged at varying time-lengths at a consistently-applied centrifugal force (2900 x gravity) (Figure 3.12).

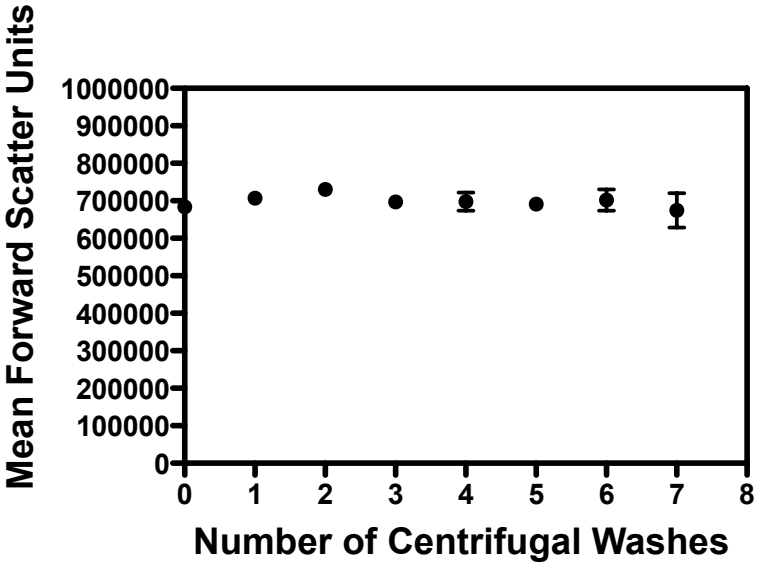

Figure 3.11 Polydisperse avidinylated-elastomeric particles (Sylgard 184) in 1X PBS (with 0.1% BSA) do not demonstrate appreciable changes in mean light scatter intensity during sequential centrifugal washes (2900 x gravity @ 2 minutes).

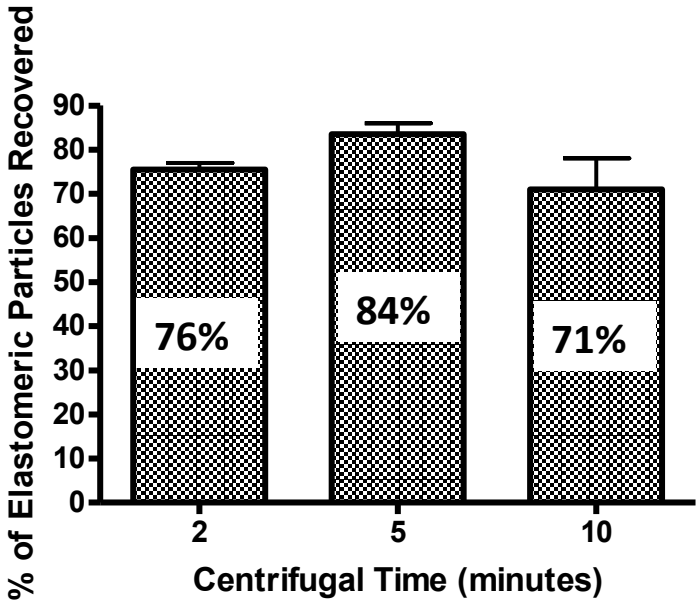

Figure 3.12 Bar graph illustrating effect of centrifugation time on particle recovery percentages of polydisperse avidinylated-elastomeric particles (Sylgard 184) in protein-rich solution (1X PBS with 0.1% BSA). Particles were centrifuged at 2900 x gravity.

Centrifugally-washing avidinylated elastomeric particles (~ 3.0 x 10^6 particles/mL) for 2 minutes followed by resuspension in the protein-rich solution resulted in a particle recovery of ~ 76%; 5 minutes resulted in 84%; and a 10 minute wash led to a 71% recovery of avidinylated-elastomeric particles. These results appear to indicate that the duration of centrifugal washes do not significantly alter the particle recovery percentage of avidinylated-elastomeric particles in a protein-rich solution (Figure 3.12).

Avidinylated-elastomeric particles were also centrifuged at different centrifugal forces (@ 5 minutes) to determine how the magnitude of the centrifugal force affects the particle recovery percentage (Figure 3.13). The results demonstrated a measurable increase in the particle recovery percentage as the centrifugal forces were increased. Avidinylated-elastomeric particles (~9.0 x 10^6 particles/mL) centrifuged at 700, 2900, and 6600 x gravity corresponded to a 78%, 88% and 95% particle recovery. These results indicate that good particle recovery can be achieved in less than 10 min by centrifugation at 6600 x gravity.

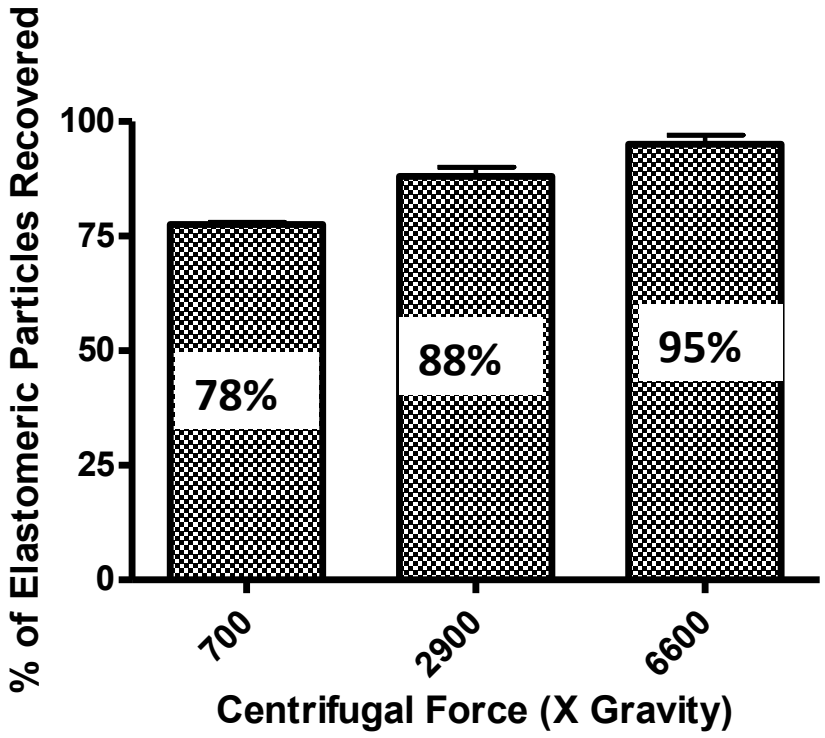

Figure 3.13 Bar graph illustrating how centrifuge force is affecting the particle recovery percentages of polydisperse avidinylated-elastomeric particles (Sylgard 184) in protein-rich solution (1X PBS with 0.1% BSA) during centrifugal washes performed for 5 minute durations.

Synthesis of Monodisperse Elastomeric Particles (Sylgard 184)

Monodisperse elastomeric particles were synthesized from Sylgard 184 at a 10:2 ratio of prepolymer (viscosity ~ 5000 cSt) to crosslinking agent (110 cSt), using a PDMS-based T-junction microfluidic device (Figure 2.14A). To ensure that the PDMS microchannels were hydrophilic, elastomeric droplet production was initiated immediately after the PDMS microfluidic template was plasma sealed to the glass microslide. Although monodisperse elastomeric droplets and particles were produced, the high viscosity (2209 cSt) resulting from the 10:2 ratio of prepolymer to crosslinking agent resulted in an exceedingly slow droplet rate (~ 1 droplet per second). To remedy the slow droplet rate, the viscosity of the Sylgard 184 was altered to a 6:4 ratio of prepolymer to crosslinking agent; thus resulting in a lowered viscosity (827 cSt). The lowered viscosity (827 cSt) resulted in an increase in droplet rate to 58 droplets per second; however droplet production was only possible for ~ 1-1.5 hours as the PDMS microchannels rapidly reverted back to a more hydrophobic state. The droplets that were collected were subsequently crosslinked to form elastomeric particles (Figure 2.14B) where the size distribution (Figure 2.14C) was used to derive a mean particle size of 22.88 μm, a standard deviation of ± 1.587 μm, and a coefficient of variation of 6.9%.

To modify the hydrophobic nature of PDMS microchannels and to increase the elastomeric droplet production time, PDMS microchannels were coated with a layer of silica using pre-established sol-gel chemistries followed by covalent attachment of a hydrophilic PEG-silane.[29]

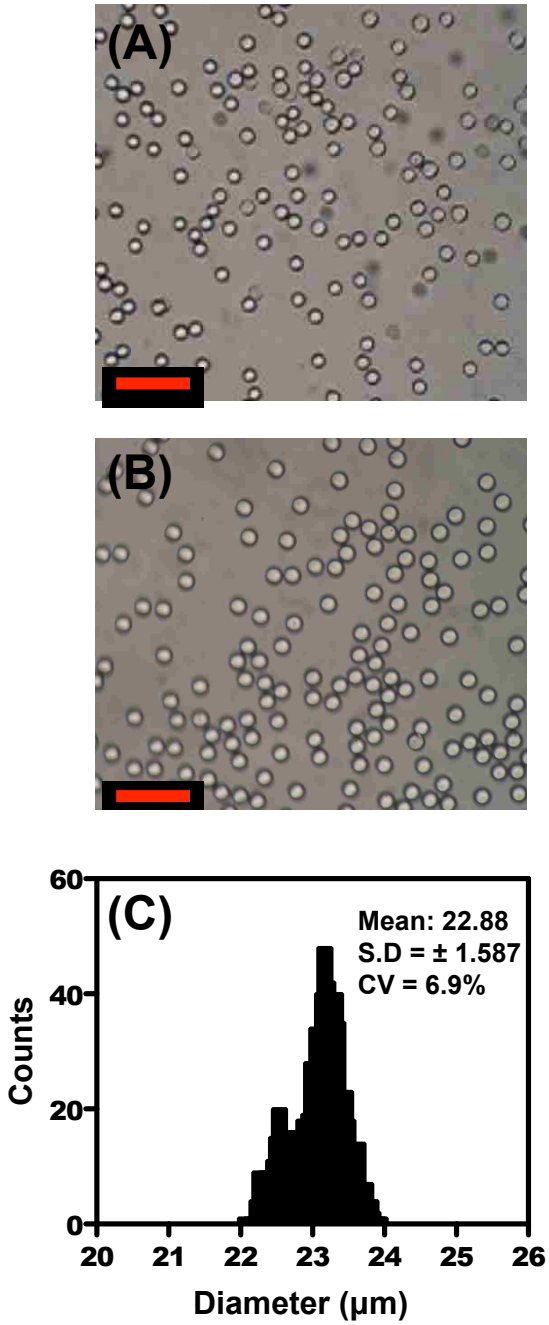

Figure 3.14 Elastomeric particles (Sylgard 184) with a narrowed size distribution were synthesized using a PDMS-based T-Junction microfluidic system without surfactant. (A) Bright field image of elastomeric particles synthesized from a 10:2 ratio of Sylgard 184 prepolymer to crosslinking agent (kinematic viscosity~ 2209 cSt). (B) Bright field image of elastomeric particles synthesized from a 6:4 ratio of Sylgard 184 prepolymer to crosslinking agent (viscosity~ 827 cSt) and (C) size histogram. Note: Red bar equals ~ 100 µm.

Attempts to coat freshly-sealed PDMS microchannels with a useable silica layer were unsuccessful, as the silica layer was excessively thick resulting in a high pressure buildup that restricted the flow of the organic PEG-silane solution. Adjustments to incubation times of the silica precursors in the microchannels could be used to modify silica layer thickness to allow less restricted flow of organic and aqueous solutions.

Alternative microfluidic systems were also pursued using glass capillary devices;[30] however flow rates of the continuous phase (ultra-pure water) and dispersed phase (10:2 ratio of prepolymer to crosslinking agent) that were within an extreme laminar flow profile ($Re << 1$) were not compatible with droplet production within the glass capillary device. The use of a lower viscosity PDMS blend, e.g., 6:4 ratio of prepolymer to crosslinking agent, may allow shearing and subsequent production of droplets.

Monodisperse elastomeric droplets (10:2 ratio of prepolymer to crosslinking agent) were also successfully produced using an emulsifying avidin protein (1μM) and a flow focusing microfluidic device (Figure 3.15A and B). This experiment was done as an attempt to produce droplets capable of binding biotinylated proteins. The size histogram (Figure 3.15C) indicated a mean droplet size of 40.10 μm; a standard deviation of ± 0.60; and a coefficient of variation of 1.5%. Although the droplets were extremely monodisperse (CV~1.5%) droplets with adsorbed avidin could not be converted into crosslinked elastomeric particles. Elastomeric droplets were clearly seen coalescing as they were being dried on a glass slide (Figure 3.15D); which was indicative of negligible crosslinking.

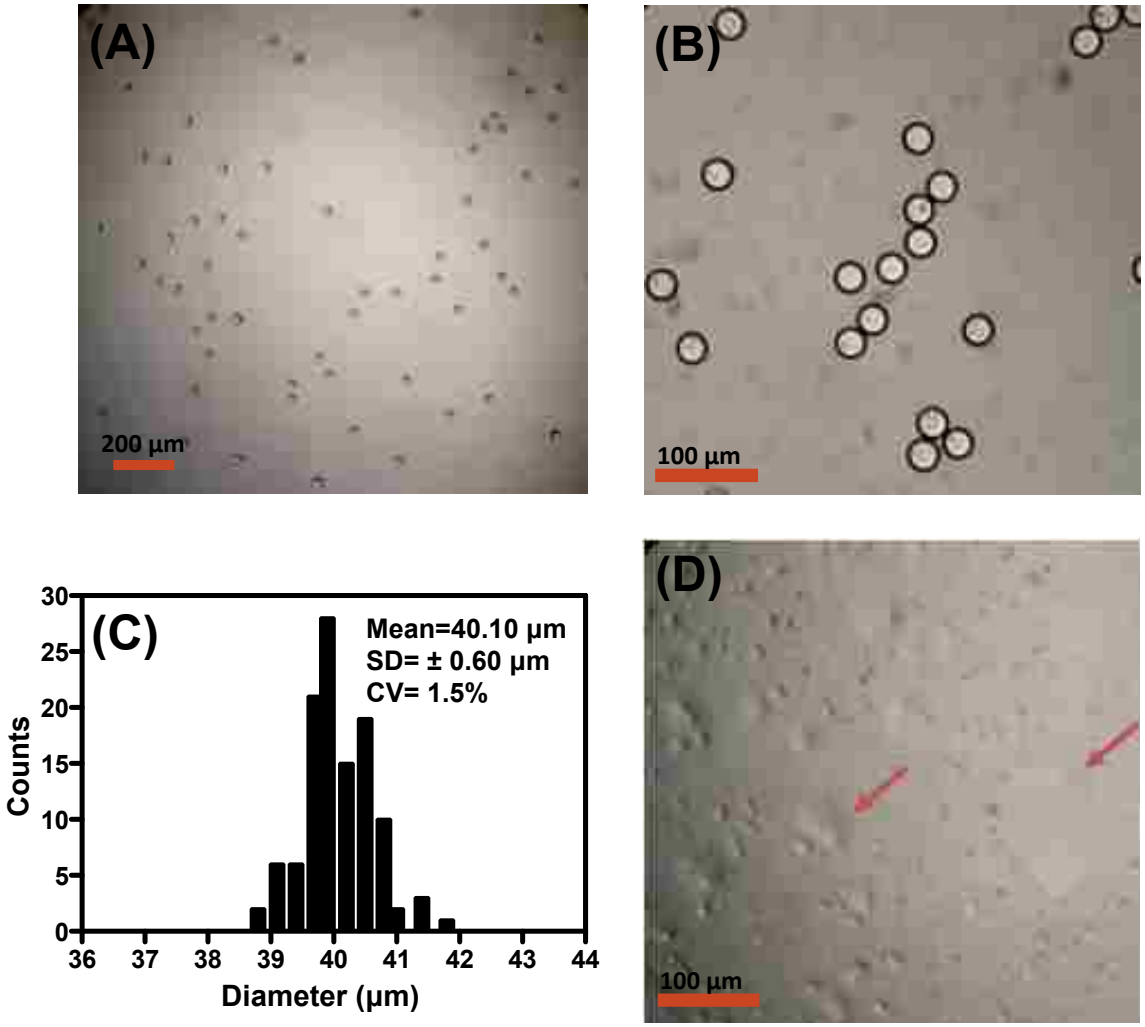

Figure 3.15 Monodisperse Elastomeric droplets (10:2 ratio of Sylgard 184 prepolymer to crosslinking agent) generated using a PDMS-based flow focusing device with an avidin protein as the emulsifying surfactant. Bright field images of elastomeric droplets at (A) 10x and (B) 20x objectives, and (C) size histogram. (D) Bright field image showing elastomeric droplets that have coalesced as they were being dried on a glass slide. Note: red arrows indicate coalescence of droplets.

Although the use of avidin protein as an emulsifying surfactant prevented elastomeric droplets from crosslinking, it does demonstrate potential for using protein as surfactant for the production of monodisperse elastomeric particles using microfluidic systems. In a separate series of experiments, bovine serum albumin (BSA) protein was successfully used to produce crosslinked monodisperse elastomeric particles. The reason that BSA but not avidin was permissive of crosslinking remains to be determined.

Synthesis of Polydisperse Elastomeric Particles (low molecular weight PDMS)

Polydisperse elastomeric particles were successfully synthesized using a lower molecular weight version of PDMS (specific gravity~0.97 and a viscosity ~ 450 cSt) with the bulk oil-in-water emulsion process in the absence of surfactant (Figure 3.16). To determine the amount of crosslinking agent required to produce crosslinked elastomeric particles, it was necessary to mix different amounts of crosslinking agent into the PDMS prepolymer prior to emulsification and thermal curing. After thermal curing, the emulsions made with different amounts of crosslinking agent were dried on glass slides and then imaged to determine if the elastomeric droplets had been converted into elastomeric particles.

Emulsions prepared with 9:1 or 7:3 ratio of PDMS prepolymer to crosslinking agent, coalesced immediately upon being dried on the glass slides (Figure 3.16A). Emulsions prepared with 5:5, 2.5:7.5, and 1.5:8.5 ratios showed no observable coalescence upon drying (Figures 3.16C,D, and E); therefore indicating that the elastomeric droplets, prepared from the bulk-emulsions, had been successfully converted into elastomeric particles upon being thermally cured.

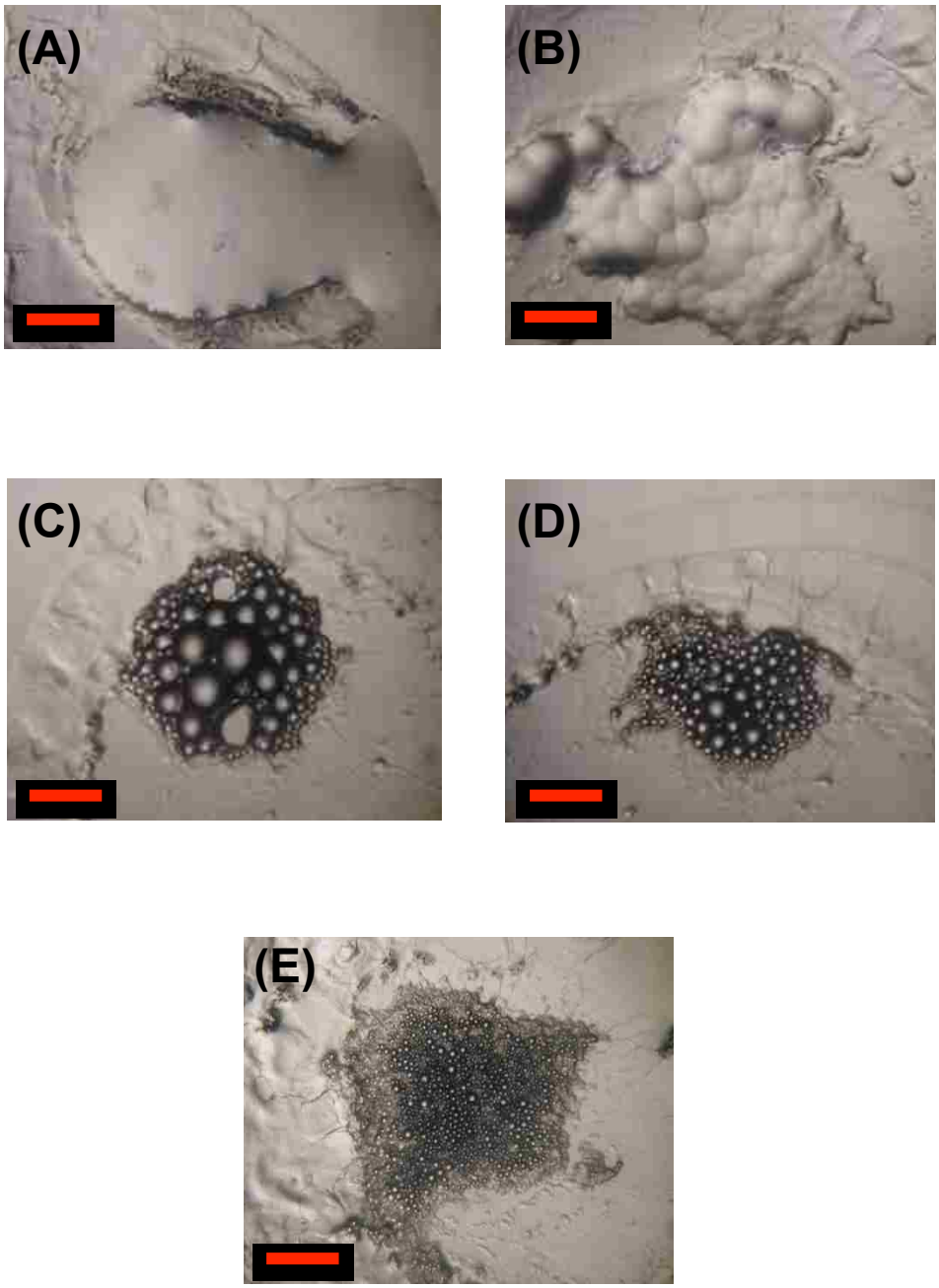

Figure 3.16 Polydisperse elastomeric particles can be synthesized from a low molecular weight PDMS elastomer (viscosity~450 cSt; specific gravity ~ 0.97) when the appropriate ratios of prepolymer to crosslinking agent are utilized. Elastomeric droplets/particles were produced using (A) 9:1, (B) 7:3, (C) 5:5, (D) 2.5:7.5, and (E) 1.5:8.5 ratios of prepolymer to crosslinking agent. All samples were dried on a glass slide prior to obtaining bright field images. Note: Red bar equals ~ 100 μm.

In the absence of quantitative data, based on visual observation of the images (Figure 3.13) it appears that the elastomeric particles are getting smaller as the crosslinking agent amount is increased. As more crosslinks are introduced into the crosslinked polymeric network, the low molecular weight PDMS prepolymers get pulled in tighter, resulting in stiffer (less compressible) and smaller particle sizes.

Synthesis of Monodisperse Elastomeric Particles (low molecular weight PDMS)

Synthesis of monodisperse elastomeric particles from low molecular weight PDMS was successfully performed using PDMS-based flow focusing and T-junction microfluidic devices with emulsifying surfactants (CTAB, SDS, and Pluronic F108). The bright field images (Figure 3.17 A,B, and C) indicate hexagonal packing of particles; indicative of extreme monodispersity. A flow rate of 5 μL/mL for the continuous phase and 0.08 μL for the dispersed phase allowed a droplet rate of ~400 droplets per second and a prolonged droplet production time of greater than 10 hours. This protocol would be suitable for scaled up production of elastomeric particles for bioassay applications. The use of a Pluronic F108 surfactant is advantageous in that it is biocompatible and non-toxic. Methodologies to functionalize the Pluronic F108 surfactant with a biotin moiety have been developed[28] and therefore make the use of Pluronic F108 surfactant an attractive emulsifying agent for the production of monodisperse elastomeric particles intended for use in biological applications (e.g., bioassays).

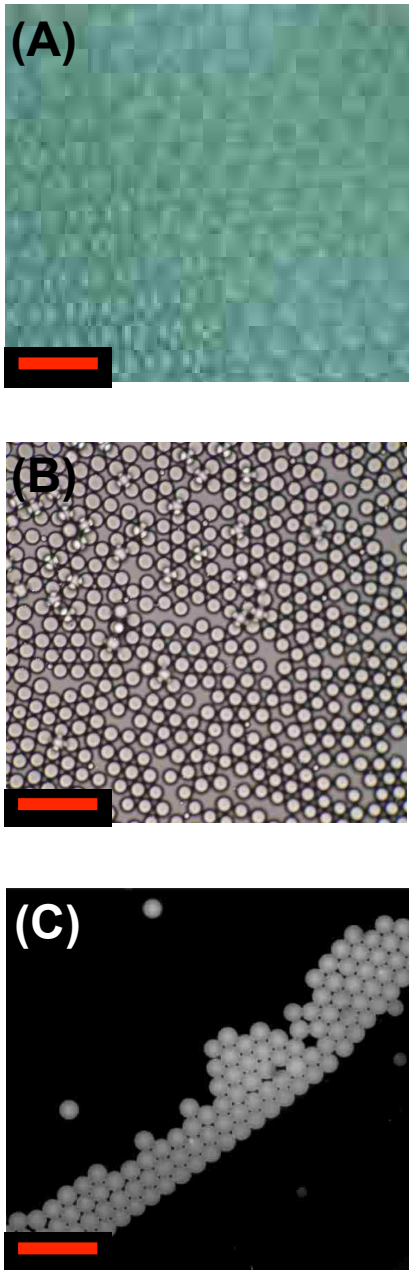

Figure 3.17 Monodisperse elastomeric particles synthesized from a low molecular weight PDMS elastomer (viscosity~450 cSt; specific gravity ~ 0.97) using PDMS-based microfluidic devices. Monodisperse elastomeric particles synthesized using (A) a flow focusing device in the presence of 0.1% CTAB surfactant and 20% glycerol; (B) a T-junction device in the presence of 0.5% SDS surfactant; and (C) a flow focusing device in the presence of 0.1% Pluronic F108 surfactant. Red bar equals ~ 100 μm.

Conclusions and Future Directions

Bulk emulsions and microfluidic systems can be successfully utilized in the synthesis of elastomeric particles from two varieties of PDMS (Sylgard 184 and low molecular weight PDMS). Monodisperse elastomeric particles can be successfully synthesized using microfluidic systems (PDMS-based flow focusing and T-junction microfluidic devices) and PDMS elastomers; however, there are limitations when the Sylgard 184 is used instead of the low molecular weight PDMS. To obtain a suitable droplet rate (~58 droplets per second), Sylgard 184 (specific gravity ~ 1.03) was used at a 6:4 ratio of prepolymer to crosslinking agent (viscosity ~ 827 cSt); this blend allowed the production of monodisperse elastomeric particles, but droplet production was only sustainable as long as the PDMS-based microchannels maintained a hydrophilic coating after plasma sealing. The rapid return of the PDMS microchannels to a hydrophobic state minimized the effectiveness of this system. The use of a low molecular weight PDMS elastomer (specific gravity ~ 0.97) appears to be an alternative approach that avoids this problem. In the presence of emulsifying surfactants (e.g., CTAB, SDS, and Pluronic F108) low molecular weight PDMS elastomer can be used to produce elastomeric droplets at a suitable rate of 400 droplets per second for at least 10 hours without interruption. A potentially promising approach for making such particles bioassay compatible would be to substitute a biotinylated version of the emulsifying Pluronic F108 as surfactant in the production process. The presence of endogenous biotin moieties would allow versatile adaptation of the particles to a variety of bioassay formats through use of appropriate avidin/biotin conjugation reagents.

References

1. Andriot, M.; Chao, S.; Colas, A.; Cray, S.; deBuyl, F.; DeGroot, J.; Dupont, A.; Easton, T.; Garaud, J.; Gerlach, E., Silicones in industrial applications. Nova Science Publishers, New York: **2009**; Vol. 84.

2. Colas, A.; Curtis, J., Silicone biomaterials: history and chemistry. *Biomaterials Science: An Introduction to Materials in Medicine. Amsterdam, Elsevier* **2004**, 80-86.

3. Sun, G.; Kappl, M.; Butt, H.-J., Confined polymer melts studied by atomic force microscopy. *Colloids and Surfaces A: Physicochemical and Engineering Aspects* **2004,** *250* (1), 203-209.

4. Shojaei-Zadeh, S.; Morris, J. F.; Couzis, A.; Maldarelli, C., Highly crosslinked poly (dimethylsiloxane) microbeads with uniformly dispersed quantum dot nanocrystals. *Journal of colloid and interface science* **2011,** *363* (1), 25-33.

5. Jiang, K.; Thomas, P. C.; Forry, S. P.; DeVoe, D. L.; Raghavan, S. R., Microfluidic synthesis of monodisperse PDMS microbeads as discrete oxygen sensors. *Soft Matter* **2012,** *8* (4), 923-926.

6. Esteves, A.; Brokken-Zijp, J.; Laven, J.; Huinink, H.; Reuvers, N.; Van, M., Influence of cross-linker concentration on the cross-linking of PDMS and the network structures formed. *Polymer* **2009,** *50* (16), 3955-3966.

7. Lisensky, G. C.; Campbell, D. J.; Beckman, K. J.; Calderon, C. E.; Doolan, P. W.; Ottosen, R. M.; Ellis, A. B., Replication and compression of surface structures with polydimethylsiloxane elastomer. *Journal of Chemical Education* **1999,** *76* (4), 537.

8. Lötters, J.; Olthuis, W.; Veltink, P.; Bergveld, P., The mechanical properties of the rubber elastic polymer polydimethylsiloxane for sensor applications. *Journal of Micromechanics and Microengineering* **1999,** *7* (3), 145.

9. Sia, S. K.; Whitesides, G. M., Microfluidic devices fabricated in poly (dimethylsiloxane) for biological studies. *Electrophoresis* **2003,** *24* (21), 3563-3576.

10. Wilder, E. A.; Guo, S.; Lin-Gibson, S.; Fasolka, M. J.; Stafford, C. M., Measuring the modulus of soft polymer networks via a buckling-based metrology. *Macromolecules* **2006,** *39* (12), 4138-4143.

11. Uchida, T.; Mills, K.; Kuo, C.-H.; Roh, W.; Tung, Y.-C.; Garner, A. L.; Koide, K.; Thouless, M.; Takayama, S., External compression-induced fracture patterning on the surface of poly (dimethylsiloxane) cubes and microspheres. *Langmuir* **2009,** *25* (5), 3102-3107.

12. Bibette, J.; Calderon, F. L.; Poulin, P., Emulsions: basic principles. *Reports on Progress in Physics* **1999,** *62* (6), 969.

13. Umbanhowar, P.; Prasad, V.; Weitz, D., Monodisperse emulsion generation via drop break off in a coflowing stream. *Langmuir* **2000,** *16* (2), 347-351.

14. Binks, B.P., Modern Aspects of Emulsion Science, in Modern Aspects of Emulsion Science. 1998, The Royal Society of Chemistry **1998**, 56-444.

15. Wilde, P., Interfaces: their role in foam and emulsion behaviour. *Current opinion in colloid & interface science* **2000,** *5* (3), 176-181.

16. Baret, J.-C.; Kleinschmidt, F.; El Harrak, A.; Griffiths, A. D., Kinetic aspects of emulsion stabilization by surfactants: a microfluidic analysis. *Langmuir* **2009,** *25* (11), 6088-6093.

17. Bancroft, W. D., The theory of emulsification, V. *The Journal of Physical Chemistry* **1913,** *17* (6), 501-519.

18. Walstra, P., Smulders, P.E. A., Emulsion Formation, In B.P. Binks (Ed.): Mordern Aspects of Emulsion Science. Royal Society of Chemistry **1998**, 56.

19. Shah, R. K.; Shum, H. C.; Rowat, A. C.; Lee, D.; Agresti, J. J.; Utada, A. S.; Chu, L.-Y.; Kim, J.-W.; Fernandez-Nieves, A.; Martinez, C. J., Designer emulsions using microfluidics. *Materials Today* **2008,** *11* (4), 18-27.

20. Nie, Z.; Seo, M.; Xu, S.; Lewis, P. C.; Mok, M.; Kumacheva, E.; Whitesides, G. M.; Garstecki, P.; Stone, H. A., Emulsification in a microfluidic flow-focusing device: effect of the viscosities of the liquids. *Microfluidics and nanofluidics* **2008,** *5* (5), 585-594.

21. Gu, H.; Duits, M. H.; Mugele, F., Droplets formation and merging in two-phase flow microfluidics. *International journal of molecular sciences* **2011,** *12* (4), 2572-2597.

22. Teh, S.-Y.; Lin, R.; Hung, L.-H.; Lee, A. P., Droplet microfluidics. *Lab Chip* **2008,** *8* (2), 198-220.

23. Atencia, J.; Beebe, D. J., Controlled microfluidic interfaces. *Nature* **2004,** *437* (7059), 648-655.

24. Nisisako, T.; Okushima, S.; Torii, T., Controlled formulation of monodisperse double emulsions in a multiple-phase microfluidic system. *Soft Matter* **2005,** *1* (1), 23-27.

25. McDonald, J. C.; Whitesides, G. M., Poly (dimethylsiloxane) as a material for fabricating microfluidic devices. *Accounts of chemical research* **2002,** *35* (7), 491-499.

26. Anna, S. L.; Bontoux, N.; Stone, H. A., Formation of dispersions using "flow focusing" in microchannels. *Applied physics letters* **2003,** *82* (3), 364-366.

27. Xu, S.; Nie, Z.; Seo, M.; Lewis, P.; Kumacheva, E.; Stone, H. A.; Garstecki, P.; Weibel, D. B.; Gitlin, I.; Whitesides, G. M., Generation of monodisperse particles by using microfluidics: control over size, shape, and composition. *Angewandte Chemie* **2004,** *117* (5), 734-738.

28. Johnson, L.M.; Gao, L.; Shields, C. W.; Smith, M.; Efimenko, K.; Cushing, K.; Genzer, J.; López, G. P., Elastomeric microparticles for acoustic mediated bioseparations. *Submitted to Journal of Nanobiotechnology* **2013**.

29. Sui, G.; Wang, J.; Lee, C.-C.; Lu, W.; Lee, S. P.; Leyton, J. V.; Wu, A. M.; Tseng, H.-R., Solution-phase surface modification in intact poly (dimethylsiloxane) microfluidic channels. *Analytical chemistry* **2006,** *78* (15), 5543-5551.

30. Vladisavljević, G. T.; Henry, J.; Duncanson, W. J.; Shum, H. C.; Weitz, D. A., Fabrication of Biodegradable Poly (Lactic Acid) Particles in Flow-Focusing Glass Capillary Devices. In *UK Colloids 2011*, Springer: 2012; pp 111-114.

Chapter 4 Elastomeric Particles Biofunctionalized and Used in Flow Cytometry-Based Assays

Biofunctionalization of Polydimethylsiloxane (PDMS)

Functionalization of polydimethylsiloxane (PDMS) surfaces can be accomplished by 1) chemical modification, which can lead to covalent attachments of bio(molecules) to the surface of PDMS; or 2) physical adsorption, in which biomolecules can be non-specifically adsorbed onto the surface. Chemical modification (i.e., covalent coupling)[1] of the PDMS surface can be a stable irreversible method for functionalizing PDMS surfaces (e.g., microfluidic microchannels) for assay activity, but the process can be 1) complicated, i.e., -there could be multiple steps involved in the chemical modification process;[2-4] 2) time consuming; and 3) expensive in regards to purchasing many of the bio-reagents needed for the process. The use of physical adsorption (also referred to as non-specific adsorption) of (bio)molecules (e.g., avidin, IgG, Protein A/G) to the surface of PDMS[5,6] can be simple, rapid, and require few selective bio-reagents. However, the use of physical adsorption as a method to functionalize PDMS surfaces is reversible, and may limit the functional activity of the adsorbed (bio)molecules. Upon non-specific adsorption of biomolecules to the surface of hydrophobic PDMS surfaces, the adsorbed biomolecules can undergo a structural relaxation and become denatured or partially denatured-leading to a partial loss of activity.[7]

As a result of chemical modification of PDMS taking multiple steps, consuming multiple reagents, and having the potential of being a time consuming process, physical adsorption can quite often become an attractive method to functionalize PDMS substrates for proof-of-concept purposes. In this dissertation we define physical adsorption as the

process where protein (e.g., avidin, BSA) or amphiphilic molecules, detergents such as cetyltrimethylammonium bromide (CTAB), non-specifically adhere to a solid surface (e.g., polystyrene, PDMS); the mechanism for this non-specific attachment can be based on Van der Walls forces, hydrophobic interactions, electrostatic interactions, and hydrogen bonding between the adsorbed (bio)molecules and the substrate.[7,8]

The efficiency with which protein(s) adsorb onto substrates can be dependent on 1) the physical and chemical properties of the proteins, i.e., such as their shape: globular (e.g., bovine serum albumin: BSA) versus rod-like (e.g., fibrinogen); 2) the isoelectric point or charge (e.g., negative or positive) of the proteins, and 3) the presence of chemical groups on the proteins that render them more hydrophobic or capable of hydrogen bonding with chemical groups on the substrate.[7] Physical and chemical properties of the substrate (e.g., topography: curvature and roughness of surface, size, and chemical groups) also affect the adsorption efficiency along with the conformation and orientation of the adsorbed proteins.[7,9,10]

It has been proposed that initial adsorption of bovine serum albumin (BSA, a globular protein) and fibrinogen (rod-like protein) to hydrophobic ($-CH_3$) and hydrophilic surfaces (-OH) reaches equilibrium (or saturation) within the first hour of exposure with saturating concentrations; after this time there are very few reported conformational changes detected at the surface of adsorption using spectroscopic methods.[7] Published reports have also demonstrated that BSA and fibrinogen adsorptions are more favorable on hydrophobic than hydrophilic surfaces.[7] This is indicated by the affinity constants for BSA adsorption on hydrophobic (K_a=5.4 M^{-1}) and hydrophilic surfaces (K_a=5.3 M^{-1}) and for fibrinogen adsorption on hydrophobic (K_a=36 M^{-1}) and hydrophilic surfaces (K_a=10.9

M^{-1}).[7] The lower affinity constants of protein adsorption to hydrophilic (-COOH, -C-OH) surfaces may simply reflect weak hydrogen bonding and ionic interactions between the hydrophilic surface and nearby proteins.[7]

Investigations on how the surface curvature affects adsorption of proteins onto solid-phase substrates have also been reported. The smaller the microparticles are, or the greater the curvature is, the greater the binding affinity of BSA (or fibrinogen) will be for solid-phase surfaces.[7] It has also been reported that the greater the curvature is the greater structural stability will be for BSA.[9,10]

The mechanism of protein adsorption onto hydrophobic surfaces appears to be dominated by hydrophobic interactions.[7,8] The adsorption of BSA is a 1-step process where BSA rapidly adsorbs to the surface (Figure 4.1).[7] This adsorption process occurs through hydrophobic surface interactions from the outer layer and the inner core of the protein. These hydrophobic interactions may cause the BSA protein to undergo partial denaturation; thus losing some of its structural integrity and shape, i.e., undergoing structural deformation as it strongly adsorbs to the hydrophobic surface (Figure 4.1).[7] Fibrinogen, by contrast, uses a multistep approach when adsorbed onto hydrophobic surfaces at high concentrations.[7] The process consists of the initial protein adsorption followed by rearrangement of the adsorbed proteins to form a tight, ordered monolayer on top of the hydrophobic surface. The fibrinogen protein rearrangement may be driven by increased hydrophobic interactions as the long axes of the proteins become aligned parallel to each other (Figure 4.1).[7]

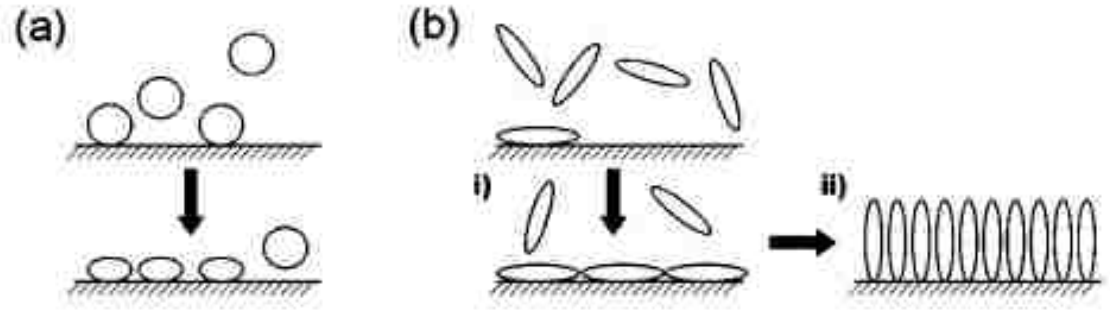

Figure 4.1 A schematic to show adsorption of (a) a globular protein (e.g., BSA) whose conformation may become distorted on interaction with the surface and (b) a rod-like protein that undergoes a multistage adsorption process where (i) initially the protein adsorbs with its long axis parallel to the surface and then (ii) rearrangement occurs to increase protein-protein interaction and surface concentration of protein.[7]

It is presumed that most proteins adsorb onto hydrophobic surfaces following one of the above-mentioned adsorption mechanism (Figure 4.1). Avidin protein is a globular protein with a molecular mass of ~ 66,000 kilodaltons (kDa). As a result of avidin having a similar shape (globular) and molecular mass to BSA, it could be presumed that avidin adsorbs onto hydrophobic PDMS surfaces using an adsorption mechanism similar to BSA. It can also be predicted that avidin adsorbs onto hydrophobic surfaces (CH_3) with a similar binding affinity constant as BSA (5.4 M^{-1}).

Avidin adsorption on PDMS surfaces has not been thoroughly investigated, but avidin has been shown to reversibly adsorb onto hydrophobic PDMS surfaces.[11] Devel et al, reported that avidin adsorbed onto hydrophobic surfaces (-CH_3) can be removed by performing a wash with a solution containing a non-ionic surfactant (octyl-β-D-glucopyranoside), which was consistent with a prevalence of hydrophobic interactions.[12]

Once avidin adsorption is complete, hydrophobic PDMS surfaces can be further functionalized by attachment of biotinylated biomolecules (e.g., small molecules, oligomers of DNA, polysaccharides).[13]

Avidin (or streptavidin) is a tetrameric protein with 4 biotin-binding subunits that are capable of being used for biotinylated biomolecule attachment (Figure 4.1). A plethora of biotinylated biomolecules (e.g., biotinylated mouse anti human prostate specific antigen: PSA) are commercially available and can be delivered in a ready-to-use format. Physical adsorption of avidin onto hydrophobic PDMS surfaces ($-CH_3$) has been used previously as a simple and rapid method to functionalize PDMS based microfluidic networks for bioassay applications.[13] Avidin protein has a high isoelectric point (PI~10.1), and along with its attached sugar molecules (mannose and N-glucosamine),[14] gives avidin a high propensity for non-specific binding to solid phase surfaces.[15] Avidin, contains a biotin-binding pocket on each of its 4 subunits; thus each avidin protein is capable of binding 4 biotins. The association constant (K_a) for the avidin/biotin complex is approximately 10^{15} M^{-1},[15] and thus makes attachment of biotinylated biomolecules to avidinylated PDMS surfaces a simple and straightforward process.[3,16,17]

Flow Cytometry-Based Assays

Flow cytometry was originally used to make measurements on biological cells (e.g., blood cells) while commercially-available microbeads were primarily used for calibration purposes; however, over the past several decades flow cytometry has become a prominent tool in bead-based assays that are used to quantify soluble protein markers. Enzyme linked immunosorbent assay (ELISA) is the standard method for quantifying soluble proteins, but there are several disadvantages in ELISA that can be improved upon

by using bead-based flow cytometry assays. ELISA only allows one type of protein assay to be performed at a time, requires multiple washing steps, and is a relatively low throughput method. By contrast, bead-based flow cytometry assays can be performed in a multiplexed format, can be made high-throughput through elimination of washing steps, and allows measurements to be performed on thousands of beads per second for improved statistical evaluation.

In this dissertation chapter, we focus on the use of non-specific adsorption of an avidin (or streptavidin) protein as a method for functionalizing PDMS-based elastomeric particles. We demonstrate that 1) avidin (or streptavidin) protein can be successfully adsorbed onto the hydrophobic surface of elastomeric particles; 2) that avidinylated-elastomeric particles can be further functionalized with a biotinylated-monoclonal antibody; and 3) that functionalized elastomeric capture microparticles (ECμPs) can be successfully used in homogeneous (no wash) assays where ligand capturing is performed in high protein backgrounds prior to flow cytometry analysis.

Materials and Methods

Synthesis of Elastomeric Particles

Synthesis of Polydisperse Elastomeric Particles

Sylgard 184 (specific gravity ~ 1.03) (1 g, at 10:2 ratio of PDMS prepolymer to crosslinking agent) or low molecular weight PDMS (specific gravity ~ 0.97) (1 g, at 1:1 ratio of PDMS prepolymer to crosslinking agent) (Dow Corning Corp., Midland, MI) were emulsified in 10 mL of ultrapure water (18.2 MΩ•cm @ 25 °C; Synergy®, EMD Millipore) using a homogenizer (Power Gen 125, Fisher Scientific) set at 6,000 RPM for ~ 60 seconds. The elastomeric droplets, with crosslinking agent, were cured at 100 °C for

~ 1 hour to form crosslinked elastomeric particles. Elastomeric particles were imaged using bright field microscopy (BH-2, Olympus) and a 4300 cool pix camera (Nikon). The scale bar was calibrated based on standardized monodisperse particles (mean diameter = 30.1 μm; standard deviation = ± 2.1 μm; and a coefficient of variation = 6.6%) (Thermo Scientific).

Synthesis of Monodisperse Elastomeric Particles

Sylgard 184 (6:4 ratio of PDMS prepolymer to curing agent) was used to form PDMS-based elastomeric droplets in a PDMS-based T-junction microfluidic device. The continuous phase contained ultrapure water (18.2 MΩ•cm @ 25 °C; Synergy®, EMD Millipore) that was filtered with a 0.22 μm pore sized Acrodisc® syringe filter (PALL Corp., Port Washington, NY). To help prevent droplets from wetting the micro channel walls, the continuous phase was first injected using a syringe pump (Nexus 3000, Chemyx Inc. Stafford, TX) at a flow rate of 5-13 μL/min, into the freshly sealed microfluidic device. The dispersed phase (Sylgard 184) was then injected into the microfluidic device using a syringe pump (Nexus 3000, Chemyx Inc. Stafford, TX) at a flow rate of 0.67 μL/min. Monodisperse elastomeric droplets were then collected off chip and cured in an oven (Model 1321F, VWR International, Cornelius Oregon) overnight at 70 °C.

Functionalization of Polydisperse Elastomeric Particles

Avidin Adsorption

Polydisperse elastomeric particles (2.5 x 10^7 particle/mL) from Sylgard 184 (10:2 ratio of prepolymer to crosslinking agent) and low molecular weight PDMS (1:1 ratio of prepolymer to crosslinking agent) were incubated in a 1 μM avidin-FITC (Molecular

Probes, Eugene, Oregon) solution in 1 mL of 1X PBS for 30 minutes at room temperature with continuous rocking. Elastomeric particle solutions were subsequently centrifugally-washed (2900 x gravity at 2 minutes) and then imaged using an epifluorescence microscope (Zeiss Axio Imager) and a Luca S EMCCD camera (Andor Technology, Belfast N., Ireland) with Andor imaging software (Andor-Solis) and an inverted fluorescence microscope (Zeiss Axiotron; model: AXT03) with a Hitachi CCD digital camera (model: KPD591U).

Adsorption Studies

Polydisperse elastomeric particles (2.5 x 10^7 particles/mL) (10:2 ratio of Sylgard 184 prepolymer to crosslinking agent) were incubated in a 1 μM avidin-FITC solution in a total volume of 1 mL of 1X PBS for 30 minutes at room temperature with continuous rocking. The elastomeric particles with the adsorbed avidin-FITC were then analyzed with flow cytometry and then centrifuged 4 x sequentially for 5 minutes at different centrifugal forces (700, 2900, 6000, and 14,000 x gravity). After centrifugation and gentle removal of the supernatant, the elastomeric particles were resuspended in a 1X PBS (with 0.1% BSA) solution followed by flow cytometry analysis. Flow cytometry analysis was performed after every centrifugal wash/resuspension cycle.

Polydisperse elastomeric particles (1.0 x 10^7 particles/mL) (10:2 ratio of Sylgard 184 prepolymer to crosslinking agent) were incubated with 30 nM streptavidin-phycoerythrin (PE) (Invitrogen, Eugene, Oregon) or 1 μM unconjugated avidin protein (Molecular Probes, Eugene, Oregon) in 500 μL of 1X PBS at room temperature with continuous rocking for 30 minutes. Elastomeric particles with adsorbed streptavidin-PE were then centrifugally washed (2900 x gravity for 5 mins) then analyzed using flow

cytometry (Accuri C6). Elastomeric particles (~5.0 x 10^6 particle/mL) with streptavidin-PE were then incubated in 1 mL of PBS with 0.003% tween 20 or 0.1% bovine serum albumin (BSA) (Sigma-Aldrich) for ~ 30 minutes at room temperature with continuous rocking. Samples were then centrifugally washed and analyzed with flow cytometry. Elastomeric particles (5.0 x 10^6 particles/mL) with adsorbed avidin protein were incubated with a 100 nM solution of BSA conjugated to AlexaFluor-647 (Invitrogen, Eugene, Oregon) in 1 mL of 1X PBS for 30 minutes at room temperature with continuous rocking. Samples were then centrifugally washed and analyzed using flow cytometry.

Avidin and Streptavidin Titrations

Polydisperse elastomeric particles (2.5 x 10^7 particles/mL) (10:2 ratio of Sylgard 184 prepolymer to crosslinking agent) were incubated with different concentrations of avidin-FITC (0, 20, 40, 80, 100 and 1000 nM) and streptavidin AlexaFluor-647 (Invitrogen, Eugene, Oregon) (0, 20, 40, 80, and 100 nM) in 1 mL of 1X PBS for 30 minutes at room temperature at continuous rocking. Samples were then centrifugally-washed (2900 x gravity for 5 minutes) and then analyzed using flow cytometry (Accuri C6).

IgG Titration

Polydisperse elastomeric particles (2.5 x 10^7 particle/mL) were incubated in 1 μM of unconjugated avidin (Molecular Probes, Eugene, Oregon) in a total volume of 1 mL of 1X PBS for 30 minutes at room temperature with continuous rocking. Avidinylated-elastomeric particles were then centrifugally-washed (2900 x gravity for 5 minutes) and resuspended in 1 mL of the washing blocking buffer (1X PBS with 0.1% BSA) where they were incubated for 30 minutes at room temperature with continuous

rocking. The avidinylated-elastomeric particles (5.0 x 10^6 particle/mL) in 1 mL of 1X PBS were then incubated with varying concentrations (0, 2, 4, 6, and 8 nM) of the biotinylated mouse anti human PSA monoclonal IgG (Abcam, Cambridge, MA) for 30 minutes at room temperature with continuous rocking. Elastomeric capture microparticles (ECμPs) were then centrifugally-washed and resuspended in 500 μL of the washing blocking buffer after which the samples were incubated with a 7 nM solution of goat anti mouse IgG-phycoerythrin (PE) (Abcam, Cambridge, MA) for 30 minutes at room temperature with continuous rocking. The elastomeric particles were then analyzed using flow cytometry.

Prostate Specific Antigen (PSA) Titrations (no wash)

Five x 10^5 ECμPs –elastomeric particles functionalized with mouse anti-human PSA monoclonal antibodies (HyTest Inc., Turku, Finland)– were incubated with different concentrations (0, 1, 5, 10, 20, 30 nM) of prostate specific antigen (PSA) (Meridian Life Sciences Inc., Memphis, TN) in 200 μL (or 20 μL) of aqueous media (1X PBS with 1 mg/mL of BSA and 10% human plasma diluted with PBS containing 1 mg/mL of BSA) for 30 minutes with continuous rocking at room temperature. Without washing, enough mouse anti-human PSA monoclonal antibody-FITC (detection antibody) (HyTest Inc., Turku, Finland) was added to make a 1 nM solution that was incubated for 30 minutes with rocking at room temperature. The ECμPs were then analyzed with an Accuri C6 flow cytometer without washing. All bioassay data was fitted to a one-site binding curve with the following equation, $Y = \frac{F_{max}*x}{K_d+x}$ using PRISM (Graph Pad) version 5.0b. The dependent variable (Y) is the median fluorescence intensity (MFI, y-axis), the

independent variable (x) is the ligand analyte concentration (x-axis), K_d is the dissociation constant and F_{max} is the maximum MFI.

Functionalization of Monodisperse Elastomeric Particles

Monodisperse elastomeric microparticles (~10^5 particles/mL) were incubated in 1 μM avidin (Molecular Probes, Eugene, Oregon) or streptavidin-Alexa Fluor® 647 conjugate (Invitrogen, Eugene, Oregon) in 1X PBS for 30 minutes at room temperature with continuous rocking. Elastomeric particles were then centrifugally washed (1200 x gravity for 15 minutes). The supernatant was gently removed and the particles were then resuspended in the washing/blocking buffer (1X PBS with 0.1 % BSA). A biotinylated mouse anti human high density lipoprotein (HDL) monoclonal antibody (Abcam, Cambridge, MA) was then added to make a ~ 7 nM solution; the solution was incubated for 30 minutes at room temperature with continuous rocking. Elastomeric capture microparticles (ECμPs) were then centrifugally washed and resuspended in the washing/blocking buffer. Detection of the attached monoclonal antibody was performed by incubating ECμPs in a 7 nM solution of goat anti mouse IgG-phycoerythrin (PE) (Abcam, Cambridge, MA) for 30 minutes at room temperature with continuous rocking followed by flow cytometry analysis.

Flow Cytometry Analysis

An Accuri C6 flow cytometer (BD Biosciences) was used for all flow cytometry analyses. Green fluorescence (e.g., FITC) and orange fluorescence (e.g., PE) of particles were excited at 488 nm and detected at 530 nm ± 40 nm and 580 ± 40 nm, respectively. Red fluorescence of Alexa-640 was excited at 635 nm and detected at 675 ± 25 nm.

Fluorescence and light scatter intensities were recorded as arbitrary units on a relative scale ranging from 10 to 6,500,000.

Results

The hydrophobic surface of PDMS-based materials (e.g., PDMS-based microfluidics) allows for the non-specific adsorption of proteins. Generally this has been interpreted as a negative attribute associated with PDMS. In this dissertation report, we can demonstrate that it is possible to utilize the natural biofouling nature of PDMS materials to functionalize PDMS-based elastomeric particles using the non-specific adsorption of avidin protein (Figure 4.2) followed by further functionalization via attachment of biotinylated biomolecules.

Figure 4.2 Non-specific adsorption of avidin protein onto the hydrophobic surface of elastomeric particles.

Functionalization of Polydisperse Elastomeric Particles

Avidin Adsorption

Polydisperse elastomeric particles synthesized from PDMS-based elastomers using the bulk-emulsion process in the absence of surfactant, were functionalized using non-specific adsorption of avidin-FITC (Figure 4.3). The fluorescent images indicate that a large molecular weight PDMS elastomer (10:2 ratio of Sylgard 184 prepolymer to

crosslinking agent) (Figure 4.3A) along with a low molecular weight PDMS elastomer (1:1 ratio of low molecular weight PDMS prepolymer to crosslinking agent) (Figure 4.3B) can be easily functionalized with non-specific avidin adsorption.

Adsorption Studies

The adsorption of avidin protein to the hydrophobic surface of polydisperse elastomeric particles (Sylgard 184) resulted in a strong attachment that resisted desorption under the influence of strong shear forces that were generated via centrifugation. The synthesized elastomeric particles (~2.5 x 10^7 particles/mL) that were initially analyzed with flow cytometry showed a median fluorescence intensity (MFI) of 252 (Figure 4.4). Once avidin-FITC adsorption was performed on the elastomeric particles, the MFI increased to 6,962 (Figure 4.4). After performing a centrifugal wash at 700 x gravity in the washing blocking buffer (1X PBS with 0.1% BSA) the MFI of the particles was 9,605; the subsequent centrifugal-washes on the same sample in the washing blocking buffer were performed at 2900, 6600, and 14000 x gravity demonstrated MFIs of 9,412, 8,833, and 9,598, respectively (Figure 4.4). These results demonstrated no appreciable loss of fluorescence on the measured particles; thus indicating that the adsorbed avidin-FITC was not being removed from the elastomeric particles during centrifugal-washes performed at high centrifugal forces.

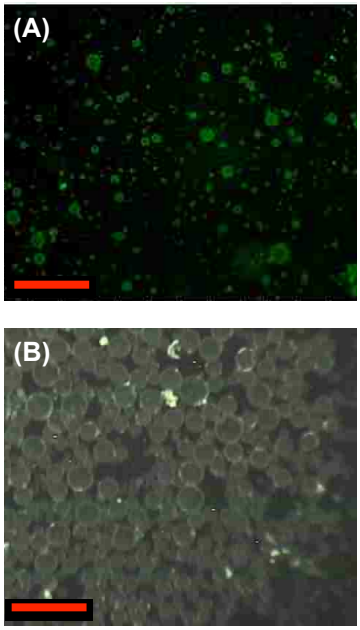

Figure 4.3 Non-specific adsorption of avidin-FITC protein onto polydisperse elastomeric particles synthesized from (A) Sylgard 184 and (B) low molecular weight PDMS. Note: Red bar equals ~ 100 μm

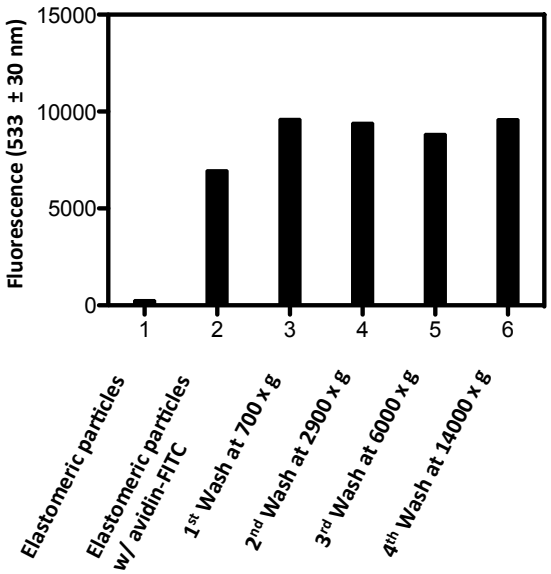

Figure 4.4 Avidin-FITC maintains non-specific adsorption to the surface of polydisperse elastomeric particles (Sylgard 184) subsequent to multiple washes involving high centrifugal forces.

To establish if surfactants (detergents) were capable of removing adsorbed protein from the surface of polydisperse elastomeric particles (Sylgard 184), elastomeric particles (~5.0 x 10^6 particle/mL) with adsorbed streptavidin-PE were incubated with a 0.003% tween 20 solution. The elastomeric particles were centrifugally washed and then analyzed with flow cytometry where the particles were identified and gated for fluorescence analysis on the basis of their light scattering distribution profile (forward scatter versus side scatter plot) (Figure 4.5A). The initial MFI of the elastomeric particles with adsorbed streptavidin-PE was 17,792 (Figure 4.5B). Once the elastomeric particles with adsorbed streptavidin-PE were incubated with a solution of 0.003% tween 20 and centrifugally washed, the MFI plummeted to 479 (Figure 4.5B); indicative that the tween 20 had removed a significant amount of the adsorbed streptavidin-PE from the surface of the elastomeric particles.

To evaluate the affects of incubating protein-functionalized elastomeric particles in the presence of other soluble proteins, elastomeric particles (5.0 x 10^6 particles/mL) with adsorbed streptavidin-PE were incubated with a solution of 0.1% BSA and then centrifugally washed. The initial MFI of the elastomeric particles with adsorbed streptavidin-PE was 13,078 (Figure 4.5C). Once the elastomeric particles with adsorbed streptavidin-PE were incubated with a solution of 0.1% BSA the particles displayed a MFI value of 13,163 (Figure 4.5C); indicative that the soluble BSA protein does not remove the adsorbed streptavidin-PE from the surface of the elastomeric particles.

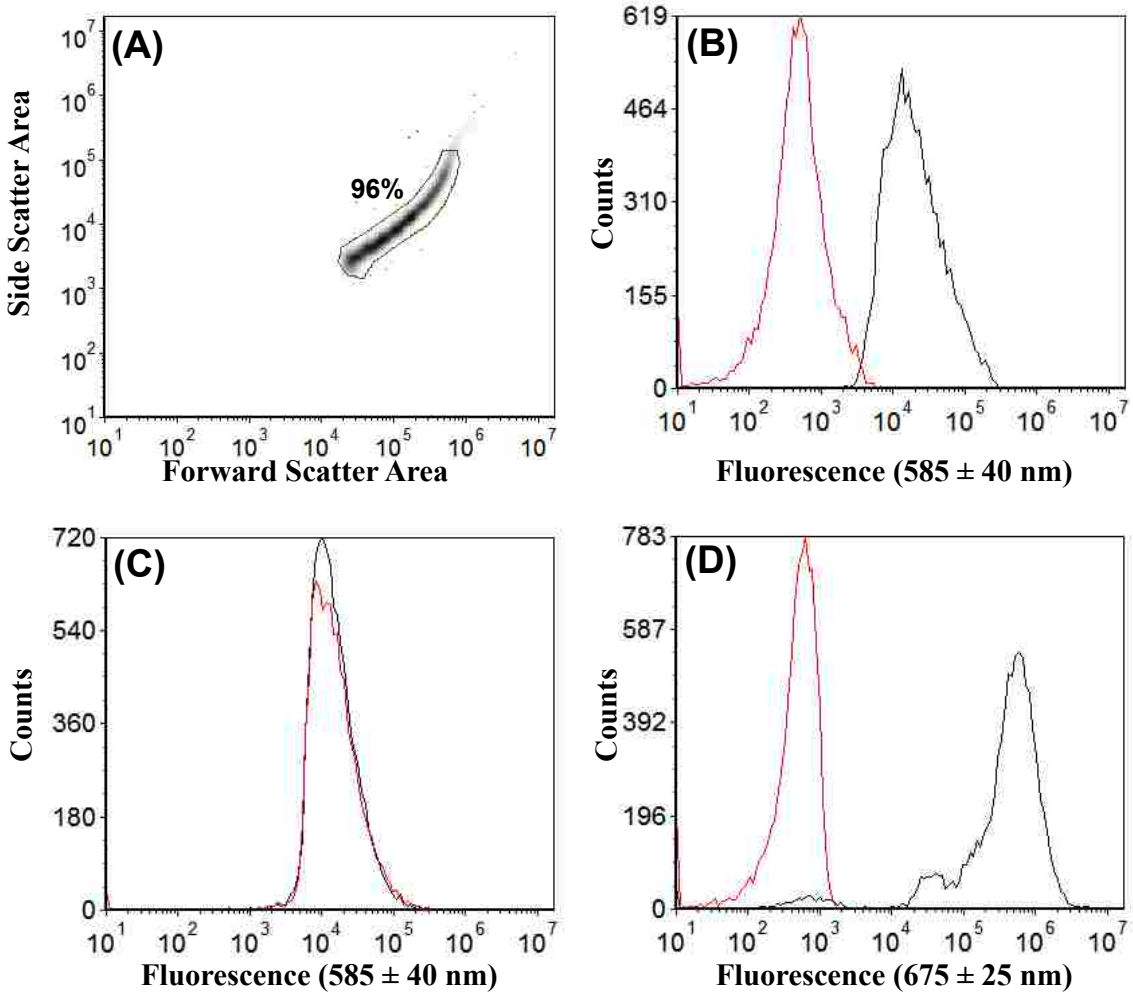

Figure 4.5 Protein non-specifically adsorbs to the hydrophobic surface of polydisperse elastomeric particles (Sylgard 184). (A) A density scatter plot (forward scatter versus side scatter) was used to identify elastomeric particles. (B) Elastomeric particles were treated with streptavidin-phycoerythrin (PE)(**black trace**) followed by incubation with 0.003% tween 20 (**orange trace**). (C) Elastomeric particles were treated with streptavidin-(PE) (**black trace**) followed by incubation with 0.1% BSA (**orange trace**). (D) Avidinylated-elastomeric particles (**orange trace**) were incubated with BSA conjugated to AlexaFluor-647 (**black trace**). Note: The density scatter plot was performed using an inverse gray-scale where the darkest parts indicate the most densely populated areas and the lightest parts indicate the least densely populated areas of the scatter plot. 96% of all detected particles fell within the light scatter region that was selected (gated) for fluorescence analysis.

To determine if BSA protein can be adsorbed to the surface of elastomeric particles that have already undergone avidin (unconjugated) protein adsorption, avidinylated-elastomeric particles (5.0 x 10^6 particles/mL) were incubated with a solution of BSA conjugated to AlexaFluor-647 and then centrifugally washed. The initial MFI of the avidinylated-elastomeric particles was 512 (Figure 4.5D). Upon incubation with a 100 nM solution of BSA AlexaFluor-647 the particles displayed a MFI value of 452,220 (Figure 4.5D); indicative that avidinylated-elastomeric particles adsorb soluble BSA protein in solution. Adsorption of high quantities of BSA AlexaFluor-647 to the surface of elastomeric particles may also reflect the non-specific binding of the AlexaFluor component of the labeled BSA to the particles.

Avidin and Streptavidin Titrations

Avidin-FITC and streptavidin-PE titration curves were performed on polydisperse elastomeric particles (2.5 x 10^7 particles/mL) to ascertain an approximate concentration range that could be used to saturate the surface of elastomeric particles. Centrifugal-washes were performed on all samples prior to performing flow cytometry measurements. The avidin-FITC titration (0, 20, 40, 80, 100 and 1000 nM) did not appear to give any type of trend that could be used for a best-fit curve; however, a 100 nM concentration of avidin-FITC corresponded to the highest MFI value (~ 11,640) measured using flow cytometry (Figure 4.6A). In regards to the avidin-FITC titration, inclusion of 200 and 400 nM concentrations would have likely provided a better binding curve.

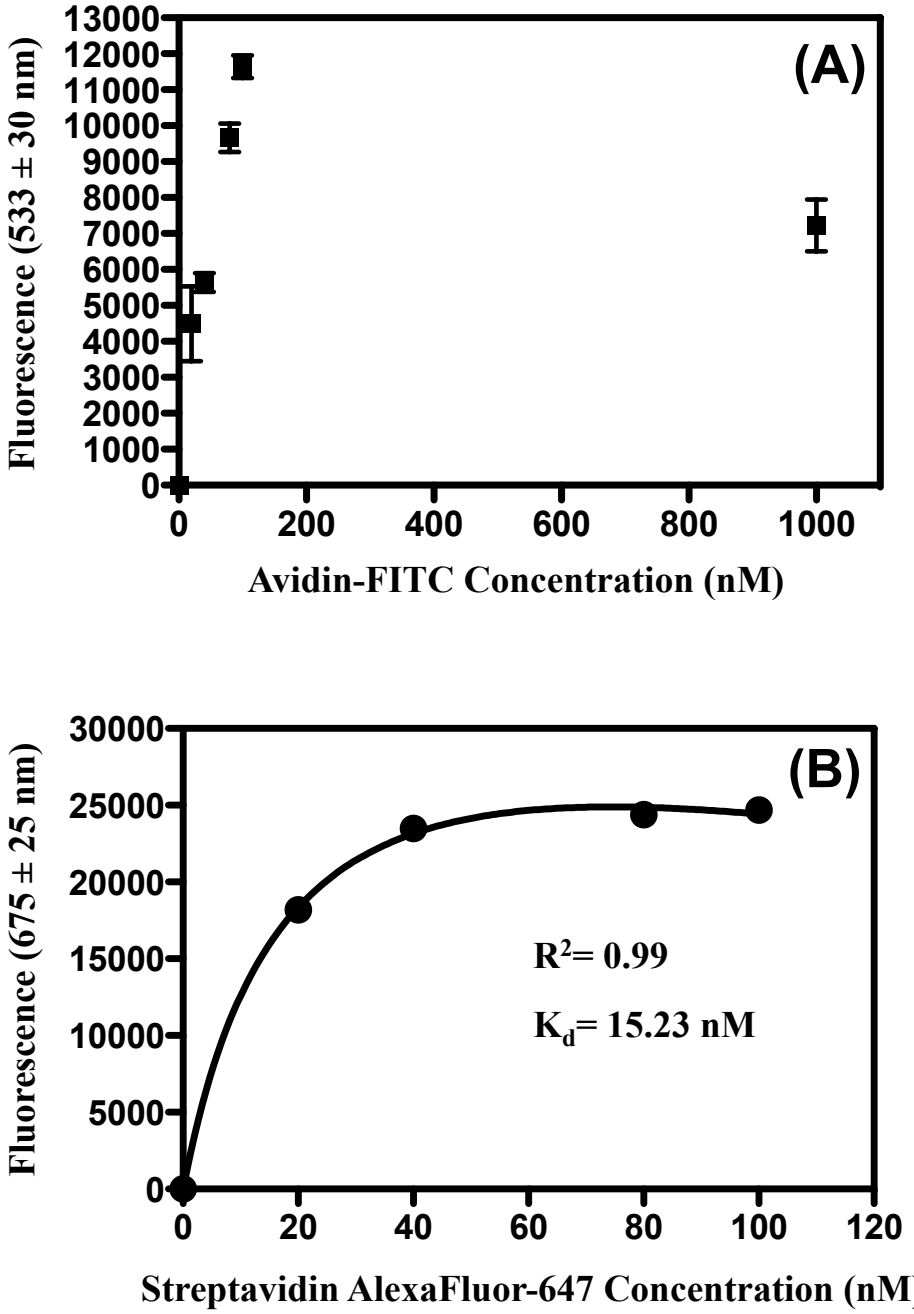

Figure 4.6 Polydisperse elastomeric particles were used in (A) avidin-FITC and (B) streptavidin AlexaFluor-647 titrations. For (A) Error bars indicate SD of 2 separate determinations.

A streptavidin AlexaFluor-647 titration (0, 20, 40, 80, and 100 nM) was also performed and was successfully fit to a 1-site binding curve (Langmuir Isotherm: R^2= 0.99 and K_d= 15.23 nM) using GraphPad PRISM version 5.0b (Figure 4.6B). Based on the 1-site binding curve it appears that saturation occurs around 60-100 nM.

Functionalization with a Biotinylated Antibody

Once elastomeric particles have been functionalized with an avidin (or streptavidin) protein, elastomeric particles can be further functionalized with a biotinylated antibody to form elastomeric capture microparticles (ECμPs). The attached biotinylated antibodies can then be easily detected and quantified using a secondary antibody conjugated to a fluorochrome (e.g., phycoerythrin) along with flow cytometry analysis (Figure 4.7).

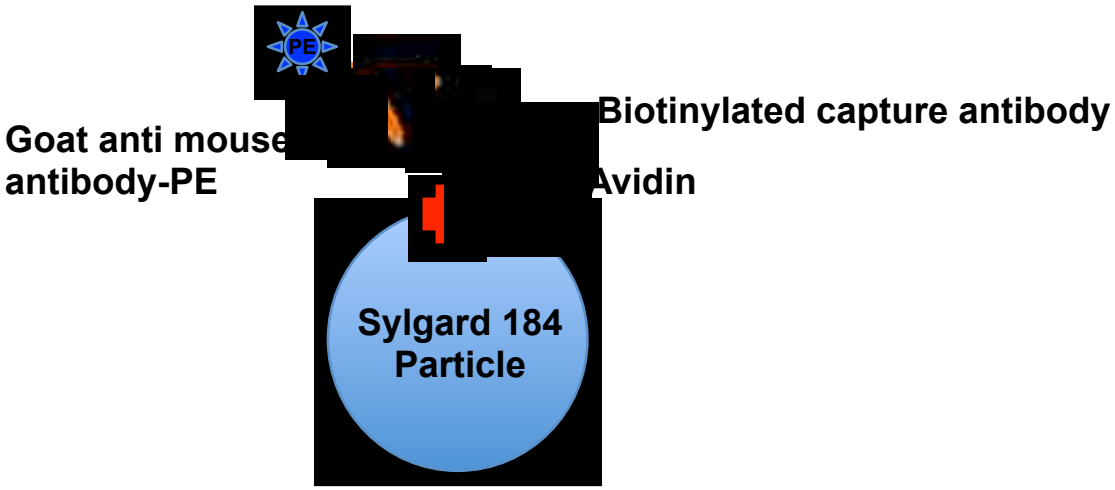

Figure 4.7 Schematic diagram showing an attached biotinylated antibody (e.g., mouse anti human PSA) on the surface of avidinylated-elastomeric particles being detected by a secondary antibody (e.g., goat anti mouse IgG) conjugated to a phycoerythrin (PE) fluorochrome.

Avidinylated-elastomeric particles were prepared by incubation with unconjugated avidin at a concentration of 1 μM (~10 times the maximal binding concentration) for 30 min. To form elastomeric capture microparticles (ECμPs), avidinylated-elastomeric particles (5.0 x 10^6 particles/mL) were centrifugally washed and then incubated with varying concentrations (0, 2, 4, 6, and 8 nM) of a biotinylated antibody (mouse anti human monoclonal IgG). ECμPs were then centrifugally washed prior to being detected using a goat anti mouse IgG conjugated to phycoerythrin (PE) in conjunction with flow cytometry (Figure 4.8). The biotinylated-IgG titration did not demonstrate any type of trend that could be used for a best-fit curve; however, a 6 nM concentration of biotinylated-IgG corresponded to the highest MFI value (~ 23,971). It appears that maximal levels of binding may be expected in the presence of 4-6 nM of the biotinylated-IgG.

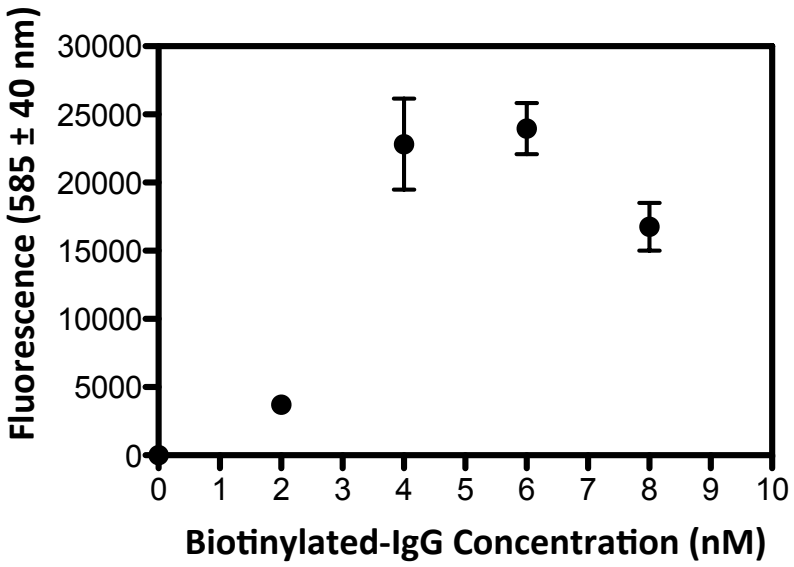

Figure 4.8 Polydisperse avidinylated-elastomeric particles used in an IgG (biotinylated-mouse anti human PSA monoclonal) titration that was detected and quantified using a goat anti mouse polyclonal-phycoerythrin and flow cytometry analysis. Error bars indicate SD of 2 separate determinations.

Prostate Specific Antigen (PSA) Titrations (no wash)

Polydisperse ECμPs can be used in a human prostate specific antigen (PSA) assay that is detected and quantified using a sandwich assay configuration and flow cytometry analysis (Figure 4.9). To ensure ultra-specific detection of PSA in solution, a monoclonal pair of PSA antibodies were used. The biotinylated monoclonal capture antibody was specific for epitope 1 on human PSA, and the monoclonal detection antibody-(FITC) was specific for epitope 5 on human PSA.

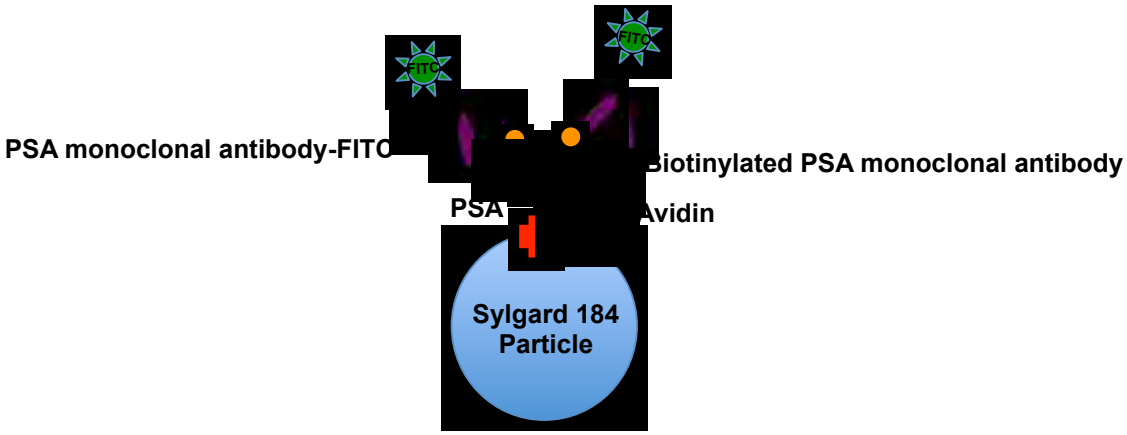

Figure 4.9 Polydisperse elastomeric capture microparticles (ECμPs) (10:2 ratio of Sylgard 184 prepolymer to crosslinking agent) are used to detect and quantify prostate specific antigen (PSA) in solution utilizing a sensitive sandwich immunoassay configuration in conjunction with flow cytometry analysis.

Polydisperse ECμPs (5.0×10^5 particles/mL) were successfully used in a homogeneous (no wash) human PSA sandwich assay where the specific and selective capturing of PSA occurred in 200 µL of 1X PBS with a high protein background (~ 1 mg/mL BSA). The PSA titration (0, 1, 5, 10, 20, and 30 nM) was successfully fit to a 1-site binding curve (R^2= 0.997; K_d = 1.141 nM) and demonstrated low non-specific binding of the human PSA antigen (Figure 4.10A). The lowest detected PSA

concentration was 1 nM and demonstrated very low background indicative that lower concentrations of PSA may be possible in simple buffer solutions with high protein content.

To determine if polydisperse ECμPs could be utilized in affinity capture assays conducted in small liquid volumes, ECμPs (50,000 particles/mL) were utilized in a human PSA sandwich assay where capturing of PSA occurred in 20 µL of PBS with a high protein content. The PSA titration was successfully fit to a 1-site binding curve (R^2 = 0.987) and demonstrated low non-specific binding of the human PSA antigen (Figure 4.10B). The lowest detected PSA concentration was 1 nM and demonstrated very low background that is suggestive that detection of lower PSA concentrations are possible in small liquid volumes with high protein content. The dissociation constant (K_d = 13.40 nM) that was calculated from the fitted 1-site binding curve was significantly higher than the K_d value calculated from Figure 3.11A (K_d = 1.141 nM). The increased K_d value may be the result of a decrease in the mixing efficiency that occurred because of the small volume (20 µL) that was used for the capturing of the PSA antigen. Small volumes in 500 µL PCR tubes may allow surface tension to minimize the mixing efficiency of the liquid within the tube; thus a lack of mixing can minimize the association of the ligand to the receptor, therefore leading to an increase in the calculated K_d value.

To evaluate if polydisperse ECμPs could be utilized in affinity capture assays in human plasma, ECμPs (5.0×10^5 particles/mL) were successfully used in a PSA sandwich assay performed in 200 µL of 1% human plasma (diluted in 1X PBS with high protein content). The PSA titration was successfully fit to a 1-site binding curve (R^2= 0.986; K_d = 1.071 nM) and demonstrated low non-specific binding of the human PSA

antigen (Figure 4.10C). The lowest detected PSA concentration was 1 nM and demonstrated very low background indicative that lower concentrations of PSA may be possible in biological milieu (e.g., plasma, blood). However, since there appears to be no inflection to the fitted curve, it may be likely that the actual saturation (Bmax) of the binding curve is much higher than the one derived from the fitted 1-site binding curve. As a result of this, the actual Kd may be higher than the one calculated from our fitted data.

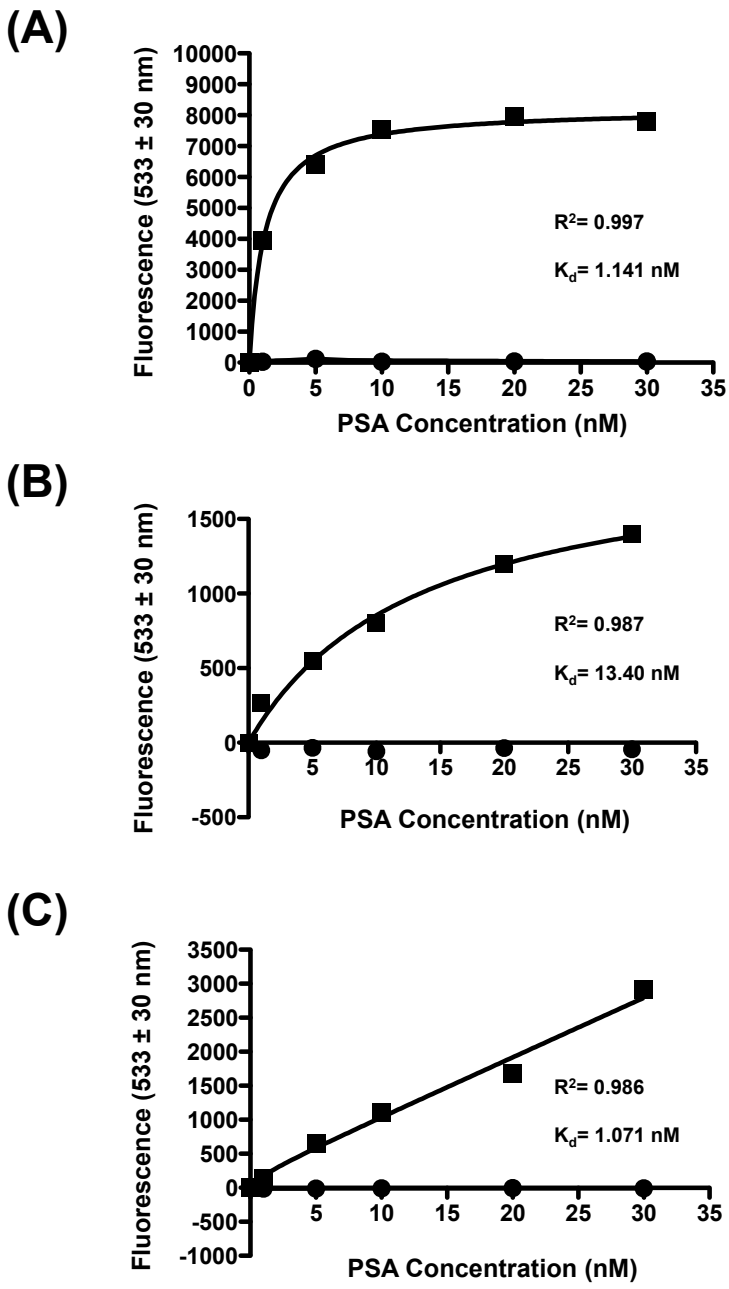

Figure 4.10 Elastomeric capture microparticles (ECμPs) capture human PSA in high protein backgrounds prior to detection antibody treatment and flow cytometry analysis. (A) 5.0 x 10^5 ECμPs capture human PSA in 200 µL of 1 mg/ml BSA in PBS , (B) 50,000 ECμPs capture human PSA in 20 µL of 1 mg/ml BSA in PBS , and (C) 5.0 x 10^5 ECμPs capture human PSA in 200 µL of 1% human plasma that was diluted with PBS containing 1 mg/ml BSA. Note: (■) denotes ECμPs with capture antibody and (●) denotes particles without capture antibody.

Functionalization of Monodisperse Elastomeric Particles

Monodisperse elastomeric particles synthesized using a 6:4 ratio of Sylgard 184 prepolymer to crosslinking agent with a PDMS-based T-junction microfluidic system, can be functionalized with the same avidin/biotin conjugation reagents that were utilized to form the polydisperse ECμPs. To identify the appropriate monodisperse elastomeric particle population using flow cytometry, a density scatter plot (forward scatter versus side scatter) using an inverse gray-scale was utilized (Figure 4.11A). The gated monodisperse elastomeric particles displayed a forward scatter coefficient of variation (CV) of ~ 3.91%; however, the gated particles only amounted to 26% of the total particles counted using the flow cytometer. As a result of this, filtering methodologies can be incorporated to reduce the presence of unwanted particle populations (e.g., satellite particles); it is hypothesized that these unwanted particles may have arisen as a result of the microchannels in the PDMS-based microfluidic device reverting back to their hydrophobic nature and thus resulting in less control over the size distribution of the produced droplets and particles.

The monodisperse elastomeric particle population displayed an initial autofluorescence MFI of 2053 (Figure 4.9B). Once the elastomeric particles were incubated with 1 μM streptavidin AlexaFluor-647 (~66 x the Kd to achieve binding saturation) the MFI increased to ~ 8.8 x 10^6; indicative that streptavidin had been successfully adsorbed to the surface of the monodisperse elastomeric particles (Figure 4.11B).

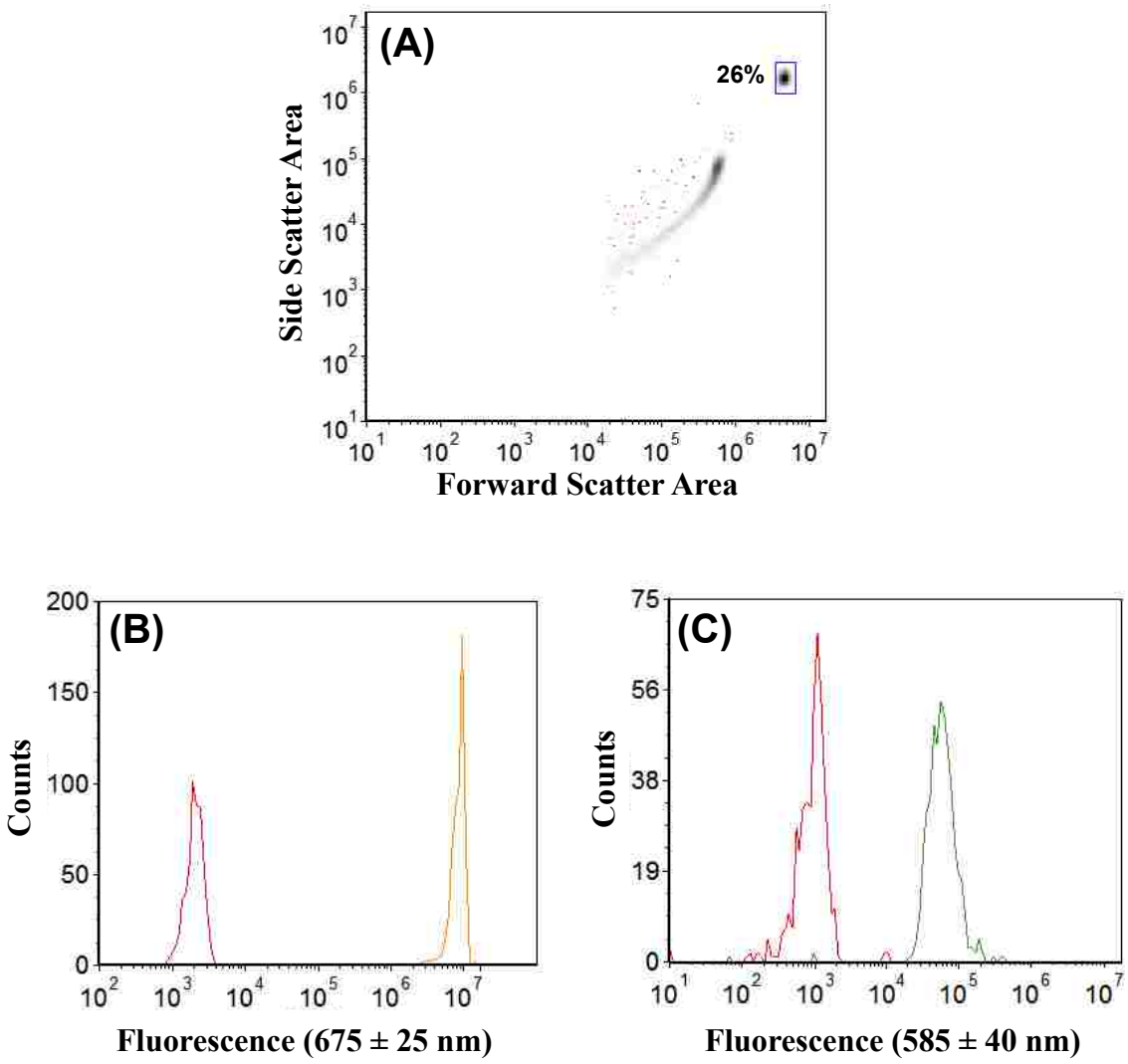

Figure 4.11 A monodisperse elastomeric particle population (6:4 ratio of Sylgard 184 prepolymer to crosslinking agent) was functionalized using non-specific adsorption of avidin and streptavidin followed by further functionalization using a biotinylated high density lipoprotein (HDL) antibody. (A) Density scatter plot (forward versus side scatter) indicating the appropriate monodisperse particle population used for analysis. (B) Fluorescence histogram comparing untreated elastomeric particles (red trace) to elastomeric particles treated with streptavidin AlexaFluor-647 (yellow trace). (C) Fluorescence histogram comparing avidinylated-elastomeric particles that were not treated with the biotinylated HDL antibody (mouse anti human HDL IgG) prior to centrifugal washes and secondary antibody treatment (goat anti mouse IgG-phycoerythrin) (red trace) to avidinylated-elastomeric particles that were treated with the biotinylated HDL antibody prior to centrifugal washes and secondary antibody treatment (green trace).

To determine if avidinylated-elastomeric particles were capable of binding biotinylated IgGs to become ECμPs, avidinylated-elastomeric particles (pre-incubated 30 min with 1 μM unconjugated avidin) were centrifugally washed and then incubated with a solution of biotinylated high density lipoprotein (HDL) antibody (mouse anti human HDL IgG). Detection of the attached biotinylated HDL antibody was accomplished by performing centrifugal washing to remove unbound biotinylated antibody followed by incubation with a secondary antibody (goat anti mouse IgG antibody-PE) and flow cytometry analysis. To determine the non-specific binding of the secondary antibody, a control was also performed in which the avidinylated-elastomeric particles were incubated (without the biotinylated-IgG) with just the secondary antibody prior to flow cytometry analysis. The avidinylated-elastomeric particles that were incubated with only the secondary antibody, displayed an initial MFI of ~ 1031 (Figure 4.9C). Avidinylated-elastomeric particles that were incubated with the biotinylated IgG prior to centrifugal washes and secondary antibody treatment displayed a MFI of ~ 57,240 (Figure 4.9C); indicative that the biotinylated-IgG was successfully attached to the surface of the avidinylated-elastomeric particles.

Conclusions and Future Directions

Polydisperse elastomeric particles synthesized from Sylgard 184 (10:2 prepolymer to crosslinking agent) and low molecular weight PDMS (1:1 prepolymer to crosslinking) can be easily functionalized with an avidin or streptavidin protein using non-specific adsorption. The adsorption of avidin-FITC protein to the hydrophobic surface of polydisperse elastomeric particles (Sylgard 184) is a relatively strong attachment but can be easily removed by incubation in a surfactant solution (0.003%

tween 20). Once the polydisperse elastomeric particles are functionalized with an unconjugated avidin protein, the 4-biotin binding pockets that are associated with an avidin protein allow further functionalization with commercially-purchased biotinylated antibodies. In this report, the polydisperse elastomeric particles were functionalized into elastomeric capture microparticles (ECμPs) that were successfully used in PSA sandwich assays that were conducted in high protein content backgrounds (physiologic buffer, exceedingly small liquid volumes, and 1% human plasma) followed by flow cytometry analysis without prior washing. Our results demonstrated that polydisperse ECμPs have potential to be used in homogeneous (no wash) medically-relevant bioassays (e.g., high density lipoprotein) where the capturing of analytes is specifically and selectively performed in high protein backgrounds (e.g., plasma, blood, cerebral spinal fluid, urine) followed by flow cytometry analysis.

The sensitivity of assays performed with ECμPs in conjunction with flow cytometry analysis can be enhanced by using monodisperse ECμPs. A monodisperse elastomeric particle population synthesized from Sylgard 184 (6:4 ratio prepolymer to crosslinking) was successfully functionalized with avidin adsorption followed by biotinylated high density lipoprotein (HDL) antibody attachment. However, the density scatter plot (forward scatter versus side scatter) derived from flow cytometry demonstrated that there were a significant percentage of apparent elastomeric particles (~ 74%) outside the region representing larger, more uniformly sized particles. The presence of unwanted ECμPs can function as ligand-depletion agents; thus leading to a decrease in the sensitivity and accuracy of the measurements being performed on gated ligand-bound ECμPs using flow cytometry. Mechanical filtering methods may be implemented to

remove a significant fraction of these unwanted particles prior to performing ligand capturing and flow cytometry analysis. However, the current methods used for synthesizing monodisperse elastomeric particles from Sylgard 184 (6:4 ratio of prepolymer to crosslinking agent) in microfluidic devices were limited with respect to the number of particles that could be produced from a single chip (~150,000 particles); thus limiting the ability to efficiently scale up production for bioassay applications. The use of a relatively hydrophilic polymethylmethacrylate (PMMA) polymer have been shown to produce microfluidic devices that generate monodisperse elastomeric particles.[6] The use of PMMA may allow increased production of our monodisperse elastomeric particles; thus allowing them to be used for bioassay purposes.

As indicated above in chapter 3,monodisperse elastomeric particles can be synthesized from Pluronic F108 surfactant for long stretches of time (10 hours) at a suitable rate (~ 400 droplets/hour) leading to 1.5×10^7 particles using microfluidic systems. Thus, a potentially promising alternative route for producing large numbers of monodisperse particles would be to synthesize them from a low molecular weight PDMS in combination with a biocompatible Pluronic F108 surfactant that has already been chemically modified with a biotin functional group. Evaluation of such an approach remains for future investigations beyond the scope of projects associated with this dissertation.

References

1. Sui, G.; Wang, J.; Lee, C.-C.; Lu, W.; Lee, S. P.; Leyton, J. V.; Wu, A. M.; Tseng, H.-R., Solution-phase surface modification in intact poly (dimethylsiloxane) microfluidic channels. *Analytical chemistry* **2006,** *78* (15), 5543-5551.

2. Jang, Y.; Oh, S. Y.; Park, J.-K., In situ electrochemical enzyme immunoassay on a microchip with surface-functionalized poly (dimethylsiloxane) channel. *Enzyme and microbial technology* **2006,** *39* (5), 1122-1127.

3. Huang, B.; Wu, H.; Kim, S.; Kobilka, B. K.; Zare, R. N., Phospholipid biotinylation of polydimethylsiloxane (PDMS) for protein immobilization. *Lab on a Chip* **2006,** *6* (3), 369-373.

4. Xiao, D.; Zhang, H.; Wirth, M., Chemical modification of the surface of poly (dimethylsiloxane) by atom-transfer radical polymerization of acrylamide. *Langmuir* **2002,** *18* (25), 9971-9976.

5. Yu, L.; Li, C. M.; Liu, Y.; Gao, J.; Wang, W.; Gan, Y., Flow-through functionalized PDMS microfluidic channels with dextran derivative for ELISAs. *Lab Chip* **2009,** *9* (9), 1243-1247.

6. Eteshola, E.; Leckband, D., Development and characterization of an ELISA assay in PDMS microfluidic channels. *Sensors and Actuators B: Chemical* **2001,** *72* (2), 129-133.

7. Roach, P.; Farrar, D.; Perry, C. C., Interpretation of protein adsorption: surface-induced conformational changes. *Journal of the American Chemical Society* **2005,** *127* (22), 8168-8173.

8. Tilton, R. D.; Robertson, C. R.; Gast, A. P., Manipulation of hydrophobic interactions in protein adsorption. *Langmuir* **1991,** *7* (11), 2710-2718.

9. Lundqvist, M.; Sethson, I.; Jonsson, B.-H., Protein adsorption onto silica nanoparticles: conformational changes depend on the particles' curvature and the protein stability. *Langmuir* **2004,** *20* (24), 10639-10647.

10. Roach, P.; Farrar, D.; Perry, C. C., Surface tailoring for controlled protein adsorption: effect of topography at the nanometer scale and chemistry. *Journal of the American Chemical Society* **2006,** *128* (12), 3939-3945.

11. Wong, I.; Ho, C.-M., Surface molecular property modifications for poly (dimethylsiloxane)(PDMS) based microfluidic devices. *Microfluidics and nanofluidics* **2009,** *7* (3), 291-306.

12. Deval, J.; Umali, T. A.; Lan, E. H.; Dunn, B.; Ho, C.-M., Reconfigurable

hydrophobic/hydrophilic surfaces in microelectromechanical systems (MEMS). *Journal of Micromechanics and Microengineering* **2003,** *14* (1), 91.

13. Jiang, X.; Xu, Q.; Dertinger, S. K.; Stroock, A. D.; Fu, T.-m.; Whitesides, G. M., A general method for patterning gradients of biomolecules on surfaces using microfluidic networks. *Analytical chemistry* **2005,** *77* (8), 2338-2347.

14. Sakahara, H.; Saga, T., Avidin–biotin system for delivery of diagnostic agents. *Advanced drug delivery reviews* **1999,** *37* (1), 89-101.

15. Diamandis, E. P.; Christopoulos, T. K., The biotin-(strept) avidin system: principles and applications in biotechnology. *Clinical chemistry* **1991,** *37* (5), 625-636.

16. Dong, Y.; Phillips, K. S.; Cheng, Q., Immunosensing of Staphylococcus enterotoxin B (SEB) in milk with PDMS microfluidic systems using reinforced supported bilayer membranes (r-SBMs). *Lab on a Chip* **2006,** *6* (5), 675-681.

17. Scott Wilbur, D.; Pathare, P. M.; Hamlin, D. K.; Stayton, P. S.; To, R.; Klumb, L. A.; Buhler, K. R.; Vessella, R. L., Development of new biotin/streptavidin reagents for pretargeting. *Biomolecular engineering* **1999,** *16* (1), 113-118.

Chapter 5 Elastomeric Particles Function as Negative Acoustic Contrast Particles

Acoustic Contrast Factor

Biological cells (erythrocytes, spores, fungi, phagocytes), common sediments, plastics, sand, metals,[1] and commercially-available microspheres (e.g., Spherotech) have a positive acoustic contrast value (Figure 5.1) and therefore function as positive acoustic contrast particles and are acoustically forced to pressure nodes under an acoustic standing wave.[2] Because all biological cells and most commercially-available microspheres function as positive acoustic contrast particles, the use of acoustic-based separations, based on acoustic contrast, have rarely been implemented in biological problems[1] (e.g., acoustic separation of ligand-bound capture particles from cells in a biological sample). As a result of this, the development of a particle that functions as a negative acoustic contrast particle is highly desirable and promising for biological applications (Figure 4.1).

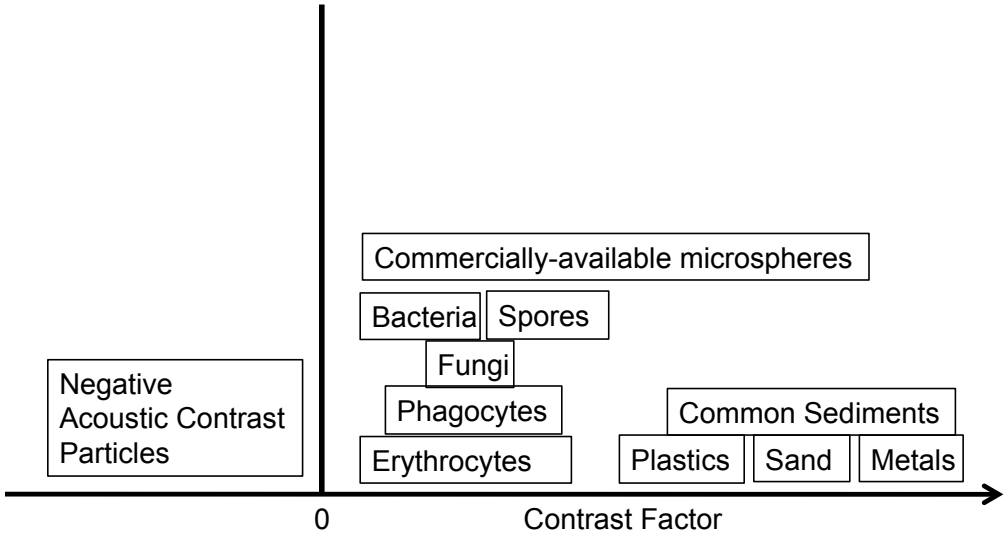

Figure 5.1 Schematic diagram of contrast factors of various materials. Figure modified and reproduced from Kaduchak et al.[1]

Secondary Acoustic Forces

Interesting acoustic phenomena that can affect the focusing and separation of acoustically active particles (e.g., negative and positive acoustic contrast particles) under an acoustic standing wave field are acoustic secondary forces - also referred to as Bjerknes forces $F_B(x)$.[3] These interparticle forces are caused by acoustic waves that are scattered by particles in close proximity and can produce attractive and repulsive forces in which the magnitude of $F_B(x)$ is described by an equation reported by Crum et al.[4]

$$F_B(x) = 4\pi r^6 \left[\frac{\left(\rho_p - \rho_o\right)^2 \left(3(\cos\theta)^2 - 1\right)}{6\rho_o d^4} v_{(x)}^2 - \frac{\omega^2 \rho_o \left(\beta_p - \beta_o\right)^2}{9d^2} p_{(x)}^2 \right] \qquad \textbf{(1)}$$

The magnitude of the secondary acoustic force $F_B(x)$ is directly proportional to the radius of the particle (r), the distance between particles (d), the angular frequency of the particle (ω) also referred to as $2\pi f$, the density of the particle (ρ_p) and the surrounding medium (ρ_o), and the compressibility of the particle (β_p) and the surrounding medium (β_o). The second term $\frac{\left(\rho_o - p_p\right)^2 \left(3(cos\theta)^2 - 1\right)}{6\rho_o d^4} v_{(x)}^2$ on the right side of the equation is dependent upon the velocity amplitude ($v_{(x)}$), where the third term $\frac{\omega^2 \rho_o (\beta_p - \beta_o)^2}{9d^2} p_{(x)}^2$ on the right side of the equation is dependent upon the pressure amplitude ($p_{(x)}$). A negative value (-) for $F_B(x)$ exerts attractive forces moving particles together to form aggregates at their respective nodal (or antinodal) regions. However a positive value (+) generates repulsive forces moving particles away from one another. An important factor

determining the sign (+ or -) of $F_B(x)$ is the angle (θ) and orientation of the particles within the primary acoustic standing wave field, where θ is the angle between the line defined by the center of two particles and the direction of the propagated primary acoustic standing wave. If particles are lined up parallel to the propagation of the primary acoustic standing wave, the value for θ will become 0° and therefore $\cos\theta = 1$; and thus the velocity amplitude-dependent expression will likely have a positive value. A positive value for the velocity amplitude-dependent expression of the equation will likely allow a positive value for $F_B(x)$; thus generating repulsive Bjerknes forces. However, if particles are lined up perpendicular to the direction of the propagated primary acoustic standing wave, the value for θ will become 90° and therefore $\cos\theta = 0$; and thus the velocity-dependent expression becomes zero. A zero value for the velocity amplitude-dependent expression makes the sign (+ or -) of $F_B(x)$ dependent upon the pressure amplitude-dependent expression making it likely that the pressure amplitude-dependent expression will be greater than the velocity amplitude-dependent expression of the equation (0 value); thus giving a negative value for $F_B(x)$ and generating attractive Bjerknes forces.

The elastomeric particles that are synthesized in this dissertation report from PDMS elastomers, Sylgard 184 (specific gravity ~ 1.03) and low molecular weight PDMS (specific gravity ~ 0.97), have densities that are similar to aqueous solutions ~1 g/cm^3. As a result of the density similarities, the value of the velocity amplitude-dependent expression of the Bjerknes force equation (**1**) becomes 0, and thus the magnitude and sign (+ or -) becomes dependent on the pressure amplitude-dependent expression of the equation; and thus, as long as there is a voltage applied to the piezoelectric transducer to generate a pressure amplitude, the value of $F_B(x)$ will be (-)

and generate attractive Bjerknes forces. As a result of this, it appears reasonable to conclude that any Bjerknes forces associated with elastomeric particles will likely be in the form of attractive interparticle forces.

In this dissertation, we hypothesize that compressible PDMS-based elastomeric particles function as negative acoustic contrast particles under an ultrasonic acoustic pressure standing wave and that elastomeric particles can be affected by attractive forces that cause aggregates to form at pressure antinodes. This report demonstrates 1) the negative acoustic contrast properties of elastomeric particles that were synthesized from two PDMS-based elastomers, Sylgard 184 (specific gravity ~ 1.03) and low molecular weight PDMS (specific gravity ~ 0.97); and 2) the application of using an ultrasonic acoustic pressure standing wave to separate elastomeric negative acoustic contrast particles from positive acoustic contrast particles (blood cells and commercially-available polystyrene particles); and 3) elastomeric particles being affected by attractive forces, that cause elastomeric particles to clump at pressure antinodes.

Materials and Methods

Synthesis of Polydisperse Elastomeric Particles

Sylgard 184 (specific gravity ~ 1.03) (1 g, at 10:2 ratio of PDMS prepolymer to crosslinking agent) or low molecular weight PDMS (specific gravity ~ 0.97) (1 g, at 1:1 ratio of PDMS prepolymer to crosslinking agent) (Dow Corning Corp., Midland, MI) were emulsified in 10 mL of ultrapure water (18.2 MΩ•cm @ 25 °C; Synergy®, EMD Millipore) using a homogenizer (Power Gen 125, Fisher Scientific) set at 6,000 RPM for ~ 60 seconds. The elastomeric droplets, with crosslinking agent, were cured at 100 °C for ~ 1 hour to form crosslinked elastomeric particles.

Silicon Acoustofluidic Device

A silicon acoustofluidic device was fabricated in silicon via photolithography using a photomask designed from AutoCAD software (Autodesk Inc., San Rafael, CA) and deep reactive ion etching (DRIE) using a protocol described by Suthanthiraraj et al.[5] DRIE allowed specific micro-channel patterns to be etched onto the surface of the silicon wafer (WaferNet Inc., San Jose, CA). A borosilicate glass slide (Borofloat 33, Schott North America, Inc., Elms Ford, NY) with 1 mm holes drilled through it to accommodate inlet and outlet ports (tube connection sites) was then sealed on top of the etched silicon wafer using anodic bonding.[6] To allow easy insertion of silicone tubing (Cole-Parmer Instrument Company, Vernon Hills, IL) into inlet and outlet ports, square PDMS blocks, with punctured holes, were aligned and plasma sealed on top of the inlet and outlet ports.[6] Silicone tubing was then inserted and epoxy glued into the PDMS inlet and outlet ports. To complete the fabrication, a lead zirconate titanate piezoelectric transducer (PZT: 5 mm width x 30 mm length x ~1 mm thickness) (Boston Piezo-Optics Inc., Bellingham, MA) was attached to the bottom side of the chip using cyanoacrylate glue.

Square Glass Microcapillary Acoustofluidic Device

An acoustofluidic device was fabricated out of a borosilicate micro glass square cell (Friedrich & Dimmock, Inc, Millville, NJ). The device was constructed by gluing a PZT (5 mm width x 30 mm length x ~ 1 mm thickness) (Boston Piezo-Optics Inc., Bellingham, MA) to one of the four flat sides of the square microcapillary using cyanoacrylate glue. A second PZT can also be glued to the microcapillary to function as a feedback PZT to ensure that an acoustic standing wave is being generated in the fluid-filled cavity of the acoustofluidic device. To allow easy flow of particle/cell suspensions

silicone tubing (Cole-Parmer, Vernon Hills, IL) was attached to both ends of the glass microcapillary. To support the fragile glass microcapillary, the device was mounted on a glass microslide (Corning Inc., Corning, NY) with crosslinked PDMS cubes that secured the attachment of the glass microcapillary and raised it approximately 1 cm above the microslide surface.

Acoustic Focusing and Separation

Samples were flowed (20-100 μL/min) through the acoustofluidic devices using a microsyringe pump (Nexus 3000, Chemyx Inc. Stafford, TX). To focus and separate particles and blood cells, the PZT was actuated using a waveform generator (33250A, Agilent, Santa Clara, CA) at a frequency of 3.101 MHz at 20-50 volts peak-to-peak. To monitor and image the focusing and separation of particles and blood cells, commercially available Nile Red (NR)-polystyrene particles (10.2 μm in diameter) (Spherotech Inc., Lake Forest, IL) were used, and Nile Red dye (Sigma-Aldrich, St. Louis, MO) was used to label elastomeric particles and blood cells; this was accomplished by incubation in an aqueous Nile Red solution (100 μM) in 1 mL of phosphate buffered saline (1X PBS with 7.4 pH: 10 mM Na_2HPO_4; 1 mM KH_2PO_4; 138 mM NaCl; 3 mM KCl) for 30 minutes followed by centrifugal washing (PBS) to remove unbound dye. Focusing and separation of particles (and blood cells) was monitored and imaged using an epifluorescence microscope (Zeiss Axio Imager) and a Luca S EMCCD camera (Andor Technology, Belfast N., Ireland) with Andor imaging software (Andor-Solis).

Results

Elastomeric Particles (Sylgard 184)

A silicon acoustofluidic device (Figure 5.2A,B) that functions as a 1/2λ resonator (i.e., 2 pressure antinodes at the side walls and 1 pressure node at the center of the microchannel) was used to demonstrate the negative acoustic contrast property of polydisperse elastomeric particles that were synthesized from Sylgard 184 (10:2 ratio of prepolymer to crosslinking agent). Nile Red (NR)-elastomeric particles (~1.0 x 10^7 particles/mL) were dispersed while being flowed (20 μL/min) through the acoustic focusing device with the acoustic field off (Figure 4.3A). Once an ultrasonic acoustic pressure standing wave field was applied (3.101 MHz at 20 $V_{peak\text{-}peak}$), NR-elastomeric particles were rapidly focused to pressure antinodes at the side walls of the microchannel (Figure 5.3B). The application of the acoustic pressure standing wave field demonstrated that elastomeric particles synthesized from Sylgard 184 function as negative acoustic contrast particle.

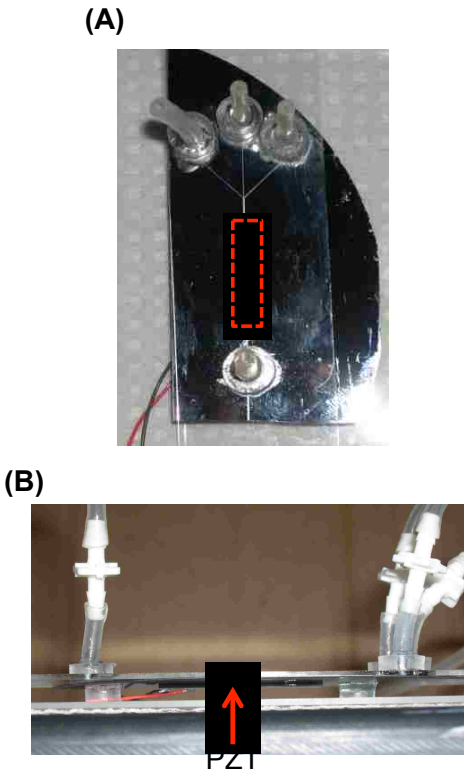

Figure 5.2 Silicon acoustic focusing device that was used for acoustic focusing and separation. (A) top view and (B) side view showing the actuating PZT coupled to the silicon acoustic focusing device. Note: The red dashed box indicates where initial acoustic focusing and separation occurs.

Once elastomeric particles (2.5 x 10^7 particles/mL) that were synthesized from Sylgard 184 were shown to possess negative acoustic contrast properties, the application of acoustically separating them from a high concentration of human blood (10% dilution in 1X PBS with 0.1% BSA) with continuous flow (20 μL/min) was demonstrated. Upon application of the acoustic pressure standing wave field (3.101 MHz at 20 $V_{peak\text{-}peak}$) the NR-elastomeric particles were rapidly focused to the pressure antinodes while blood cells were focused to the pressure node at the center of the microchannel (Figure 5.3C). The activation of the acoustic pressure standing wave field demonstrated that the separated elastomeric particles at the pressure antinodes were forming aggregates and experiencing

a decrease in their flow velocity; the decrease in flow velocity of the focused elastomeric particles is a result of the applied acoustic forces and the laminar flow profile within the acoustofluidic device. Though, work needs to be performed in order to understand and control the aggregation of focused elastomeric particles at pressure antinodes the results clearly demonstrate that elastomeric particles synthesized from Sylgard 184 (10:2 ratio of prepolymer to crosslinking agent) function as negative acoustic contrast particles and can be efficiently separated from human blood using an ultrasonic acoustic standing wave field within an acoustofluidic device.

Elastomeric Particles (low molecular weight PDMS)

Since previous studies performed in our laboratory have demonstrated efficient production of monodisperse elastomeric particles using a low molecular weight PDMS, it became essential to determine their acoustic contrast properties. Polydisperse elastomeric particles were utilized for proof-of-concept experimentation. A low-cost square glass microcapillary that functions as a 1/2λ acoustic resonator (Figure 5.4A), was used to determine the negative acoustic contrast properties of polydisperse elastomeric particles that were synthesized from a low molecular weight PDMS (1:1 ratio of prepolymer to crosslinking agent). Elastomeric particles (~ 1.25×10^8 particles/mL) were equally dispersed with no flow in the acoustofluidic device with the acoustic field off (Figure 5.4B).

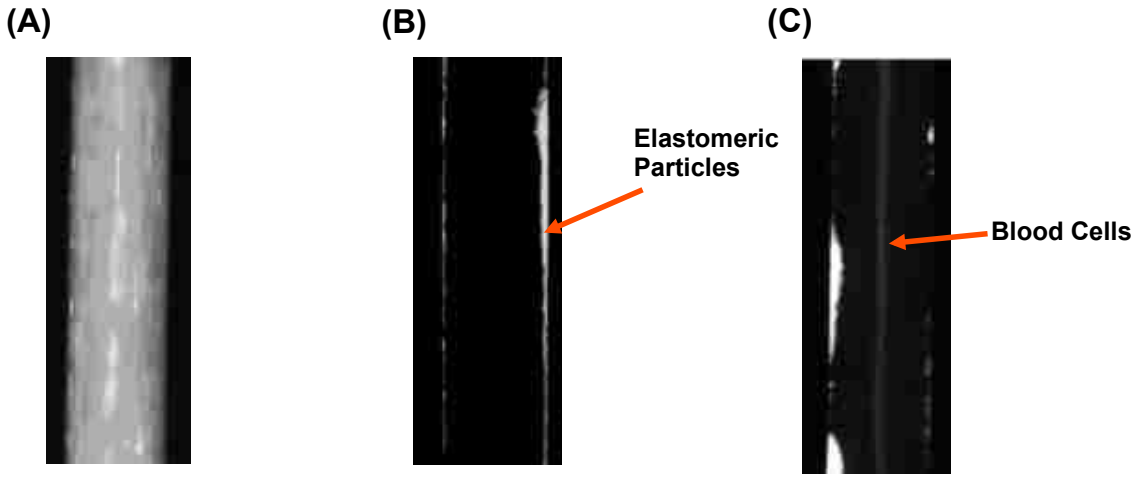

Figure 5.3 Polydisperse elastomeric particles synthesized from Sylgard 184 (10:2 ratio of prepolymer to crosslinking agent) function as negative acoustic contrast particles and can be separated from 10% human blood. Nile Red (NR)- Elastomeric particles flowed (20 μL/min) through the acoustic focusing device with the acoustic field (A) off and then (B) on. (C) A mixture of (NR) elastomeric particles and (NR) human blood (10% dilution in 1X PBS with 0.1% BSA) flowed (20 μL/min) through the silicone-based acoustofluidic device with the ultrasonic acoustic standing field on.

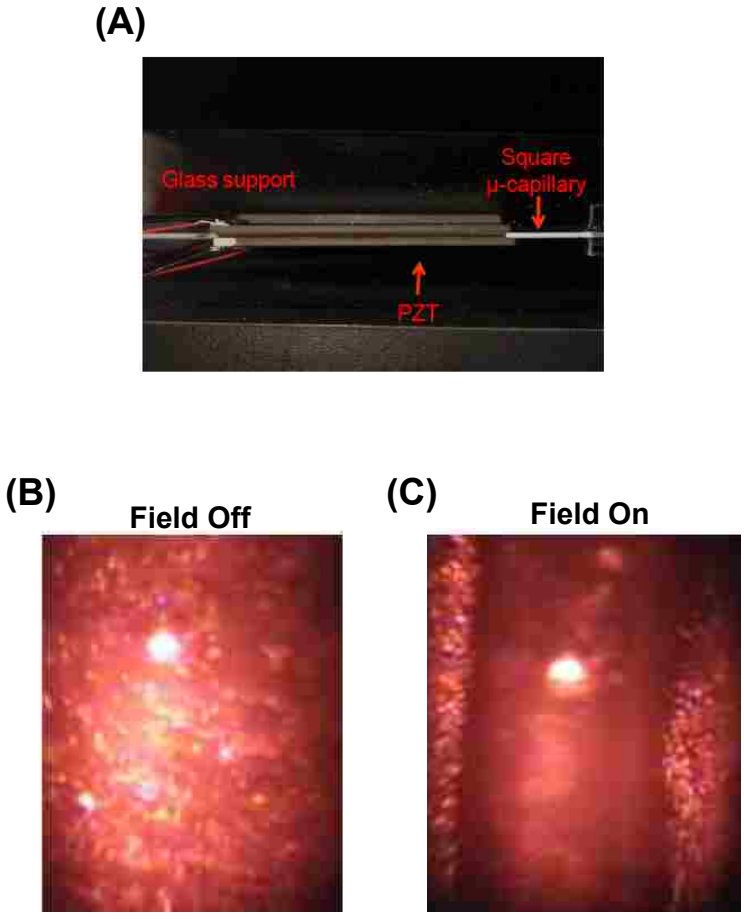

Figure 5.4 Elastomeric particles synthesized from a low molecular weight PDMS (1:1 ratio of prepolymer to crosslinking agent) are shown to function as negative acoustic contrast particles using a low-cost glass square microcapillary that functions as an acoustofluidic device. (A) Image of a square glass microcapillary that has been converted into an acoustofluidic chip by way of coupling PZTs to the surface. Elastomeric particles suspended in the microchannel with the field (B) off and then (C) on. Note: Image of the square glass microcapillary (A) was taken by Menake Piyasena and is used with his granted permission.

Once an ultrasonic acoustic pressure standing wave field was applied (3.101 MHz at 50 $V_{peak\text{-}peak}$), elastomeric particles were rapidly focused to pressure antinodes at the side walls of the microchannel; however there does appear to be a particle aggregate at the pressure antinode along the right side of the microchannel wall (Figure 5.4C). The focusing of elastomeric particles at the pressure antinodes clearly demonstrates the negative acoustic contrast properties of elastomeric particles that are synthesized from a low molecular weight PDMS.

To determine if elastomeric particles synthesized from low molecular weight PDMS could be separated from positive acoustic contrast particles, elastomeric particles (~2.5 x 10^7 particles/mL) were mixed with commercially-available polystyrene particles (~6.4 x 10^5 particle/mL) and flowed (100 μL/min) through a square glass microcapillary acoustofluidic device. The mixture was dispersed while being flowed with the acoustic field off (Figure 5.5A). Upon activation of the ultrasonic acoustic pressure standing wave field (3.101 MHz at 50 $V_{peak\text{-}peak}$) elastomeric particles rapidly focused to pressure antinodes while polystyrene particles were focused to the central pressure node of the microchannel (Figure 5.5B). The activation of the acoustic pressure standing wave field demonstrated that 1) elastomeric particles synthesized from low molecular weight PDMS possess negative acoustic contrast properties and can be separated from positive acoustic contrast particles (polystyrene); and 2) once these elastomeric particles are focused at pressure antinodes they experience a significant decrease in their flow velocity. These results indicate that elastomeric particles synthesized from a low molecular weight PDMS (1:1 ratio of prepolymer to crosslinking agent) function as negative acoustic

contrast particles and can be separated from positive acoustic contrast particles (polystyrene particles).

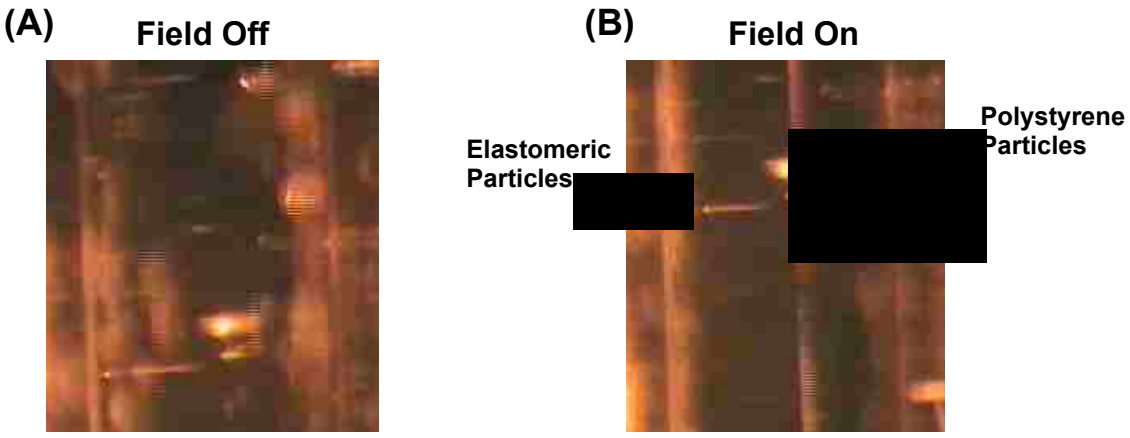

Figure 5.5 Elastomeric particles synthesized from low molecular weight PDMS (1:1 ratio of prepolymer to crosslinking agent) function acoustically separated from positive acoustic contrast particles. A mixture of elastomeric particle and polystyrene particles flowed (100 μL/min) in an acoustofluidic device with the acoustic field (A) off and then (B) on.

Conclusions and Future Directions

Elastomeric particles that possess negative acoustic contrast properties can be synthesized from two varieties of PDMS elastomers, Sylgard 184 (specific gravity 1.03) and a low molecular weight PDMS (specific gravity ~ 0.97). Elastomeric particles synthesized from Sylgard 184 and low molecular weight PDMS were successfully separated from positive acoustic contrast particles (blood cells and polystyrene) upon activation of the ultrasonic acoustic pressure standing field. The negative acoustic contrast property of PDMS-based elastomeric particles has potential to be used in capture assays where the capturing of specific analytes is performed on elastomeric capture

microparticles (ECμPs) in solutions containing particulate matter that functions as positive acoustic contrast particles (e.g., biological cells, commercially-available particles, plastics, sand, and metals).[1] Upon capturing and concentrating the desired analyte on the surface of the ECμPs, the application of an ultrasonic acoustic standing wave field could be used to separate and concentrate ligand-bound ECμPs from background generating particles that function as positive acoustic contrast particles.[2] Once ligand-bound ECμPs are separated and concentrated at pressure antinodes, and the background generating particles at pressure nodes, it may be possible to perform on-chip flow cytometry or collect and remove the concentrated ligand-bound ECμPs from the acoustofluidic device prior to performing spectroscopic analysis (e.g., flow cytometry, mass spectrometry).[2]

Acoustic focusing of elastomeric particles at the pressure antinodes along the side walls of the microchannel has a tendency to form isolated aggregates in the presence of no flow or reduced flow rates. The generation of these aggregates at pressure antinodes could have a negative impact on the laminar flow profile within the microchannel, and thus make it more difficult to flow focused particles into collecting outlet channels (e.g., trifurcation). It seems possible that these formed aggregates or clumps at the side walls of the microchannel maybe caused in part by secondary acoustic forces (Bjerknes attractive forces). As a result of elastomeric particles (Sylgard 184 and low molecular weight PDMS) having a density that is similar to their surrounding medium, any secondary forces experienced by the elastomeric particles would probably be attractive Bjerknes forces. However, in a video showing the focusing of elastomeric particles synthesized from low molecular weight PDMS to pressure antinodes, it can be observed with the acoustic field on (without flow) that elastomeric particles that appear relatively distant

from the densely populated clumps at the side pressure antinode, appear to be migrating in the direction of the formed clumps. It also appears that there may be periodic clumping that is occurring throughout the microchannel. Previous results published by Evander et al.,[7] demonstrated that it was possible to produce an acoustic standing wave down the length of the microchannel. This result, along with the periodic clumping of elastomeric particles at the pressure antinodes along the side walls of the microchannel, may be due in part to an acoustic standing wave that is being propagated down the length of the microchannel. An experimental method to determine if there is an acoustic standing wave being propagated down the microchannel is to perform the acoustic focusing of the elastomeric microparticles multiple times and observe if the elastomeric particle clumps form at the same positions at the pressure antinodes as previously noted. If the clumps form at precisely the same position down the entire length of the microchannel, then there would certainly be an increased probability that an acoustic standing wave was being propagated down the microchannel.

A reduction of these clumping forces may also be possible by lowering the voltage applied on the actuating PZT which directly affects the pressure amplitude and therefore the acoustic forces that are exerted on the particles.[3] Another option is to increase the flow rate to a level that still maintains laminar flow but generates enough shear forces to overcome these clumping forces that are causing aggregation at the side walls. A high concentration of particles may also increase the clumping forces that are generated during the application of the acoustic field.[3] Flow rates, voltages applied on the actuating PZT, and the concentration of the particles can all be experimentally

controlled to determine if modification to these variables can minimize the amount of aggregation that is occurring during the activation of an acoustic standing wave field.

References

1. Kaduchak, G.; Ward, M. D., Apparatus for separating particles utilizing engineered acoustic contrast capture particles. **2011**, Patent No., US 8,083,068 B2.

2. Cushing, K. W.; Piyasena, M. E.; Carroll, N. J.; Maestas, G. C.; Lopez, B. A.; Edwards, B. S.; Graves, S. W.; Lopez, G. P., Elastomeric Negative Acoustic Contrast Particles for Affinity Capture Assays. *Analytical chemistry* **2013**, *85* (4), 2208-2215.

3. Laurell, T.; Petersson, F.; Nilsson, A., Chip integrated strategies for acoustic separation and manipulation of cells and particles. *Chemical Society Reviews* **2007,** *36* (3), 492-506.

4. Crum, L.A., Acoustic force on a liquid droplet in an acoustic stationary wave, *J. Acoust. Soc. Am.* 1971, *50*, 157–163.

5. Austin Suthanthiraraj, P. P.; Piyasena, M. E.; Woods, T. A.; Naivar, M. A.; López, G. P.; Graves, S. W., One-dimensional acoustic standing waves in rectangular channels for flow cytometry. *Methods* **2012,** *57* (3), 259-271.

6. Saarela, V.; Franssila, S.; Tuomikoski, S.; Marttila, S.; Östman, P.; Sikanen, T.; Kotiaho, T.; Kostiainen, R., Re-usable multi-inlet PDMS fluidic connector. *Sensors and Actuators B: Chemical* **2006,** *114* (1), 552-557.

7. Evander, M.; Lenshof, A.; Laurell, T.; Nilsson, J., Acoustophoresis in wet-etched glass chips. *Analytical chemistry* **2008,** *80* (13), 5178-5185.

Chapter 6 Elastomeric Negative Acoustic Contrast Particles for Affinity Capture Assays

Kevin W. Cushing,[a,b] Menake E. Piyasena,[a] Nick J. Carroll,[a,†] Gian C. Maestas,[a] Beth Ann López,[a] Bruce S. Edwards,[d] Steven W. Graves,*[,a,b] and Gabriel P. López,*[a,c]

[a] Center for Biomedical Engineering, Department of Chemical and Nuclear Engineering, The University of New Mexico, Albuquerque, NM 87131, USA.
[b] National Flow Cytometry Resource, Los Alamos National Laboratory, Los Alamos, NM 87545, USA.
[c] NSF Research Triangle Materials Research Science and Engineering Center, Depts. of Biomedical Engineering and Mechanical Engineering & Materials Science, Duke University, Durham, NC 27708, USA.
[d] Department of Pathology, School of Medicine, The University of New Mexico, Albuquerque, NM 87131, USA.

[†]*Current Address: Harvard School of Engineering and Applied Sciences, Pierce Hall, 29 Oxford Street, Cambridge, MA 02138, USA.*

* Corresponding authors: Gabriel P. López
NSF Research Triangle MRSEC
Duke University
Box 90271
Durham, NC 27708, USA.
Email: gabriel.lopez@duke.edu
Phone: 919-660-5435

Steven W. Graves
Center for Biomedical Engineering
MSC01 1141
1 University of New Mexico
Albuquerque, NM 87131-0001, USA
Email: graves@unm.edu
Phone: 505-277-2043

(Published: *Anal. Chem.*, **2013**, *85* (4), pp 2208–2215)

Abstract

This report describes the development of elastomeric capture microparticles (ECμPs) and their use with acoustophoretic separation to perform microparticle assays via flow cytometry. We have developed simple methods to form ECμPs by crosslinking droplets of common commercially available silicone precursors in suspension followed by surface functionalization with biomolecular recognition reagents. The ECμPs are compressible particles that exhibit negative acoustic contrast in ultrasound when suspended in aqueous media, blood serum or diluted blood. In this study, these particles have been functionalized with antibodies to bind prostate specific antigen and immunoglobulin (IgG). Specific separation of the ECμPs from blood cells is achieved by flowing them through a microfluidic acoustophoretic device that uses an ultrasonic standing wave to align the blood cells, which exhibit positive acoustic contrast, at a node in the acoustic pressure distribution while aligning the negative acoustic contrast ECμPs at the antinodes. Laminar flow of the separated particles to downstream collection ports allows for collection of the separated negative contrast (ECμPs) and positive contrast particles (cells). Separated ECμPs were analyzed via flow cytometry to demonstrate nanomolar detection for prostate specific antigen in aqueous buffer and picomolar detection for IgG in plasma and diluted blood samples. This approach has potential applications in the development of rapid assays that detect the presence of low concentrations of biomarkers in a number of biological sample types.

Introduction

Acoustic microfluidic systems are of significant utility in the analysis and separation of a number of biological samples, including blood.[1-4] Whole blood comprises 45-50% hematocrit (blood cell volume) and a plethora of serum proteins. Many serum proteins are biomarkers for a number of pathologies, including cancers, inflammatory responses, and infectious diseases.[5-9] Sensitive and rapid quantification of such biomarkers is very useful for early diagnoses and for monitoring the therapeutic success of many clinical treatments.[10] To detect and quantify low concentrations of serum biomarkers, it is often necessary to remove blood cells prior to analysis.[11] This is most commonly performed via centrifugation,[12,13] which is time consuming, labor intensive, and requires milliliters of blood. Once the serum protein containing supernatant is obtained, immunoassays can be performed to detect and quantify low concentrations of the desired biomarker present in the serum,[14,15]. Other more specific protein purification and enrichment methods such as: 2-D gel electrophoresis, chromatography, precipitation or filtration can also be performed prior to analysis, for example using mass spectrometry.[16-19]

Acoustic standing waves offer an alternative to centrifugation for blood cell separation. Initial work on this approach concentrated blood cells, which generally exhibit positive acoustic contrast, to nodes in a standing wave where they aggregated and sedimented out of solution to leave clarified plasma.[20] Based on similar acoustic principles, many acoustophoretic flow through systems have been developed by Laurell *et al.* to separate blood cells from serum, lipids, and platelets.[21-26] In general this approach uses flow channels in a rigid substrate to which a acoustic driver (e.g., a PZT crystal) is

attached to generate a standing acoustic wave across the channel. Drive frequencies are chosen to match the dimensions of the channel such that the wavelength of the standing wave has fractional harmonics across the channel (e.g., 1/2l, 3/2l, etc.), which creates acoustic nodes and antinodes across the channel. Cells are concentrated to the nodes and separated from the plasma by collecting the focused cells downstream in microfluidic channels. As described below there is a significant dependence of particle size to the magnitude of the force imparted on a particle by the standing wave, which allows for size dependent acoustophoretic fractionation of components such as platelets.[25] Of interest here is the observation that particles exhibiting negative contrast, such as lipids, can be separated by collecting them as they are driven to the antinode.[21,22,23]

The primary acoustic force on particles in an acoustic standing wave field can be calculated from the following equations.[22,23,27]

$$F_p = -\left(\frac{\pi p^2 V_p \beta_o}{2\lambda}\right)\varphi(\beta,\rho)\sin(2kx) \qquad \textbf{(1)}$$

$$\varphi(\beta,\rho) = \frac{5\rho_p - 2\rho_o}{2\rho_p + \rho_o} - \frac{\beta_p}{\beta_o} \qquad \textbf{(2)}$$

The magnitude of the primary acoustic force is directly proportional to the volume of the particles (V_p), the pressure amplitude of the field (p^2) the applied frequency ($1/\lambda$), and the acoustic contrast factor $\varphi(\beta,\rho)$. The value of the acoustic contrast factor depends on the density of the particles (ρ_p) and the suspension media (ρ_o) and the compressibility of the particles (β_p) and the suspension media (β_o). If $\varphi(\beta,\rho)$ has a positive value then the acoustic field will exert a time-averaged force moving particles to

the acoustic pressure node of a standing wave (positive contrast particles). However, if $\varphi(\beta, \rho)$ has a negative value then the acoustic field will exert a time-averaged force moving particles to acoustic pressure antinodes in a standing wave (negative contrast particles). A more detailed description of the acoustic forces exerted on particles under an acoustic standing wave field can be found in Bruus et al.[28]

In this report we demonstrate facile synthesis of elastomeric particles from a common water insoluble elastomer, crosslinked polydimethylsiloxane (Dow Corning Sylgard 184), which we hypothesized would (i) exhibit negative acoustic contrast, and thus (ii) allow their continuous separation from blood cells in an acoustic microfluidic chip. We introduce the concept of negative contrast elastomeric capture microparticles (ECμPs) and demonstrate the use of ECμPs in model antigen and antibody capture assays conducted in buffer, plasma and diluted whole blood in an acoustic sample preparation chip. As ECμPs are separated continuously from blood cells they are collected into fractions, which are then analyzed using flow cytometry.[29] This continuous separation of ECμPs via acoustophoresis has the potential to greatly simplify immunoassays by obviating the need for centrifugation and lysis steps that are normally used to remove the background generating blood cells that are present at $5x10^9$ cells per mL. Finally, simple and rapid separations, such as acoustophoretic ECμPs displaying high affinity antibodies, have the potential to improve the sensitivity of detection for biomarkers by reducing the number of sample preparation steps that can lead to non-specific loss of biomarkers of interest. [30] This analysis could be performed directly on ECμPs (e.g., through particle based immunoassays and flow cytometric detections) or through other subsequent analysis methods (e.g., mass spectrometry) on separated ECμPs.

Materials and Methods

Acoustic Focusing and Separation

Samples were flowed (45 μL/min) through the acoustic sample preparation chip (see supplementary information (SI) for details of fabrication of the chip) using a microsyringe pump (Nexus 3000, Chemyx Inc. Stafford, TX). To focus and separate particles and blood cells, the PZT was actuated using a waveform generator (33250A, Agilent, Santa Clara, CA) at a frequency of 2.91 MHz at 10 volts peak-to-peak. To monitor and image the focusing and separation of particles and blood cells, commercially available Nile Red (NR)-polystyrene particles (PS) (Spherotech Inc., Lake Forest, IL) were used, and Nile Red dye (Sigma-Aldrich, St. Louis, MO) was used to label elastomeric particles and blood cells; this was accomplished by incubation in an aqueous Nile Red solution (100 μM) in 1 mL of phosphate buffered saline (1X PBS with 7.4 pH: 10 mM Na_2HPO_4; 1 mM KH_2PO_4; 138 mM NaCl; 3 mM KCl) for 30 minutes followed by centrifugal washing (PBS) to remove unbound dye. Focusing and separation of particles (and blood cells) was monitored and imaged using an epifluorescence microscope (Zeiss Axio Imager) and a Luca S EMCCD camera (Andor Technology, Belfast N., Ireland) with Andor imaging software (Andor-Solis). This software was used to perform intensity analysis of line scans across the width of the microchannel. The average of 17 scans from bottom to top was used to generate fluorescence histograms using PRISM® software (version 5.0b, GraphPad).

Synthesis of Elastomeric Particles

Sylgard 184 (1 g, 10:2 ratio of PDMS prepolymer to crosslinking agent) (Dow Corning Corp., Midland, MI) was emulsified in 10 mL of ultrapure water (18.2 MΩ•cm

@ 25 °C; Synergy®, EMD Millipore), using a homogenizer (Power Gen 125, Fisher Scientific) set at 6K RPM for ~ 60 seconds. The droplets were cured at 100 °C for ~ 1 hour to form crosslinked elastomeric particles. Elastomeric particles were imaged using bright field microscopy (BH-2, Olympus) and a 4300 cool pix camera (Nikon). The scale bar was calibrated based on standardized monodisperse particles (mean = 30.1 μm; standard deviation = ± 2.1 μm; and a coefficient of variation = 6.6%) (Thermo Scientific). A Coulter counter (Z2 Coulter Particle Count and Size Analyzer, Becton Dickinson) was used to determine the concentration and the size distribution of the polydisperse elastomeric particles.

Biofunctionalization of Polydisperse Elastomeric Particles

Elastomeric particles (2.5×10^7) where incubated in 1 μM avidin (Molecular Probes, Eugene, Oregon) in PBS for 30 minutes with continuous rocking at room temperature. They were then centrifugally (2900 g for 5 minutes) washed and resuspended in washing/blocking buffer (PBS with 0.1 % BSA). A biotinylated mouse anti-human prostate specific antigen (PSA) monoclonal antibody (capture antibody; HyTest Ltd., Turku, Finland; catalog # 4P33B Mab8A6; lot # 10/11-P33B-8A6) was added to make a 6 nM solution; the solution was incubated for 30 minutes with rocking at room temperature. The resulting ECμPs were centrifugally washed and resuspended in the washing/blocking buffer.

Separation Efficiency Measurements

1.5×10^5 ECμPs were fluorescently labeled with a goat anti-mouse antibody (PE) and mixed with 0.1% porcine whole blood in 200 μL of total volume (diluted in PBS with 0.1% BSA). The initial fraction of ligand-bound ECμPs to porcine blood cells was

determined based on flow cytometry gating ((fluorescence (585 ± 20 nm) vs. forward side scatter). The mixture was then flowed (45 μL/min) through the acoustic sample preparation chip with the acoustic field on (2.91 MHz at 10 Volts peak-to-peak) and the 3 separated fractions at the trifurcation were collected through the outlet silicone tubing. Once collected, the fractions were analyzed in an Accuri C6 flow cytometer where gating was performed, as mentioned-above, to determine the percentages of ligand-bound ECμPs and porcine blood cells in each of the collected fractions.

Preparation of Plasma

1 mL samples of whole porcine blood containing sodium heparin (Bioreclamation) were centrifuged in 1.7 mL polypropylene microcentrifuge tubes using a Galaxy 14D microcentrifuge (VWR, Radnor, PA) at 2000 g for 10 minutes. Supernatant (plasma) was carefully pipetted into microcentrifuge tubes and stored in 0.5 mL aliquots at -20 °C.

PSA Titration in Physiological buffer

5 x 10^5 ECμPs –elastomeric particles functionalized with mouse anti-human PSA monoclonal antibodies (HyTest Inc., Turku, Finland)– were incubated with different concentrations (0, 1, 5, 10, 20, 30 nM) of prostate specific antigen (PSA) (Meridian Life Sciences Inc., Memphis, TN) in 200 μL of washing/blocking buffer for 30 minutes with continuous rocking at room temperature. Without washing, enough mouse anti-human PSA monoclonal antibody-FITC (detection antibody) (HyTest Inc., Turku, Finland) was added to make a 1 nM solution that was incubated for 30 minutes with rocking at room temperature. The ECμPs were then analyzed with an Accuri C6 flow cytometer without washing. All bioassay data was fitted to a one-site binding curve with the following

equation, $Y = \frac{F_{max}*x}{K_d+x}$ using PRISM (Graph Pad) version 5.0b. The dependent variable (Y) is the median fluorescence intensity (MFI, y-axis), the independent variable (x) is the ligand analyte concentration (x-axis), K_d is the dissociation constant and F_{max} is the maximum MFI.

IgG-PE Titration in 10% Plasma

5 x 10^5 ECμPs –elastomeric particles functionalized with mouse anti-human PSA monoclonal antibodies (Abcam, Cambridge MA)– were incubated with different concentrations, (0, 21, 42, 84, 168, 336, 672 pM) of goat anti-mouse IgG-phycoerythrin (PE) (Abcam, Cambridge MA) in 200 µL of 10% volume porcine plasma (diluted in the washing/blocking buffer) for 30 minutes with continuous rocking at room temperature. ECμPs were then analyzed in an Accuri C6 flow cytometer without prior washing.

Titration in 0.1% Blood, Acoustic Separation, and Flow Cytometry

ECμPs –again, elastomeric particles (5 x 10^5) functionalized with mouse anti-human PSA monoclonal antibodies– were incubated with different concentrations (0, 21, 42, 84, 168, 336, 672 pM) of goat anti mouse IgG-(PE) (Abcam, Cambridge MA) in 200 µL of 0.1 % volume whole porcine blood (porcine blood was diluted in washing/blocking buffer) for 30 minutes with continuous rocking at room temperature. Samples were then flowed (45 µL/min) through the acoustic sample preparation chip with the acoustic field on (2.91 MHz; 10 V peak-to-peak supplied to the PZT) and collected through the outlet silicone tubings. Once collected, ligand-bound ECμPs were analyzed in an Accuri C6 flow cytometer without prior washing.

Flow Cytometry Gating in Bioassays

Flow cytometry (Accuri C6) data on ECμPs was acquired by gating on forward and side scatter parameters to exclude debris and doublets. The median fluorescence intensity of gated ECμPs was used to formulate the binding curves shown within the manuscript.

RESULTS

Particle Separation Approach

Particles (or cells) with different acoustic contrast properties can be focused (i.e., acoustically positioned to nodal or antinodal planes) and then separated using an acoustic sample preparation chip with a downstream trifurcation (Figure 6.1a) (see SI Figure S6.1 for an image of an actual acoustic sample preparation chip).[22] After acoustic focusing, laminar flow carries particles continuously into outlet channels at the trifurcation for collection (Figure 6.1a). The attached acoustic transducer (PZT) has an appropriate size to allow resonance at the frequency (2.91 MHz) that corresponds to a wavelength that is twice the width (252 μm) of the acoustic focusing channel (Figure 6.1b). Thus a resonant acoustic standing wave is established in the fluid-filled cavity of the chip and the field exerts a time-averaged force that focuses positive contrast particles (e.g., blood cells) to the center pressure node and negative contrast particles (e.g., elastomeric particles) to the two pressure antinodes at the sides of the channel (Figure 6.1b).[21,22]

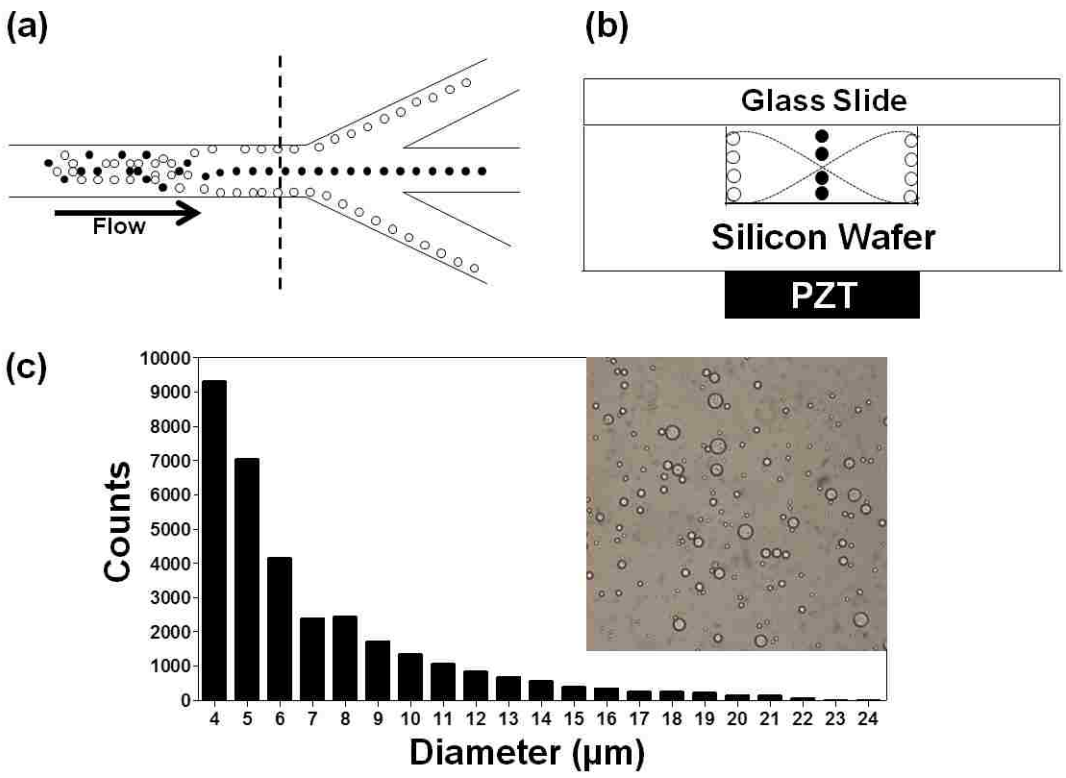

Figure 6.1 (a) Schematic diagram depicting the separation approach for elastomeric negative acoustic contrast particles (white) from positive acoustic contrast particles (e.g., blood cells) (black) at the trifurcation in a silicon acoustic sample preparation chip. (b) Cross-section, at dashed line in (a), of the chip, with the positive contrast particles focused at the pressure node and the negative contrast particles focused at the pressure antinodes under an acoustic standing wave field. Note: Images are not drawn to scale. (c) Bright field image and size histogram of PDMS-based elastomeric particles prepared by bulk emulsification.

Particle Synthesis

Polydisperse elastomeric particles were synthesized using an oil-in-water bulk emulsion process without the use of detergent. The synthesis method is straightforward and allows polydisperse elastomeric particles to be rapidly synthesized (~1 hour) with a bulk concentration of 1.3 x 10^8 particles/mL. The diameters of particles produced by this method varied from submicron to approximately 21 μm in diameter (Figure 6.1c). As prepared, these particles were unstable in regards to particle aggregation; adsorption of avidin allowed the elastomeric particles to maintain stability during centrifugal washes (2900 g for 5 minutes) performed in a washing/blocking buffer.

Acoustic Focusing and Separation

Acoustic focusing experiments were performed on Nile Red labeled ECμPs (NR-ECμPs) to examine their acoustic contrast properties and the optimal operating conditions of the acoustic sample preparation chip (e.g., particle concentrations, flow rates, resonance frequency, and applied voltage on the actuating PZT). The field of view of the epifluorescence microscopic objective (2.5x, NA of 0.3) was large enough to capture the entire width (252 μm) of the central micro-channel in the acoustic sample preparation chip and was positioned to capture fluorescent images in the central micro-channel upstream of the trifurcation. NR-ECμPs (2.5 x 10^7 particle/mL) were flowed (45 μL/min) continuously through the acoustic sample preparation chip with the acoustic field off (Figure 6.2a) and then on (Figure 6.2b); the concomitant increase in Nile Red fluorescence at the sides of the micro-channel, indicated an increase in the concentration of NR-ECμPs at the pressure antinodes. Histograms of the average fluorescence intensity measured across the channel width confirm the relatively uniform distribution of

fluorescence particles across the channel width in the absence of the acoustic field (Figure 6.2a), and the focusing of the NR-ECμPs at the side-walls of the channels upon imposition of the acoustic field (Figure 6.2b). The NR-ECμPs thus exhibit negative acoustic contrast and are focused to the pressure antinodes along the sides of the micro-channel walls upon imposition of a resonant frequency (2.91 MHz) to the acoustic sample preparation chip.

To evaluate the ability of ECμPs to be acoustically separated from positive contrast particles and the ability of the acoustic sample preparation chip to support effective separations, NR-ECμPs (2.5 x 10^7 particles/mL) were separated from positive contrast, Nile Red labeled polystyrene particles (NR-PS: 2.5 x 10^6 particles/mL) (Figure 6.2c). Further, to demonstrate that ECμPs could be continuously separated from blood cells NR-ECμPs (2.5 x 10^7 particles/mL) were separated from Nile Red stained blood cells (NR-blood cells: 0.1% volume whole porcine blood) (Figure 6.2d) using the same acoustic set-up described above.

Separation at Trifurcation

As a result of laminar flow within the micro-channel (R_e = 7.4), acoustically focused ECμPs flow directly into the peripheral outlet channels at the trifurcation for collection. NR-ECμPs (2.5 x 10^7 particles/mL) were continuously flowed (45 µL/min) through the acoustic sample preparation chip. Figure 4.3 shows images at the trifurcation, with the field off (Figure 6.3a) and then on (Figure 6.3b); the concomitant increase in Nile Red fluorescence at the sidewalls of the side outlet channels of the trifurcation demonstrated that ECμPs were acoustically manipulated into side outlet channels for continuous collection.

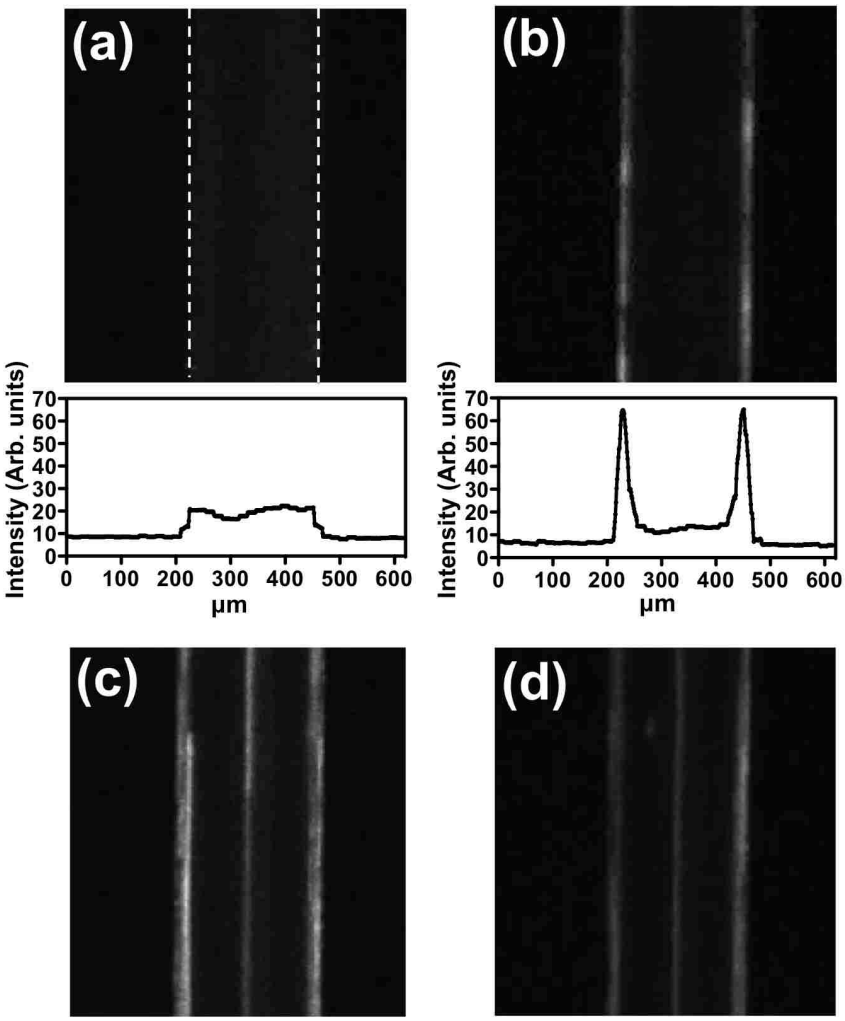

Figure 6.2 ECμPs function as negative contrast particles and can be separated from positive contrast particles using an acoustic sample preparation chip. These images were captured via an epifluorescence microscope with a 2.5x objective. Each sample was flowing at 45 µL/min. Fluorescence microscopy images along with histograms of average intensity profiles for Nile Red (NR) stained ECμPs with the field (a) off and then (b) on. (c) NR-ECμPs separated from NR-PS particles with the field on. (d) NR-ECμPs separated from NR-blood cells with the field on. Note: white dashed lines in (a) indicate micro-channel borders.

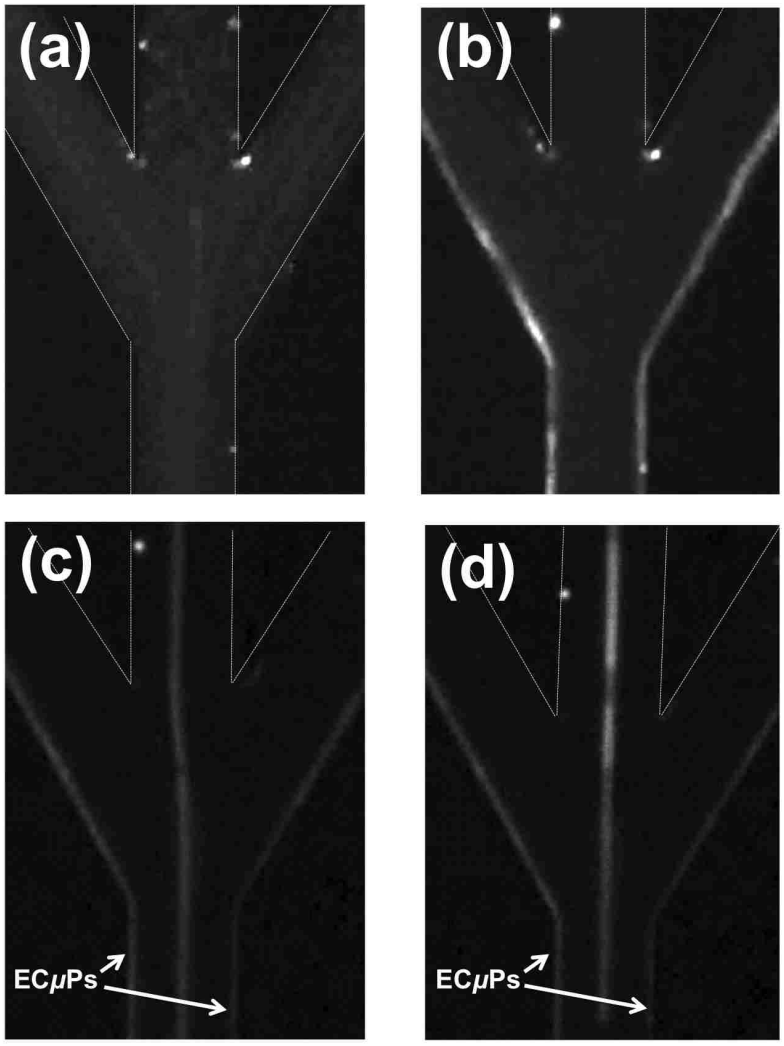

Figure 6.3 (a) Fluorescence microscopy images of NR-ECμPs with the field (a) off and then (b) on. (c) NR-ECμPs separated from NR-PS particles with the field on. (d) NR-ECμPs separated from NR-blood cells (0.1% volume whole porcine blood) with the field on. Each sample was flowing at 45 μL/min. Note: white dashed lines indicate micro-channel borders that are not otherwise visible due to presence of NR-ECμPs.

To evaluate whether ECμPs can be separated, concentrated, and collected apart from positive contrast particles, polydisperse NR-ECμPs (2.5×10^7 particles/mL) were continuously separated from NR-PS particles (2.5×10^6 particle/mL) at the trifurcation (Figure 6.3c). Laminar flow also allowed acoustically focused and separated NR-ECμPs and NR-blood cells (from 0.1% porcine whole blood) to maintain focusing and allow shunting into designated outlet channels at the trifurcation for collection. Focused NR-ECμPs flowed into side outlet channels and NR-blood cells flowed directly into the center outlet channel at the trifurcation (Figure 6.3d).

ECμPs used in Bioassays

Biospecific Functionalization of Negative Contrast Particles

Biofunctionalization of elastomeric particles was accomplished by non-specifically adsorbing avidin to the hydrophobic surface of the elastomeric particles. To demonstrate their specific biotin-binding ability, avidinylated elastomeric particles were titrated with biotin-4-fluorescein; controls were performed where avidinylated elastomeric particles were pre-incubated with free biotin (biotin-block) followed by incubation with biotin-4-fluorescein (see SI Figure S6.2). Our results indicate that (i) avidin protein can be non-specifically adsorbed to bare elastomeric particles, and (ii) adsorbed avidin protein maintains biotin-binding functionality and binds biotin with minimal non-specific adsorption. Once elastomeric particles have been functionalized with avidin they can be further functionalized with a biotinylated capture antibody (see SI Figure S6.3). These results demonstrate that negative contrast elastomeric particles can be biofunctionalized using simple avidin/biotin conjugation reagents.

PSA Sandwich Assays Performed in Physiological Buffer

ECμPs were used in a titration assay for prostate specific antigen (PSA) in PBS (0.1 % BSA) in which anti-human PSA monoclonal antibody-FITC was used as the secondary (detection) antibody in a sandwich assay configuration. The assay data exhibited high signal-to-noise (Figure 6.4a) and very low background indicative of biospecific analysis and were fit to a one-site binding curve (R^2=0.89) where saturation was approached near 30 nM PSA. To estimate the limit of detection (LOD) for this analysis, a propagation of errors model was used as described by Long and Winefordner.[31] First, the standard deviation of the blank samples (S_B) was determined ($S_B = 1568;\ n = 3$). Next, a line was fit to points from triplicate determinations that represented the most linear region of the binding curve (PSA concentrations: 0, 1, and 5 nM PSA). The best fit for a straight line was calculated by non-linear regression to a straight line model using PRISM version 5.0 software (GraphPad). Calculated best fit values included the slope (m = 2903) and MFI axis intercept (i= 3706) of the line as well as standard errors for each (Sm = 1605 and Si = 4724, respectively). These values were used to calculate LOD using the equation $LOD = \frac{k\left(S_B^2+S_i^2+\left(\frac{i}{m}\right)^2 S_m^2\right)^{1/2}}{m}$ in which k =3, the number of standard deviations of separation between two points that equaled a 99% probability of being different. The LOD was calculated to be approximately 6 nM.

IgG-PE Binding Assays Performed in 10% Porcine Plasma

To examine biospecific binding of ECμPs in a complex solution of proteins, an IgG capture assay was performed in 10% whole porcine plasma (diluted with 0.1% BSA in PBS). ECμPs were used in a titration binding assay for a polyclonal goat anti-mouse

IgG-phycoerythrin (PE). The standard assay data exhibited high signal-to-noise (Figure 6.4b) and very low background indicative of biospecific adsorption and were fitted to a one-site binding curve. This fit well (R^2=0.99) but provided a linear response implying that we did not achieve saturation over our titration range. The calculated *LOD* using propagation of errors ($k = 3;\ S_B = 16;\ S_i = 237.5;\ S_m = 0.8145;\ m = 47.75;\ i = 454.6$) for all 6 points (0, 21, 42, 187, 334, 668 pM IgG-PE) on the binding curve, was calculated to be approximately 15 pM.

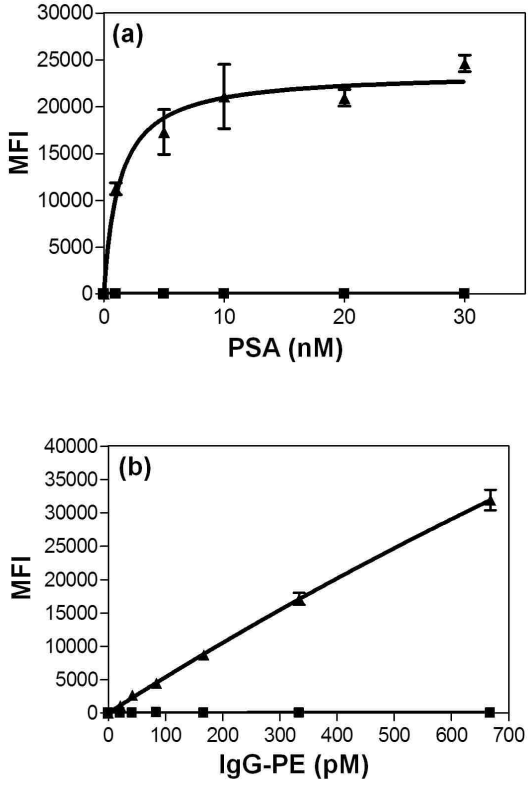

Figure 6.4 ECμPs as platforms for protein capture assays in flow cytometry. Note: (▲) denotes ECμPs with capture antibody and (■) denotes particles without capture antibody. (a) ECμPs used in a sandwich assay for prostate specific antigen (PSA) in physiological buffer (PBS). (b) ECμPs used in a binding assay for goat anti-mouse IgG-phycoerythrin performed in 10% volume porcine plasma diluted with PBS. Note: all data points were obtained from triplicate experiments analyzed by gated flow cytometric analysis. Error bars represent the standard deviation of the mean for 3 separate determinations of median fluorescence intensity.

ECμPs and Blood Cells Collected from Trifurcation

Ligand-bound ECμPs (Ligand = goat anti mouse IgG antibody-PE) were separated from porcine blood cells using an acoustic sample preparation chip. To determine the effectiveness of separating ECμPs from blood cells, separation efficiency measurements were performed by analysis via flow cytometry of fractions collected from each leg of a trifurcation. Control experiments (see SI Figure S6.4) were performed to determine gating regions in flow cytometry scatter plots (fluorescence (585 ± 20 nm) versus forward scatter) that allow identification and quantitation of ligand-bound ECμPs and blood cells. A mixture (73% blood cells; 27% ligand-bound ECμPs, Figure 6.5a) was prepared and then flowed through the acoustic sample preparation chip with the acoustic field on. The outputs from the two peripheral outlet channels were collected and consisted mostly of ligand-bound ECμPs (95-96% ligand-bound ECμPs, 4-5% blood cells; see Figures 6.5b,d); whereas the output from the central outlet channel consisted mostly of blood cells (98% blood cells, 2% ligand-bound ECμPs; see Figure 6.5c). Our results thus indicate that ligand-bound ECμPs can be efficiently separated away from blood cells using an acoustic sample preparation chip with a downstream trifurcation.

IgG-PE Binding Performed in 0.1% Blood with Acoustic Separation Prior to Assay

ECμPs were used in an IgG-PE assay in which IgG capture was performed in 0.1 % porcine blood prior to separation from blood cells, collection of the ECμPs using an acoustic sample preparation chip, and their subsequent analysis via flow cytometry. The blood was diluted to 0.1% (or 5 x 10^6 cells/ml) to eliminate acoustic scattering from cells that is known to occur in whole or high concentration blood.[32] High concentrations of red cells under an acoustic standing wave field can generate acoustic scattering that

results in secondary acoustic forces (i.e., interparticle forces on red cells).[32] These secondary acoustic forces can cause red cells to aggregate or experience repulsive forces,[32] and thus result in decreased focusing and lower separation efficiencies. Future work will examine the maximum concentration of blood that can be used in conjunction with ECμPs. Nonetheless, the blood concentrations used are consistent with those used in ELISA assays.[33] The assay data exhibited high signal-to-noise and very low background indicative of biospecific binding and were fit to a one-site binding curve (R^2=0.99) where we had a near linear response implying that we did not reach saturation over our titration range (Figure 6.5e). The calculated LOD using propagation of errors ($k = 3;\ S_B = 184;\ S_i = 424.4;\ S_m = 1.456;\ m = 21.53;\ i = 513.3$) for all 6 points ($0, 21, 42, 187, 334, 668$ pM IgG-PE) on the binding curve, was calculated to be approximately 65 pM.

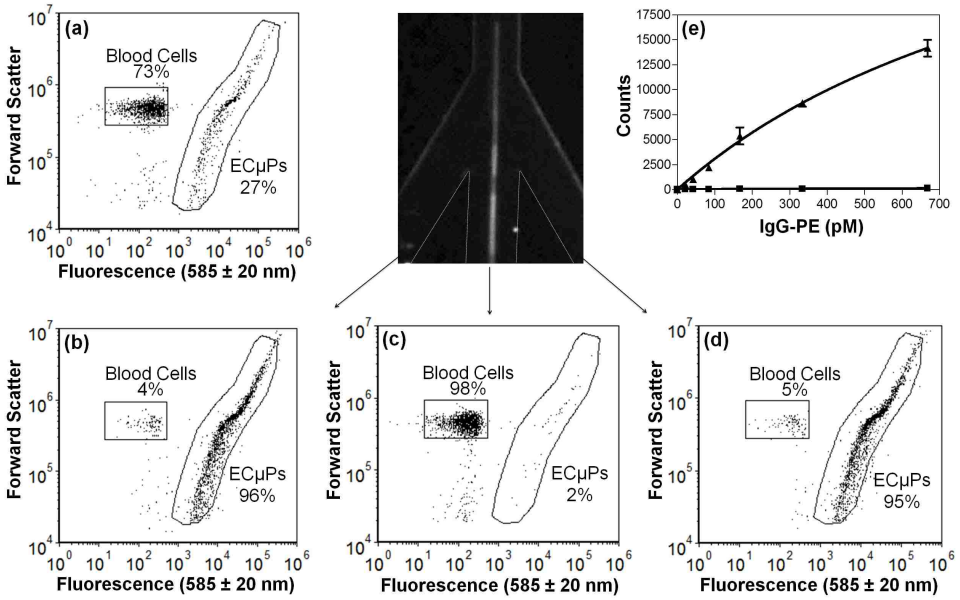

Figure 6.5 ECμPs used in an assay in diluted blood where acoustic separation and collection was achieved using the acoustic sample preparation chip prior to flow cytometry analysis. (a) Flow cytometry scatter plot (forward scatter versus fluorescence (585 ± 20 nm)) showing the initial mixture (inlet) of ligand-bound ECμPs and blood cells. (b) Scatter plot of the collected fraction of the left peripheral outlet channel. (c) Scatter plot of the collected fraction from the central outlet channel. (d) Scatter plot of the collected fraction of the right peripheral outlet channel. (e) IgG-PE binding assay in 0.1 % porcine blood from ECμPs separated and collected using an acoustic sample preparation chip, prior to flow cytometry analysis. (▲) denotes ECμPs with capture antibody and (■) denotes particles without capture antibody. Note: all data points were obtained in triplicate. Error bars represent the standard deviation of the mean for 3 separate determinations of median fluorescence intensity.

Discussion

We have synthesized PDMS-based ECμPs that possess negative acoustic contrast and specific biorecognition properties. We have demonstrated that ECμPs enable binding and acoustophoretic separation of ligand analytes from complex biological samples (e.g., blood) containing large concentrations of cells. Furthermore, we have demonstrated that when the separated ECμPs are analyzed via flow cytometry, highly sensitivity and selective detection of serum proteins is possible.

Sylgard 184^{TM} and PDMS-based elastomers, in general, are water insoluble elastomers whose compressibility (inverse of bulk modulus) can be adjusted based on the amount of crosslinking agent added.[34] To date, we have only used Sylgard 184™ based elastomeric microparticles that were synthesized using standard PDMS prepolymer to crosslinking agent ratios of 10:1 and 10:2;[35] both samples exhibited negative acoustic contrast. Incorporating other amounts, i.e., increasing or decreasing the amount of crosslinking agent, may allow adjustments to be made in how elastomeric microparticles respond to acoustic radiation fields. Other compressible water-insoluble elastomers such as other silicones, natural rubbers, polyurethanes, butyl rubbers, polybutadienes, styrene butadienes, fluoroelastomers, polyether block amides, ethylene-vinyl acetates, and polyacrylic rubber[36], have the potential to be synthesized into negative contrast particles using emulsion-based methodologies such as those employed herein.

The acoustic separation of ligand-bound ECμPs s from blood cells in the acoustic sample preparation chip occurs rapidly, within seconds or less, and occurs with continuous flow. The acoustic sample preparation chip allows for ligand-bound ECμPs to be rapidly collected without (i) performing time-consuming centrifugal washes to remove

blood cells, and (ii) without other time-consuming protein isolation steps such as 2-D gel electrophoresis or other protein separation steps (e.g., precipitation, chromatography, filtering) that are performed prior to mass spectrometry analysis. The use of flow cytometry, as compared to other detection methods of analysis (e.g., ELISA, spectrofluorimetry), is advantageous in that it allows ECμPs to be used in homogeneous (no wash) blood-based assays where unbound fluorescently labeled ligands provide minimal background.[37]

The PSA assay was conducted in PBS buffer, and was primarily used to demonstrate that ECμPs can be used as platforms for binding of medically-relevant antigens. We note that the PSA concentration range tested was not in the diagnostically-relevant range (4 - 10 ng/mL).[38] However, our lowest PSA concentration (1 nM) was detected with a high signal-to-noise ratio and thus shows potential to detect PSA at even lower concentrations. Future work will emphasize the use of optimal antibodies and fluorophores for such assays to further improve limits of detection. Furthermore, the use of monodisperse elastomeric microparticles may provide greater potential to optimize the functionalization of ECμPs; thus enabling detection of PSA at lower concentration levels.

The ability to bind ligands specifically in the presence of abundant serum proteins is a necessary component of accurate and sensitive immunoassay platforms for the detection of low concentration levels of biomarkers in blood. Our detection of 21 pM IgG-PE (~3 ng/mL) in blood-based samples (Figures 6.4b and 6.5e) is commensurate with the clinically relevant detection limits for other biomarkers commonly detected in diagnostics using blood-based samples.[38] Furthermore, the continuous flow format of acoustophoresis will make it possible to couple this approach directly to a conventional

flow cytometer or to perform cytometry directly on the focused streams as has been done in other microfluidic systems.[4,39]

We present the first demonstration of engineered particles with negative contrast in acoustic based microfluidic bioanalytical systems. The negative contrast property of ECμPs, along with the use of acoustic sample preparation microfluidic systems have the potential to enable the development of bioassay systems where the acoustic sample preparation chip is coupled directly to a flow cytometer. The continuous feed of separated ligand-bound ECμPs directly into a flow cytometer may allow for a significantly decreased time-to-analysis along with increased analysis rates. Further improvements could use ECμPs in portable systems where a disposable acoustic flow cell is used to separate ECμPs from blood cells before analysis by a low cost flow cytometer.[4,39] In pursuit of making ligand-bound ECμP measurements more accurate and sensitive using flow cytometry, we are developing methods (such as those based on microfluidics, see SI Figure S6.5) to synthesize monodisperse elastomeric particles. Such monodisperse particles would be simpler to identify in flow cytometry as discreet populations with consistent optical properties. Furthermore, their singular size would make their time dependent movement in an acoustic standing waves more predictable and simplify efficient separations using ECμPs.

ACKNOWLEDGMENT

We thank Travis Woods and Robert Applegate for technical assistance. We also appreciate helpful discussions with Andrew Goumas, Carl Brown, Greg Kaduchak, and Michael Ward. We are grateful for the funding that supported this work from the National Science Foundation (Research Triangle MRSEC: DMR 1121107, DMR 0611616) and the National Institutes of Health (NIH RR020064, NIH RR001315).

Five figures as noted in the text. This material is available free of charge via the Internet at http://pubs.acs.org

References

1. Laurell, T.; Petersson, F.; Nilsson, A., Chip integrated strategies for acoustic separation and manipulation of cells and particles. *Chemical Society Reviews* **2007,** *36* (3), 492-506.

2. Nam, J.; Lim, H.; Kim, D.; Shin, S., Separation of platelets from whole blood using standing surface acoustic waves in a microchannel. *Lab on a Chip* **2011,** *11* (19), 3361-3364.

3. Gossett, D. R.; Weaver, W. M.; Mach, A. J.; Hur, S. C.; Tse, H. T. K.; Lee, W.; Amini, H.; Di Carlo, D., Label-free cell separation and sorting in microfluidic systems. *Analytical and bioanalytical chemistry* **2010,** *397* (8), 3249-3267.

4. Piyasena, M. E.; Suthanthiraraj, P. P. A.; Applegate, R. W., Jr.; Goumas, A. M.; Woods, T. A.; Lopez, G. P.; Graves, S. W., Multinode Acoustic Focusing for Parallel Flow Cytometry. *Analytical Chemistry* **2012,** *84* (4), 1831-1839.

5. Meng, Z.; Veenstra, T. D., Targeted mass spectrometry approaches for protein biomarker verification. *Journal of Proteomics* **2011**, *74* (12), 2650-2659.

6. Greenwald, J.; Burstein, G.; Pincus, J.; Branson, B., A rapid review of rapid HIV antibody tests. *Current Infectious Disease Reports* **2006**, *8* (2), 125-131.

7. Stevens, E. V.; Liotta, L. A.; Kohn, E. C., Proteomic analysis for early detection of ovarian cancer: A realistic approach? *International Journal of Gynecological Cancer* **2003**, *13*, 133-139.

8. Toner, M.; Irimia, D., Blood-on-a-chip. In *Annual Review of Biomedical Engineering*, **2005**; Vol. 7, pp 77-103.

9. Prabhakar, U.; Eirikis, E.; Davis, H. M., Simultaneous quantification of proinflammatory cytokines in human plasma using the LabMAP (TM) assay. *Journal of Immunological Methods* **2002**, *260* (1-2), 207-218.

10. Etzioni, R.; Urban, N.; Ramsey, S.; McIntosh, M.; Schwartz, S.; Reid, B.; Radich, J.;Anderson, G.; Hartwell, L., The case for early detection. *Nature Reviews Cancer* **2003**, *3*, 243-252.

11. Stern, E.; Vacic, A.; Rajan, N. K.; Criscione, J. M.; Park, J.; Ilic, B. R.; Mooney, D. J.; Reed, M. A.; Fahmy, T. M., Label-free biomarker detection from whole blood. *Nature Nanotechnology* **2010**, *5* (2), 138-142.

12. Hou, H. W.; Bhagat, A. A. S.; Lee, W. C.; Huang, S.; Han, J.; Lim, C. T., Microfluidic Devices for Blood Fractionation. *Micromachines* **2011,** *2* (3), 319-343.

13. Gervais, L.; de Rooij, N.; Delamarche, E., Microfluidic Chips for Point-of-Care Immunodiagnostics. *Advanced Materials* **2011,** *23* (24), H151-H176.

14. Wang, R. E.; Tian, L.; Chang, Y.-H., A homogeneous fluorescent sensor for human serum albumin. *Journal of Pharmaceutical and Biomedical Analysis* **2012,** *63*, 165-169.

15. Jani, I. V.; Janossy, G.; Brown, D. W. G.; Mandy, F., Multiplexed immunoassays by flow cytometry for diagnosis and surveillance of infectious diseases in resource-poor settings. *The Lancet infectious diseases* **2002,** *2* (4), 243-250.

16. Williams, D.; Ackloo, S.; Zhu, P.; Bowden, P.; Evans, K. R.; Addison, C. L.; Lock, C.; Marshall, J. G., Precipitation and selective extraction of human serum endogenous peptides with analysis by quadrupole time-of-flight mass spectrometry reveals posttranslational modifications and low-abundance peptides. *Analytical and Bioanalytical Chemistry* **2010,** *396* (3), 1223-1247.

17. Bischoff, R.; Luider, T. M., Methodological advances in the discovery of protein and peptide disease markers. *Journal of Chromatography B* **2004,** *803* (1), 27-40.

18. Prazeres, S.; Santos, M. A.; Ferreira, H. G.; Sobrinho, L. G., A practical method for the detection of macroprolactinaemia using ultrafiltration. *Clinical endocrinology* **2003,** *58* (6), 686-690.

19. Harper, R. G.; Workman, S. R.; Schuetzner, S.; Timperman, A. T.; Sutton, J. N., Low-molecular-weight human serum proteome using ultrafiltration, isoelectric focusing, and mass spectrometry. *Electrophoresis* **2004,** *25* (9), 1299-1306.

20. Cousins, C.; Holownia, P.; Hawkes, J.; Price, C.; Keay, P.; Coakley, W., Clarification of plasma from whole human blood using ultrasound. *Ultrasonics* **2000,** *38* (1), 654-656.

21. Petersson, F.; Nilsson, A.; Holm, C.; Jönsson, H.; Laurell, T., Continuous separation of lipid particles from erythrocytes by means of laminar flow and acoustic standing wave forces. *Lab on a Chip* **2005,** *5* (1), 20-22.

22. Petersson, F.; Nilsson, A.; Holm, C.; Jönsson, H.; Laurell, T., Separation of lipids from blood utilizing ultrasonic standing waves in microfluidic channels. *Analyst* **2004,** *129* (10), 938-943.

23. Grenvall, C.; Augustsson, P.; Folkenberg, J. R.; Laurell, T., Harmonic microchip acoustophoresis: a route to online raw milk sample precondition in protein and lipid content quality control. *Analytical chemistry* **2009,** *81* (15), 6195-6200.

24. Lenshof, A.; Ahmad-Tajudin, A.; Järås, K.; Swärd-Nilsson, A. M.; Åberg, L.; Marko-Varga, G.; Malm, J.; Lilja, H.; Laurell, T., Acoustic whole blood plasmapheresis chip for prostate specific antigen microarray diagnostics. *Analytical chemistry* **2009,** *81* (15), 6030-6037.

25. Lenshof, A.; Laurell, T., Continuous separation of cells and particles in microfluidic systems. *Chemical Society Reviews* **2010,** *39* (3), 1203-1217.

26. Dykes, J.; Lenshof, A.; Åstrand-Grundström, B.; Laurell, T.; Scheding, S., Efficient Removal of Platelets from Peripheral Blood Progenitor Cell Products Using a Novel Micro-Chip Based Acoustophoretic Platform. *PLoS One* **2011,** *6* (8), e23074.

27. Castillo, J.; Svendsen, W. E.; Dimaki, M., *Micro and nano techniques for the handling of biological samples*. CRC Press: **2011**.

28. Bruus, H., Acoustofluidics 7: The acoustic radiation force on small particles. *Lab on a Chip* **2012,** *12* (6), 1014-1021.

29. Galbraith, D. W., Analysis of higher plants by flow cytometry and cell sorting. *Int. Rev. Cytol* **1989,** *116*, 165-228.

30. Nash, M. A.; Yager, P.; Hoffman, A. S.; Stayton, P. S., A Mixed Stimuli-Responsive Magnetic and Gold Nanoparticle System for Rapid Purification, Enrichment, and Detection of Biomarkers. *Bioconjugate chemistry* **2010,** *21* (12), 2197.

31. Long, G. L.; Winefordner, J., Limit of detection a closer look at the IUPAC definition. *Analytical chemistry* **1983,** *55* (07), 712A-724A.

32. Weiser, M.; Apfel, R.; Neppiras, E., Interparticle forces on red cells in a standing wave field. *Acta Acustica united with Acustica* **1984,** *56* (2), 114-119.

33. Mabuka, J.; Nduati, R.; Odem-Davis, K.; Peterson, D.; Overbaugh, J., HIV-Specific Antibodies Capable of ADCC Are Common in Breastmilk and Are Associated with Reduced Risk of Transmission in Women with High Viral Loads. *PLoS Pathogens* **2012,** *8* (6), e1002739.

34. Wilder, E. A.; Guo, S.; Lin-Gibson, S.; Fasolka, M. J.; Stafford, C. M., Measuring the modulus of soft polymer networks via a buckling-based metrology. *Macromolecules* **2006,** *39* (12), 4138-4143.

35. Mata, A.; Fleischman, A. J.; Roy, S., Characterization of polydimethylsiloxane (PDMS) properties for biomedical micro/nanosystems. *Biomedical microdevices* **2005,** *7* (4), 281-293.

36. Lopez, G.P.; Carroll, N.; Cushing, K.; Petsev, D. N., Synthesis of Stable Elastomeric Negative Acoustic Contrast Particles. US Patent Application 20,120,065,329: **2012**.

37. Nolan, J. P.; Lauer, S.; Prossnitz, E. R.; Sklar, L. A., Flow cytometry: a versatile tool for all phases of drug discovery. *Drug discovery today* **1999,** *4* (4), 173-180.

38. Paul, B.; Dhir, R.; Landsittel, D.; Hitchens, M. R.; Getzenberg, R. H., Detection of prostate cancer with a blood-based assay for early prostate cancer antigen. *Cancer research* **2005**, 65 (10), 4097.

39. Austin Suthanthiraraj, P. P.; Piyasena, M. E.; Woods, T. A.; Naivar, M. A.; Lopez, G. P.; Graves, S. W., One-dimensional acoustic standing waves in rectangular channels for flow cytometry. *Methods* **2012,** 57 (3), 259-271.

Supporting Information

Elastomeric Negative Acoustic Contrast Particles for Affinity Capture Assays

Kevin W. Cushing,[a,b] Menake E. Piyasena,[a] Nick J. Carroll,[a, †] Gian C. Maestas,[a] Beth Ann López,[a] Bruce S. Edwards,[d] Steven W. Graves,*[,a,b] and Gabriel P. López,*[a,c]

[a] Center for Biomedical Engineering, Department of Chemical and Nuclear Engineering, The University of New Mexico, Albuquerque, NM 87131, USA.
[b] National Flow Cytometry Resource, Los Alamos National Laboratory, Los Alamos, NM 87545, USA.
[c] NSF Research Triangle Materials Research Science and Engineering Center, Depts. of Biomedical Engineering and Mechanical Engineering & Materials Science, Duke University, Durham, NC 27708, USA.
[d] Department of Pathology, School of Medicine, The University of New Mexico, Albuquerque, NM 87131, USA.

[†] *Current Address: Harvard School of Engineering and Applied Sciences, Pierce Hall, 29 Oxford Street, Cambridge, MA 02138, USA.*

* Corresponding author(s):

Gabriel P. López
NSF Research Triangle MRSEC
Duke University
Box 90271
Durham, NC 27708, USA.
Email: gabriel.lopez@duke.edu
Phone: 919-660-5435

Steven W. Graves
Center for Biomedical Engineering
MSC01 1141
1 University of New Mexico
Albuquerque, NM 87131-0001, USA
Email: graves@unm.edu
Phone: 505-277-2043

Silicon Acoustic Sample Preparation Chip

An acoustic sample preparation chip was fabricated in silicon via photolithography using a photomask designed from AutoCAD software (Autodesk Inc., San Rafael, CA) and a deep reactive ion etching (DRIE) using a protocol described by Suthanthiraraj et al.[1] DRIE allowed specific micro-channel patterns to be etched onto the surface of the silicon wafer (WaferNet Inc., San Jose, CA). A borosilicate glass slide (Borofloat 33, Schott North America, Inc., Elms Ford, NY) with 1 mm holes drilled through it to accommodate inlet and outlet ports (tube connection sites) was then sealed on top of the etched silicon wafer using anodic bonding.[1] To allow easy insertion of silicone tubing (Cole-Parmer Instrument Company, Vernon Hills IL) into inlet and outlet ports, square PDMS blocks, with punctured holes, were aligned and plasma sealed on top of the inlet and outlet ports.[2] Silicone tubing was then inserted and epoxy glued into the PDMS inlet and outlet ports. To complete the fabrication, a lead zirconate titanate piezoelectric transducer (PZT: 5 mm width x 30 mm length x ~1 mm thickness) (Boston Piezo-Optics Inc., Bellingham, MA) was attached to the bottom side of the chip using cyanoacrylate glue.

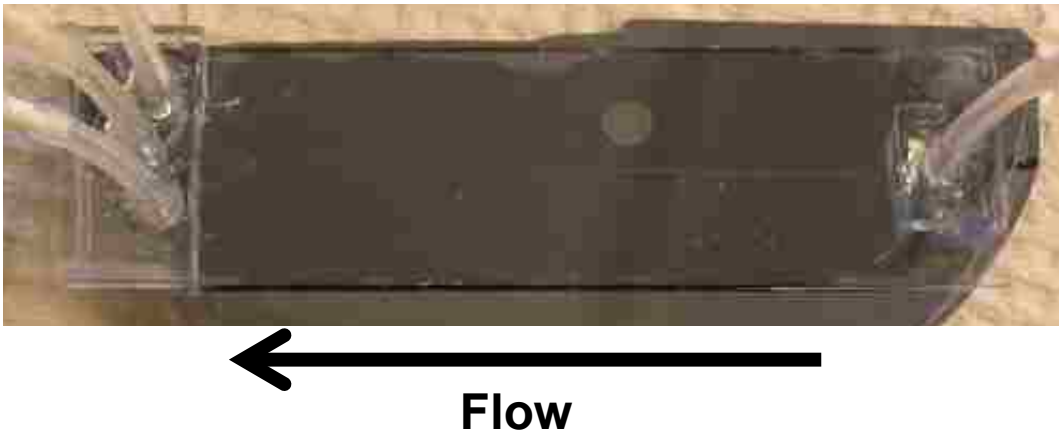

Figure S6.1 Acoustic sample preparation chip.

1. Austin Suthanthiraraj, P. P.; Piyasena, M. E.; Woods, T. A.; Naivar, M. A.; Lopez, G. P.; Graves, S. W., One-dimensional acoustic standing waves in rectangular channels for flow cytometry. *Methods* **2012,** 57 (3), 259-271.

2. Saarela,V.; Franssila, S.; Tuomikoski, S.; Marttila, S.; Östman, P.; Sikanen, T.; Kotiaho, T.; Kostiainen, R., Re-usable multi-inlet PDMS fluidic connector. *Sensors and Actuators B: Chemical* **2006,** *114* (1), 552-557.

Avidin Adsorption and Biotin-Binding

Elastomeric particles (2.5×10^7) where incubated in 1 μM avidin (Molecular Probes, Eugene, Oregon) in 1 mL of phosphate buffered saline (1X PBS with 7.4 pH: 10 mM Na_2HPO_4; 1 mM KH_2PO_4; 138 mM NaCl; 3 mM KCl) for 30 minutes with continuous rocking at room temperature. They were then centrifugally (2900 g for 5 min) washed and resuspended in 1 mL of washing/blocking buffer (0.1 % BSA in PBS) and incubated with continuous rocking at room temperature for 30 minutes. 5.0×10^5 avidinylated-elastomeric particles were then incubated in 200 μL in PBS with different concentrations of biotin-4-fluorescein (0, 0.1, 1, 10, 100 nM; Invitrogen) for 30 minutes with continuous rocking at room temperature. The particles were then analyzed with an Accuri C6 flow cytometer without prior washing. The biotin-block controls were performed in a similar manner but were incubated with 400 μM of free-biotin (Sigma-Aldrich) prior to incubation with biotin-4-fluorescein.

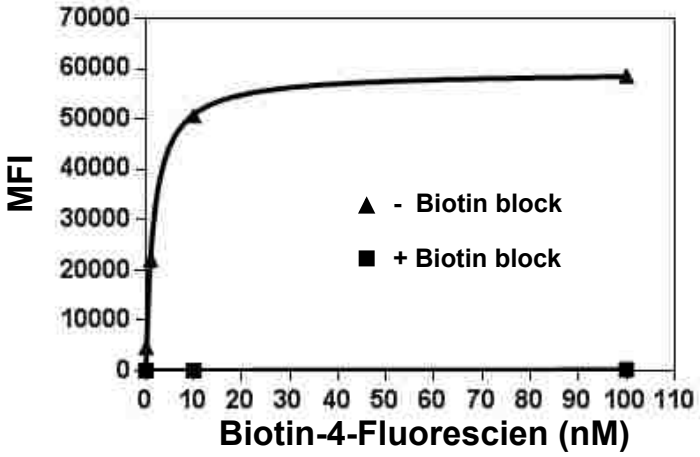

Figure S6.2 Binding curve for avidinylated-elastomeric particles that were incubated with different concentrations of biotin-4-fluorescein and then analyzed using flow cytometry (Accuri C6). The data were fit to a 1-site binding model (R^2= 0.99) using GraphPad PRISM 6.

Attachment of Biotinylated Capture Antibody

Avidinylated-elastomeric particles (2.5×10^7) were prepared as described above. A biotinylated mouse anti-human PSA monoclonal antibody (capture antibody) (HyTest Ltd., Turku, Finland) was added to make a 6 nM antibody solution in 1 mL of PBS, which was then incubated for 30 minutes with rocking at room temperature. The resulting ECμPs were centrifugally washed and resuspended in washing/blocking buffer. 5.0×10^5 ECμPs were then incubated in 200 μL of 1 nM of goat anti-mouse IgG-phycoerythrin (PE) (detection antibody) (Abcam, Cambridge MA) for 30 minutes with rocking at room temperature. Ligand-bound ECμPs were then analyzed by flow cytometry with a 585 ± 20 nm bandpass filter without prior washing. To determine the level of non-specific binding of the detection antibody, a negative control was performed in the same way, but without the inclusion of the biotinylated capture antibody.

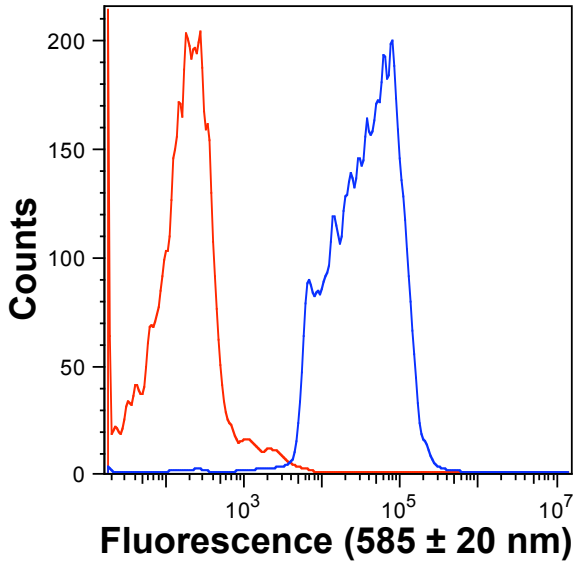

Figure S6.3 Fluorescence histograms showing the attachment of a biotinylated mouse anti human PSA monoclonal antibody (capture antibody) to avidinylated-elastomeric particles as measured by flow cytometry. Attachment of the biotinylated capture antibody was detected using a goat anti mouse polyclonal antibody-PE (detection antibody) (blue trace). To determine the non-specific binding of the detection antibody, a negative control (red trace) was performed in the same way, but without the inclusion of the biotinylated capture antibody. The median fluorescence intensity (MFI) of the negative control was 148, whereas the MFI of the sample treated with the biotinylated capture antibody was 39,270. These results indicate that ECμPs can be easily formed through the specific adsorption of high molecular weight biotinylated biomolecules (e.g., ~150,000 Da IgGs) to avidinylated PDMS microparticles.

Gating of Flow Cytometry Data for Quantifying Separation Efficiency

To identify the blood cell population in subsequent measurements of separation efficiency, 0.1 % whole porcine blood (diluted in PBS with 0.1% BSA) in 100 μL was analyzed using flow cytometry (Accuri C6). The data collected from this analysis was graphed on a scatter plot (fluorescence (585 ± 20 nm) vs. forward scatter, see Fig. S4a). The above-mentioned blood sample was then diluted into 900 μL of a common lysing buffer (recipe from Cold Spring Harbor Laboratory: 155 mM NH_4Cl; 12 mM $NaHCO_3$; and 0.1 mM EDTA in DI water) and incubated for 10 minutes at room temperature. The blood sample was then also analyzed using flow cytometry under identical conditions as mentioned-above. Based on the two analyses a gate was set to count particles with the fluorescence and scatter characteristics of blood cells (see Fig. S4a,b).

5.0×10^5 ligand-bound ECμPs (fluorescently labeled ligand = goat anti mouse IgG antibody conjugated to phycoerythrin, 1 nM) in 200 μL of PBS (0.1% BSA) were analyzed using flow cytometry. The fluorescence (585 ± 20 nm) vs. forward scatter for the ECμPs is given in Fig. S4c. The ligand-bound ECμP population was clearly distinct using these parameters from the blood cell population and thus the gating shown in Fig. S4 for each population can be used to distinguish each type of particle and to quantify separation efficiency.

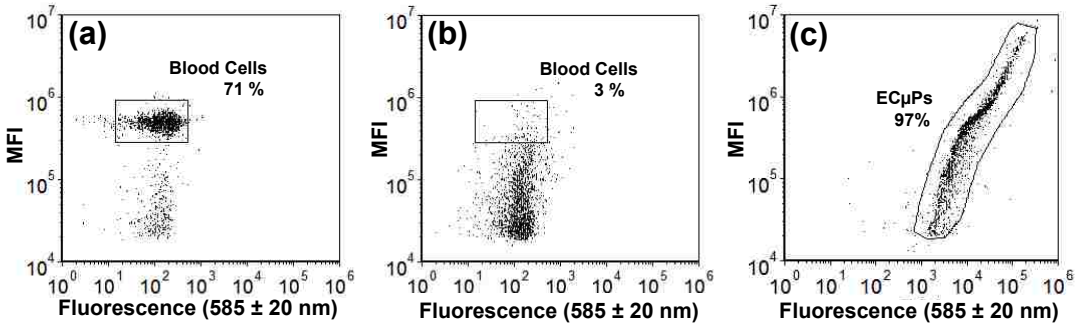

Figure S6.4 Porcine blood cells and ligand-bound ECμPs were identified using flow cytometry scatter plots (fluorescence (585±20 nm) vs. forward scatter). To quantify blood cells and ligand-bound ECμPs (fluorescently labeled ligand = goat anti mouse IgG antibody conjugated to phycoerythrin) it was necessary to determine the location of the blood cells and ligand-bound ECμPs on the scatter plots. 0.1% whole porcine blood was (a) analyzed using flow cytometry followed by lysis (b) and then re-analysis. (c) Ligand-bound ECμPs were analyzed using flow cytometry to determine the location of their appropriate gate. The numbers reported in the plots indicate the fraction of particles within the gating region in each case.

Synthesis of Monodisperse Elastomeric Particles

Sylgard 184 (20% crosslinking agent) was used to form microdroplets in a T-junction microfluidic chip (polydimethylsiloxane-based).[1] The continuous phase contained ultrapure water with 5% polyvinyl alcohol (PVA).[2] To prevent Sylgard 184 (with crosslinking agent) from wetting the micro-channel walls, the continuous phase was first injected using a syringe pump (Nexus 3000, Chemyx Inc. Stafford, TX) at a flow rate of 5 µL/min. The dispersed phase (Sylgard 184 with 20 wt.% crosslinking agent) was then injected into the microfluidic chip at a flow rate of 0.08 µL/min. Monodisperse elastomeric droplets were collected and cured at 70 °C overnight, with stirring, to form crosslinked monodisperse elastomeric particles. A Coulter counter (Z2 Coulter Particle Count and Size Analyzer, Becton Dickinson, Franklin Lakes, NJ) was used to determine the size distribution of the near-monodisperse elastomeric particles.

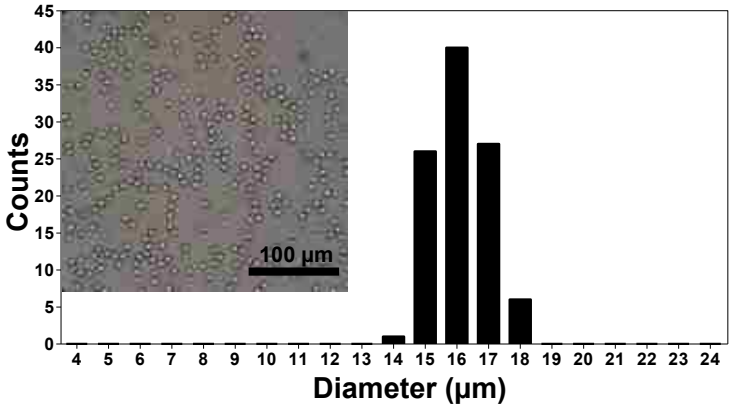

Figure S6.5 Uniformly sized elastomeric particles were synthesized using a T-Junction PDMS microfluidic chip. The mean diameter was measured to be 16.1 µm with a standard deviation (S.D.) of ± 0.9 µm and a coefficient of variation (C.V.) of 5.6 %.

1. Xu, J.; Li, S.; Tan, J.; Wang, Y.; Luo, G., Preparation of highly monodisperse droplet in a T-junction microfluidic device. *AIChE journal* **2006,** *52* (9), 3005-3010.

2. Elbert, D. L.; Hubbell, J. A., Surface treatments of polymers for biocompatibility. *Annual Review of Materials Science* **1996,** *26* (1).

Chapter 7 Conclusions and Future Directions

Particle Synthesis

Elastomeric negative acoustic contrast particles can be synthesized using PDMS-based elastomers, Sylgard 184 (specific gravity ~ 1.03) and low molecular weight PDMS (specific gravity ~ 0.97) using a bulk emulsion process and PDMS-based microfluidic systems, e.g., T-junction and flow focusing configurations. The elastomeric particles that are synthesized using the bulk-emulsion process (with or without surfactants) are polydisperse in size (submicron to a approximately 21μm in diameter) and can be produced rapidly (~ 1 hour) at high concentration levels (~1.25 x 10^8 particles/mL).

The production of PDMS-based elastomeric particles using the bulk-emulsion process is suitable for rapid proof-of-concept experimentation; however their use as accurate and sensitive platforms for flow cytometry-based assays is problematic as a result of the their large size distribution. Of several approaches evaluated for producing monodisperse particles using Sylgard 184 all were successful but limited in the ability to efficiently generate the large numbers of particles required for bioassay applications. A potentially more robust alternate approach was to use a low molecular weight PDMS (1:1 ratio of prepolymer to crosslinking agent), with a viscosity of 450 cSt, in conjunction with PDMS-based microfluidic systems (e.g., T-junction and flow focusing configurations) and a biocompatible surfactant (Pluronic® F108). Such an approach demonstrated the synthesis of ~400 monodisperse elastomeric particles per second for ~ 10 consecutive hours.

Particles Biofunctionalized and Used in Flow Cytometry-based Assays

Elastomeric particles that were synthesized from Sylgard 184 (specific gravity ~ 1.03) or low molecular weight PDMS (specific gravity ~ 0.97) in the absence of surfactant (CTAB, tween 20) were shown to be easily functionalized using non-specific adsorption of avidin or streptavidin protein. Avidin adsorbed onto the hydrophobic surface of polydisperse elastomeric particles (Sylgard 184) was shown to specifically bind biotin-4-fluorescein after elastomeric particles were blocked with a BSA protein; thus demonstrating biotin-binding functionality and minimal denaturation of the bound avidin protein.

Polydisperse elastomeric capture microparticles (ECμPs -synthesized from Sylgard 184) with a biotinylated human prostate specific antigen (PSA) monoclonal antibody were shown to be capable of capturing human PSA with a high signal-to-noise ratio in high protein content backgrounds (e.g., buffers with up to 10% human plasma and 1mg/mL BSA) and in small volumes with large amounts of protein (~20 μL of 1X PBS with 1 mg/mL BSA). The results also demonstrated that a homogeneous (no washing) sandwich assay configuration in conjunction with flow cytometry analysis can be used for high signal-to-noise ratio detection and quantification of PSA or IgG-phycoerythrin-(PE) protein bound to appropriately functionalized ECμPs. It was also shown that monodisperse ECμPs could be synthesized and functionalized for detection of HDL. These results thus establish that ECμPs can be utilized in different homogeneous assays that are detected and quantified using flow cytometry methods. Moreover, the method for functionalizing these particles with avidin was easy and straightforward; it also can allow the particles to be adapted to a wide variety of bioassays by taking

advantage of the many different biotinylated biomolecules that are commercially available.

The next logical step for future development will be methods for scaled up production and functionalization of monodisperse ECμPs. A potentially promising approach outlined above involves synthesis from low molecular weight PDMS using PDMS-based microfluidic systems (T-junction or flow focusing configuration). Functionalization of these monodisperse ECμPs could be achieved by incorporating a biotinylated Pluronic® F108 surfactant in the production process.[1] Once monodisperse elastomeric particles are thermally-crosslinked, and assuming that the biotin moiety maintains proper orientation without significant denaturation, they can be further functionalized using avidin and biotinylated-antibody (e.g., biotinylated-HDL monoclonal). Because of their more uniform size monodisperse ECμPs can allow more accurate use of fluorescence intensity as a basis for quantification of bound analyte. With appropriate calibration methods (e.g., standard curves generated using ECμPs incubated with a range of known analyte concentrations) monodisperse ECμPs offer an attractive novel approach for rapid detection and quantification of clinically important analytes circulating in blood and other fluids. .

Acoustic Focusing and Separation

Polydisperse elastomeric particles synthesized from Sylgard 184 and low molecular weight PDMS function as negative acoustic contrast particles and can be separated from positive acoustic contrast particles (blood cells and polystyrene) under the application of an acoustic standing wave field within an acoustofluidic device (silicon-based and square glass microcapillary devices).

Acoustic separation of elastomeric particles (Sylgard 184) from a 0.1% porcine (pig) blood sample, using a silicon-based acoustofluidic device with a downstream trifurcation for collection and subsequent flow cytometry analysis, demonstrated a 95-96% separation efficiency. Still, as we are using polydisperse ECμPs that vary in size from many microns in diameter to those that are only hundreds of nm in diameter, it begs the question of what separation efficiency is, as many ECμPs might be expected to separate simply based on their size (inertial focusing)[2] – without any relation to the principle of negative acoustic contrast. In fact such inertial focusing may contribute to the non-uniformity (i.e., apparent aggregation) of polydisperse ECμPs at the anti-nodes of an acoustic field under flow conditions observed above. However, data reported in this dissertation represent compelling proof of concept to support the conclusion that ECμPs can be efficiently separated and collected away from blood cells within a mixture using acoustophoresis. Future separation efficiency experiments using monodisperse ECμPs will allow a more precise quantification of the separation efficiency.

ECμPs (Sylgard 184) were successfully used in IgG-PE capturing in a diluted whole porcine blood sample (0.1% blood diluted in 1X PBS with 0.1% BSA) followed by acoustophoresis and flow cytometry analysis. The ability to detect an IgG biomolecule at a 21 pM concentration (~ 3 ng/mL) in a blood-based sample with a high protein content background (1X PBS with 0.1% BSA) demonstrates the potential of using ECμPs in medically-relevant bioassays (e.g., plasma, blood). Furthermore, the use of acoustophoresis to separate ligand-bound ECμPs prior to performing the assay, has potential to obviate the need of time-consuming preparation steps (e.g., red blood cell removal via centrifugation or lysis steps) that may cause non-specific loss of desired biomarkers leading to a reduction in the accuracy of the reported results. As a result of the continuous separation and collection of ligand-bound ECμPs using acoustophoresis, methods can be developed to allow a continuous feed of separated ligand-bound ECμPs into a flow cytometer for increased analysis rates. The use of lab-on-chip technology may also allow for rapid separation and analysis of separated and concentrated ECμPs using a low-cost flow cytometry set-up.[3,4]

References

1. Johnson, L.M.; Gao, L.; Shields, C. W.; Smith, M.; Efimenko, K.; Cushing, K.; Genzer, J.; López, G. P., Elastomeric microparticles for acoustic mediated bioseparations. *Submitted to Journal of Nanobiotechnology* **2013**.

2. Di Carlo, D.; Irimia, D.; Tompkins, R. G.; Toner, M., Continuous inertial focusing, ordering, and separation of particles in microchannels. *Proceedings of the National Academy of Sciences* **2007,** *104* (48), 18892-18897.

3. Piyasena, M. E.; Austin Suthanthiraraj, P. P.; Applegate Jr, R. W.; Goumas, A. M.; Woods, T. A.; López, G. P.; Graves, S. W., Multinode acoustic focusing for parallel flow cytometry. *Analytical chemistry* **2012,** *84* (4), 1831-1839.

4. Austin Suthanthiraraj, P. P.; Piyasena, M. E.; Woods, T. A.; Naivar, M. A.; López, G. P.; Graves, S. W., One-dimensional acoustic standing waves in rectangular channels for flow cytometry. *Methods* **2012,** *57* (3), 259-271.